Variational formulation of dynamical homogenization towards nonlocal effective media

J.F. Ganghoffer, H. Reda

Version of Record: https://www.sciencedirect.com/science/article/pii/S0997753821002333
Manuscript_cf1c6c52f555aa57141fbb6c17ba5216

Variational formulation of dynamical homogenization towards nonlocal effective media

J.F. Ganghoffer[a], H. Reda[b]

[a] LEM3, Université de Lorraine, CNRS. 7 rue Félix Savart, 57073, Metz, France
[b] Faculty of Engineering, Section III, Lebanese University, Campus Rafic Hariri, Beirut, Lebanon

Abstract

The dynamical homogenization of heterogeneous materials is performed in the low and high frequency regimes using a variational formulation of dynamical equilibrium combined with the Laplace or Fourier-Floquet-Bloch decomposition of the mechanical fields (displacement, velocity, momentum, stress). The assumed periodicity of the initial heterogeneous structure entails that the homogenization process can be carried out at the scale of a reference unit cell over which periodicity conditions apply. A dynamical Hill type macrohomogeneity condition is formulated that plays a central role in this work. The weak form of the unit cell dynamical equilibrium is formulated as the minimization of the mean field action integral expressed versus the Floquet components of the displacement and velocity. The effective dynamical moduli are evaluated in reciprocal space as unit cell averages of the microscopic properties and localization operators relating the local velocity and strain to their macroscopic counterpart. More specific dynamical models involving locality in space (thus valid for long wavelengths) but nonlocality in time (thus describing both low and high frequency regimes) are formulated, considering Cauchy type and strain gradient effective models. The range of validity of the developed dynamical generalized continuum theories is assessed by comparing the phase velocity-wavenumber plots for inclusion based composites with reference plots obtained from Bloch's theorem. The benchmark of dynamical models evidences that the nonlocal dynamical model proves able to predict with a good accuracy the dynamical behavior of 2D periodic inclusion based composites.

Keywords: elastodynamic homogenization; variational formulation; Floquet-Bloch transform; nonlocal space-time constitutive law; dispersion relations; composite materials.

1. Introduction

The present work aims to establish the nonlocal in time and space elastodynamic effective medium for periodic heterogeneous structures based on a variational characterization of dynamical equilibrium combined with Fourier transform in time or the Floquet-Bloch decomposition of the local fields. The main objective is to formulate dynamical constitutive laws of the substitution medium covering both the low and high frequency regimes, in terms of its microscopic behavior, relying on variational based homogenization methods in order to evaluate the effective dynamical properties of the formulated homogenized media.

The range of validity of the continuum theories for modeling the behavior of composites or architectured materials can be analyzed by studying their prediction capabilities in the dynamic range, especially considering the dispersion diagram, which exhibits key features for microstructured materials, most importantly the presence of acoustic branches close to the origin - at low frequencies and high wavelength -, optical branches presenting a cut-off frequency (at

high frequencies but still low wavenumbers), and the existence of band gaps in which waves cannot propagate (Rosi and Auffray, 2016). The presence of an internal microstructure in heterogeneous composite materials generally entails a dispersive behavior that can in general not be captured by the classical effective Cauchy continuum, thus requiring to increase the number of degrees of freedom or adding higher order gradients into the kinematics of the homogeneous substitution medium to formulate an enriched constitutive model at the macroscopic level. The first gradient formulations elaborated in the pioneering contributions of Mindlin (1964, 1965) can be enriched by higher order inertia terms, whereby the kinetic energy is allowed to depend on the velocity gradient. Such an enrichment allows a more accurate description of size effects manifested in the dynamical material behavior of real materials like polymer foams, porous materials (Mindlin, 1964; Askes and Aifantis, 2011) and many architected materials (Rosi et al., 2018; Ayad et al., 2019) and references therein.

Continuum models of microstructural effects in wave propagation are most of the time phenomenological in nature, with a classification into two main groups: i) those including new degrees of freedom, like micromorphic models and variants of it (see Berezovski et al., 2013) or ii) higher gradients models in the spirit of strain gradient models (Fafalis et al., 2012). Several strain gradient dynamical formulations have been developed in the literature over the last decade (Bacigalupo and Gambarotta, 2010, 2014b; Ayad et al., 2019) and references therein. Waves propagation in heterogeneous domains is accompanied by certain specific features not encountered in homogeneous materials, like their dispersive nature (the phase velocity is dependent on frequency), the existence of optical branches (some modes exhibit cut-off frequencies) and directivity (energy flows in preferred directions, which change with frequency), as explained in (Rosi and Auffray, 2016). While higher-grade continua are dispersive, they are not able to capture optical branches, due to the absence of internal degrees of freedom; moreover, the dispersion relation in these models become linear in the long wavelength limit. It has to be underlined that local generalized continuum models provide a sound description of the dynamical response only over a small window of wavelengths.

When these dynamical models are formulated in a phenomenological manner, the identification of the many material parameters involved in the wave propagation model usually requires a complicated experimental protocol (Polyzos et al., 2015; Iliopoulos et al., 2016; Réthoré et al., 2015). Moreover, such models lack a predictive capacity since the identification of their inherent materials parameters has to be repeated for each new microstructure. A methodology for the identification of the parameters of a strain-gradient dynamical constitutive model for propagating waves in media with an inner architecture is exposed in (Rosi et al., 2018). In order to circumvent this drawback, multiscale methods have been developed to link the dispersive aspects of wave propagation to microstructural features of the material. Amongst these, homogenization techniques derive the dynamical macroscopic behavior by upscaling the microscopic one, so obtaining a coarser description of the dispersive wave propagation features, but still reflecting in a predictive manner the impact of the underlying material microstructure.

The low-frequency classical homogenization theory fails to capture the physics at high frequencies, so it is clear that alternative approaches are needed. High frequency behaviors have been investigated for both architected materials and composites employing asymptotic expansion methods (Wang and Sun, 2002; Andrianov et al., 2008, 2011; Craster et al., 2010; Zhikov, 2000; Smyshlyaev, 2009; Auriault and Boutin, 2012; Karathanasopoulos et al., 2019). Bloch homogenization approach has been developed in the literature to handle high frequency homogenization (Allaire and Conca, 1998; Allaire and Piatnistski, 2005; Birman and Susline,

2006; Hoefer and Weinstein, 2011). An alternative approach to high frequency homogenization is to consider frequency dependent effective parameters of periodic media (Nemat-Nasser et al., 2011). The flourishing literature on the topic shows the existing considerable interest in generating effective continuum models of heterogeneous materials and composites that bypass the limitations of low-frequency homogenization theories.

Asymptotic homogenization is quite appealing and has witnessed important developments in the field of wave propagation over the last two decades (Fish and Chen, 2001; Guenneau et al., 2013; Bacigalupo and Gambarotta, 2010, 2012, 2014 a,b; Boutin et al., 2010; Ayad et al., 2019). Especially, dynamical models of discrete systems modeled as beams have been employed to compute their dispersion features. A methodology relying on the higher order asymptotic expansion of the inner forces and moments of structural beam type elements has been used in (Ayad et al., 2019) to compute the acoustic and optical branches of the dispersion diagrams close to resonance points of 1D and 2D periodic structures. Homogenization in the time domain has also been proposed by several authors, see e.g. (Chen and Fish, 2000; Vivar-Pérez et al., 2009), considering fast and slow time scales. Resorting to computational approaches, finite element computations over the unit cell with periodic Bloch boundary conditions have been performed to model acoustic waves scattering and to evaluate the band structure (Hussein, 2009; Huang, 2011). As an alternative strategy for the solution of the Floquet-Bloch problem, plane wave expansions of the displacement vector, elastic moduli and mass are done in Fourier series with respect to the periodicity vectors (Nemat-Nasser et al., 2011), furnishing exact dispersion relations.

The homogenized model of the periodic structure is not unique; contrariwise, it depends on both the microstructural behavior it aims to describe when using an effective continuum, and on the frequency of incident waves. Two main phenomena are primarily responsible for the effective material behavior: the so-called Bragg scattering and local resonance. While the appearance of resonances does not require a periodic microstructure and can be observed for both long and short wavelengths, Bragg scattering appears only in the short-wavelength regime thus at high frequencies (Mencik and Duhamel, 2015; Silva et al., 2016; Suiker et al., 2001; Erofeyev, 2003). The limitation of homogenization schemes to the regime of low frequencies makes them not usable in applications where high frequencies appear. High frequency homogenization schemes have been developed for such situations of wavelengths and characteristic microstructural length scales being of the same order, in which multiple scattering effects are of importance (Panasenko, 2005). Considering multiple scales has led to the formulation of an effective continuum for periodic media at diverse frequency ranges. Asymptotic homogenization techniques have been complemented by elastodynamic homogenization approaches for both periodically and randomly inhomogeneous media (Chenais et al., 2015; Colquitt, 2018; Wang and Chen, 2019). In contrast to asymptotic approaches, the elastodynamic homogenization theory is exact and does not require any scale separation hypothesis. As such, the resulting effective continuum obtained is nonlocal in space and time (Willis, 1997, 2011; Nassar et al., 2015, 2016). The development of nonlocal models in elasticity started from the pioneering works of (Eringen and Edelen, 1972), aiming to describe long-range interactions between material points. Such generalized elasticity models have been recently employed to analyze the axial and flexural dynamical response of nano beams with applications to NEMS in (Pinnola et al., 2020a), and a stress-driven nonlocal analysis of the damped vibrations of elastic nano-beams resulting from stochastic excitations has been performed in (Pinnola et al., 2020b).

Materials for which a coupling between the stress–strain and momentum–velocity constitutive relations is needed were initially proposed in (Willis, 1981) and deserve the name of elastic materials of the Willis type, or more simply Willis materials. A linear Willis material is an initially composite heterogeneous material which, after homogenization, introduces a stress to velocity and a momentum to strain coupling. This non-intuitive coupling arises from both non-local effects and from material asymmetries (Willis, 1997; Milton and Willis, 2007; Srivastava and Nemat-Nasser, 2011; Norris et al., 2012; Willis, 1981; Achenbach, 2003; Srivastava, 2015; Nassar et al., 2015; Nemat-Nasser and Willis, 2011). One mechanism in reciprocal media generating such a coupling is the asymmetry of a representative volume element; a nonlocal coupling may arise due to multiple scattering between spatially separated heterogeneities.

Willis theory was initially developed for random linear elastic composites, whereby explicit nonlocal constitutive relations have been set, relating the ensemble averages of strain and stress (Drugan and Willis, 1996). The elastodynamic homogenization theory of Willis exhibits the following salient features: (i) No approximations is one in the upscaling process from micro to macro scales, so that the resulting theory can be considered as an exact one; (ii) after homogenization, the effects of microscopic heterogeneities are reflected by the resulting non-local effective constitutive law, which otherwise takes the same form as the microscopic constitutive law; iii) for a composite comprising linear elastic constituents that obey a local in time and space constitutive law, the effective response obtained after homogenization becomes in general nonlocal both in space and time; (iv) the effective mass density becomes a second order tensor after homogenization of the microscopically scalar-valued density; (v) a non-classical coupling between the effective stress tensor and the effective velocity, and another one between the effective momentum and the effective strain tensor, occur generally in the effective constitutive law; (vi) the constitutive parameters of the effective constitutive law are non-unique, and they can be fixed by prescribing an additional eigenstrain field.

A renewed interest in Willis theory appeared in recent years due to the developments of metamaterials and their applications in different fields of engineering; it turns out that Willis theory is rich enough to encompass all types of encountered unusual effects, such as anisotropic masses, negative mass or stiffness, nonlocal effects, band gaps, optical branches. Secondly, Willis elasticity equations keep the same form under a curvilinear change of coordinates (Milton and Willis, 2007), with the consequence that the macroscopic Willis type equations can be employed to achieve elastic cloaks. Despite the renewed interest in Willis theory (Nassar, 2015; Nassar et al., 2016), numerical methods for constructing the nonlocal effective response of heterogeneous materials are still lacking in the literature, and thus the predictive capability of Willis theory for 2D and 3D heterogeneous materials has still not been fully assessed.

The main thrust of this contribution is the derivation of nonlocal dynamical models of heterogeneous materials enlarged to the high frequencies and / or short wavelengths regimes using homogenization in a 2D context, based on a variational formulation and a Fourier (in the time domain) or a full Fourier-Floquet-Bloch transform of the initial elastodynamic boundary value problem posed over the initial heterogeneous domain. The formulation of a dynamical energy equivalence extending to the dynamics the classical Hill macrohomogeneity condition plays a central role in the elaboration of the homogenized dynamical behavior; a constructive proof of this dynamical macrohomogeneity condition is provided in the present contribution. The weak form of the unit cell dynamical equilibrium is formulated as the minimization of the mean field Lagrangian entering the action integral expressed in terms of the Floquet components of the displacement and velocity fields. These components are formulated using localization operators, leading to a constitutive law in integro-differential format when expressed in direct space. From the numerical point of view, the novel aspect of this contribution is the evaluation of the effective dynamical nonlocal in time and space response of periodic 2D heterogeneous materials,

and an assessment of the capabilities of different effective media endowed with nonlocality in time or in space-time to account for the specific features of the dynamical response at medium frequencies and short wavelengths (in comparison to the unit cell linear dimension). Especially, Cauchy and strain gradient non-local in time dynamical formulations are elaborated as novel aspects in this contributions, revealing their capability to capture some salient features of the dynamical response of heterogeneous materials as reflected in the phase velocity plots of propagating waves versus wavenumber.

This contribution is organized as follows: section 2 exposes the derivation of the effective dynamical moduli of heterogeneous materials at both low and medium frequencies, in the context of Cauchy dynamical homogenization; the extension to strain gradient dynamical homogenization is performed in section 3. The full extension to short wavelength and high frequencies is achieved in section 4, using the Floquet-Bloch transform method, thereby leading to the computation of the full set of effective moduli characterizing the nonlocal in space and time response. The panel of developed dynamical models is illustrated in section 4 for inclusion based composites, providing a comparison of the different modeling strategies from the viewpoint of the prediction of the phase velocities. Finally, we summarize the main thrust of the present contribution and expose some open problems in section 5.

A few words regarding the employed notations are in order. Vectors and tensors are denoted by boldface symbols. The transpose of a tensor is written with a superscript notation, for instance $\mathbf{B}^{\mathrm{T}}$. The gradient of a tensor field $\mathbf{A}(\mathbf{y})$ with respect to the spatial variable $\mathbf{y}$ is denoted alternatively $\mathbf{A}(\mathbf{y})\otimes\nabla_{\mathrm{y}}$ (with $\otimes$ the tensor product) or $\mathrm{grad}_{\mathrm{y}}\mathbf{A}(\mathbf{y})$, with its divergence denoted $\mathbf{A}(\mathbf{y}).\nabla_{\mathrm{y}}$ or alternatively . The symmetrized dyadic product is denoted $\otimes^{\mathrm{s}}$. The dot product therein represents the internal product in the space of Cartesian tensors. The simple, double and triple contractions of tensors are written '.' ,':' , and '$\therefore$' respectively. The symbol ':=' is extensively used throughout the paper and stands for 'equality by definition'. The partial derivative is denoted equivalently with the comma notation or with the partial derivative operator ∂_{x}, so for instance for the function $\mathrm{f}=\mathrm{f}(\mathrm{x})$, its derivative writes $\mathrm{f}_{,\mathrm{x}}:=\dfrac{\partial \mathrm{f}(\mathrm{x})}{\partial \mathrm{x}}\equiv\partial_{\mathrm{x}}\mathrm{f}(\mathrm{x})$; the time derivative is denoted with an overhead dot so for instance, it holds $\dot{\mathbf{E}}:=\dfrac{\mathrm{d}\mathbf{E}}{\mathrm{dt}}$. The algebraic number i denotes the purely imaginary complex number satisfying the equality $\mathrm{i}^2=-1$.

Table 1. Nomenclature of the principal notations and symbols

$\mathbf{u},\mathbf{v}$	microscopic displacement and velocity vectors
$\mathbf{y},\mathbf{x}$	microscopic and macroscopic position vectors
$\boldsymbol{\varepsilon}(\mathbf{y}),\mathbf{E}(\mathbf{x})$	microscopic and macroscopic strain tensors
$\mathbf{C}(\mathbf{y})$	fourth order tensor of microscopic mechanical properties
$\mathbf{I}_2$	second order identity tensor - $\mathbf{G}_2$ tensor of quadratic moment of inertia
$\boldsymbol{\sigma},\boldsymbol{\Sigma}$	microscopic and macroscopic Cauchy stress tensor

$\mathbf{f}$ body force

$\mathbf{t}$ prescribed surface traction

$l_\mu(\boldsymbol{\varepsilon}, \mathbf{v})$, $L_M(\mathbf{E}, \mathbf{V})$ microscopic and macroscopic Lagrangian densities

$\mathbf{v}(\mathbf{y}, \omega)$, $\mathbf{V}(\mathbf{x}, \omega)$ microscopic and macroscopic velocity vectors in frequency domain

$\mathbf{p} := \rho\mathbf{v}, \mathbf{P}$ microscopic and macroscopic momentum vectors

$\mathbf{k}$ wave vector

$\mathbf{H}^{EE}(\mathbf{y}, \omega)$, $\mathbf{H}^{VE}(\mathbf{y}, \omega)$ displacement localization operators

$\mathbf{H}^{EE}(\mathbf{y}, \omega)$, $\mathbf{H}^{VE}(\mathbf{y}, \omega)$ velocity localization operators

$\mathbf{K}(\mathbf{x}, \omega) := \left(\mathbf{U}(\mathbf{x}, \omega) \otimes^S \nabla_x\right) \otimes \nabla_x$ frequency-dependent strain gradient tensor

$\mathbf{S}, \mathbf{Q}$ hyperstress and hypermomentum tensors

---

2. Dynamical homogenization towards strain gradient effective media at medium frequencies

The effective dynamical properties of periodic heterogeneous media - composite or architectured materials achieving in this last case an extreme contrast of microscopic properties since the matrix is then a voided phase - will be evaluated using a variational principle for the characterization of the solution in conjunction with Hill macro homogeneity condition extended to a proper account of the higher order spatial and inertia contributions. The phases within the composite unit cell pictured in Fig.1 obey Cauchy linear elasticity, but their strong contrast of mechanical properties may lead to the emergence of a richer effective medium at the macroscopic level (after homogenization).

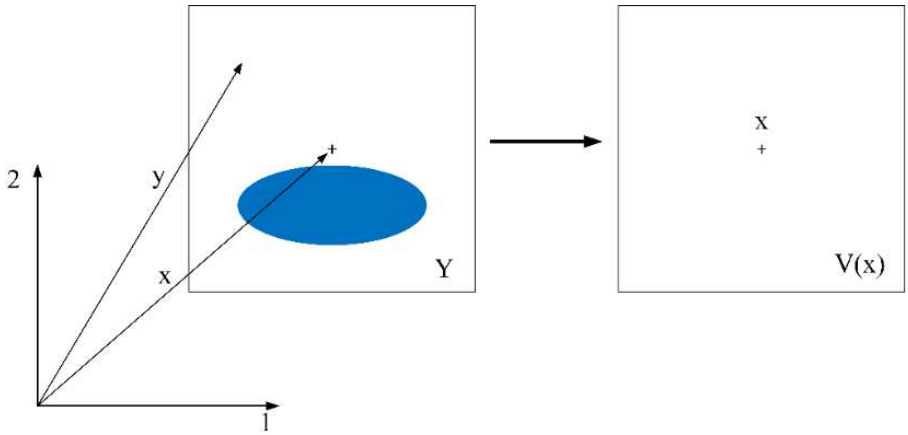

Figure 1: composite periodic unit cell Y made of two elastic materials (left) and the homogeneous substitution medium (right) with domain $\mathrm{V}(\mathbf{x})$ centered around point $\mathbf{x}$

The following vocabulary will be in use here and in the sequel: the smallest scale is called microscopic and the scale of the homogenized continuum is denoted as the macroscopic scale or level. In the same vein, the wording effective refers to properties captured at the scale of the homogenized level (the effective medium is represented on the right view of Fig.1).

The displacement and traction vectors are assumed to be fully continuous across the interface between constituents within the composite unit cell.

In order to set the state, the center of gravity of the unit cell, point $\mathbf{x}$ defined with respect to the adopted Cartesian basis, is defined implicitly by the integral relation meaning that the spatial average of relative positions within Y vanishes, viz.

$$\frac{1}{|Y|}\int_{Y}(\mathbf{y}-\mathbf{x})dV_y=\mathbf{0} \tag{2.1}$$

In Eq. (2.1), integration is done over all micropoints labelled with the position vector $\mathbf{y}$ within the unit cell. The dynamical behavior of the material at the micro level is governed by the following BVP (short cut of boundary value problem), adopting a linear elastic Hooke's law type:

$$\left|\begin{array}{l} \mathrm{div}_y\boldsymbol{\sigma}=\rho\ddot{\mathbf{u}} \\ \boldsymbol{\sigma}=\mathbf{C}(\mathbf{y}):\boldsymbol{\varepsilon} \\ \boldsymbol{\varepsilon}:=\mathbf{u}\otimes^{S}\nabla_y \\ \mathbf{u}=\mathbf{0}\ \text{ on } S_u \\ \mathbf{t}:=\boldsymbol{\sigma}.\mathbf{n}\ \text{ on } S_t=\partial\Omega/S_u \\ \mathbf{u}(\mathbf{y},0)=\mathbf{0}=\mathbf{v}(\mathbf{y},0) \end{array}\right. \tag{2.2}$$

in which $\mathbf{v}:=\dot{\mathbf{u}}$ and $\ddot{\mathbf{u}}$ denote the local velocity and acceleration respectively, $\boldsymbol{\varepsilon}:=\mathbf{u}\otimes^{S}\nabla_y$ is the linearized strain tensor and $\rho=\rho(\mathbf{y},t)$ is the mass density, a local scalar quantity varying within the unit cell. The symbol $/$ in (2.2.) denotes the set subtraction. Nil initial conditions are selected here in order to simplify the subsequent analysis in frequency domain, without however restricting the generality of the analysis to follow.

It is straightforward that the solution of BVP (2.2) can be characterized as the minimizer of the functional $S[\mathbf{u}]$, based on the spatio-temporal Lagrangian density, the scalar-valued function $l_\mu(\boldsymbol{\varepsilon},\mathbf{v}):=k_\mu(\mathbf{v})-w_\mu(\boldsymbol{\varepsilon})$, classically established as the difference between the microscopic kinetic energy $k_\mu(\mathbf{v})$ and the (microscopic) internal energy $w_\mu(\boldsymbol{\varepsilon})$ of an anisotropic linear elastic medium, selecting in a somewhat arbitrary manner initial and final times therein (respectively the real numbers t_i, t_f):

$$\begin{array}{l} S[\mathbf{u}]:=\underset{\tilde{\mathbf{u}}}{\mathrm{Min}}\int_{t_i}^{t_f}dt\int_{Y}l_\mu(\mathbf{u},\mathbf{v},\mathbf{u}\otimes\nabla_y)dV_y \\ w_\mu(\boldsymbol{\varepsilon}):=\frac{1}{2}\boldsymbol{\varepsilon}(\mathbf{y}):\mathbf{C}(\mathbf{y}):\boldsymbol{\varepsilon}(\mathbf{y}),\ k_\mu(\mathbf{v}):=\frac{1}{2}\rho\mathbf{v}.\mathbf{v}=\frac{1}{2}\mathbf{p}.\mathbf{v}\Rightarrow l_\mu(\boldsymbol{\varepsilon},\mathbf{v}):=k_\mu(\mathbf{v})-w_\mu(\boldsymbol{\varepsilon}) \end{array} \tag{2.3}$$

$\mathbf{C}(\mathbf{y})$ being the fourth order tensor of microscopic elastic moduli. The Euler equation of $S[\mathbf{u}]$ writes as the necessary stationarity condition written using the functional derivative of the action $\frac{\bar{\partial}S}{\bar{\partial}u_j}$, as explained in the **Appendix A** (considering especially relations (A3) and (A5)):

$$\begin{aligned}
&\delta S[\mathbf{u}] = 0 \Rightarrow \frac{\bar{\partial}S}{\bar{\partial}u_j} = \frac{\bar{\partial}L_M}{\bar{\partial}u_j} - \frac{d}{dt}\left(\frac{\bar{\partial}L_M}{\bar{\partial}\dot{u}_j}\right) = 0 \\
&\Rightarrow \frac{\partial l_\mu}{\partial u} - \mathrm{div}_y\left(\frac{\partial}{\partial \mathrm{grad}_y u}\right) - \frac{d}{dt}\left(\frac{\partial l_\mu}{\partial \mathbf{v}}\right) = \mathbf{0} \Rightarrow \mathrm{div}_y\left(\mathbf{C}(\mathbf{y}):\boldsymbol{\varepsilon}(\mathbf{u})\right) - \rho\dot{\mathbf{v}} = \mathbf{0} \\
&\Rightarrow \mathrm{div}_y\boldsymbol{\sigma} - \rho\dot{\mathbf{v}} = \mathbf{0}
\end{aligned} \tag{2.4}$$

The notion of functional derivative can be employed to reach the dynamical equation of motion in the more general context of a dynamical field theory, as explained in the **Appendix A**. Similarly, the microscopic Hamiltonian is defined as the sum of the internal and kinetic energies, viz. $h_\mu(\mathbf{v},\boldsymbol{\varepsilon}) := w_\mu(\boldsymbol{\varepsilon}) + k_\mu(\mathbf{v})$, referring to Eq.(2.3) for the definition of the underlying internal and kinetic energies.

2.1. Dynamic homogenization: a variational Lagrangian formulation in space-frequency domain

The dynamical equation of motion in previous BVP is rewritten in Hamiltonian form as the following set of differential equations

$$\left|\begin{aligned}
&\mathbf{p} := \rho\mathbf{v} \\
&\mathrm{div}_y\boldsymbol{\sigma} = \dot{\mathbf{p}}
\end{aligned}\right. \tag{2.5}$$

The Laplace transform allows reformulating the previous BVP in the space-frequency domain, whereby time will be replaced by the Laplace variable $p = i\omega$; recall that the Laplace transform of a function is defined as (including the origin of time in the time interval to account for the initial conditions):

$$F(p) = L(f(t)) := \int_{0^-}^{\infty} f(\mathbf{x},t)e^{pt}dt \tag{2.6}$$

The previous BVP in Eq. (2.5) then becomes after Laplace transform in space-frequency domain:

$$\left|\begin{aligned}
&\mathrm{div}_y\boldsymbol{\sigma} + i\omega\mathbf{p} = \mathbf{0} \\
&\boldsymbol{\sigma} = \mathbf{C}:\boldsymbol{\varepsilon} = \mathbf{C}(\mathbf{y}):\left(\mathbf{u}\otimes\nabla_y\right) \\
&\mathbf{p} := i\omega\rho\mathbf{u}
\end{aligned}\right. \tag{2.7}$$

In order to set the stage, the total microscopic displacement vector is decomposed additively into a homogeneous part $\mathbf{u}^{\mathrm{hom}}(\mathbf{y},\omega)$, corresponding to an exact effective Cauchy continuum and a periodic fluctuation $\tilde{\mathbf{u}}(\mathbf{y},\omega) \in H^1_{\mathrm{per}}(Y)$ of zero average, this last vector space being the Sobolev space of Y-periodic displacements; a similar decomposition holds the microscopic velocity.

It holds accordingly the following additive decomposition of the microscopic displacement and velocity in terms of their spatial average and periodic fluctuations (both functions of the microscopic spatial variable and Laplace variable), successively:

$$\begin{vmatrix} \mathbf{u}(\mathbf{y},\omega) = \mathbf{u}^{\hom}(\mathbf{y},\omega) + \tilde{\mathbf{u}}(\mathbf{y},\omega),\ \mathbf{u}^{\hom}(\mathbf{y}) = \mathbf{E}(\mathbf{x},\omega)\cdot\mathbf{y} \\ \langle\tilde{\mathbf{u}}\rangle_{\mathrm{Y}} = 0 \Rightarrow \mathbf{U}(\mathbf{x},\omega) := \langle\mathbf{u}\rangle_{\mathrm{Y}} = \mathbf{u}^{\hom}(\mathbf{y},\omega) = \mathbf{E}(\mathbf{x},\omega)\cdot\mathbf{x} \end{vmatrix} \tag{2.8}$$

$$\Rightarrow \begin{vmatrix} \mathbf{v}(\mathbf{y},\omega) = \mathbf{v}^{\hom}(\mathbf{y},\omega) + \tilde{\mathbf{v}}(\mathbf{y},\omega),\ \mathbf{v}^{\hom}(\mathbf{y}) = \dot{\mathbf{E}}(\mathbf{x},\omega)\cdot\mathbf{y} \\ \langle\tilde{\mathbf{v}}\rangle_{\mathrm{Y}} = \mathbf{0} \rightarrow \mathbf{V}(\mathbf{x},\omega) := \langle\mathbf{v}\rangle_{\mathrm{Y}} = \dot{\mathbf{E}}(\mathbf{x},\omega)\cdot\mathbf{x} \end{vmatrix}$$

The bracket notation stands for the volume averaging within the unit cell domain, so that it holds $\langle \mathrm{f} \rangle_{\mathrm{Y}} := \frac{1}{|\mathrm{Y}|}\int_{\mathrm{Y}} \mathrm{f}(\mathrm{y})\mathrm{dV}_{\mathrm{y}}$, with $|\mathrm{Y}|$ the unit cell volume or area (in 2D), and dV_{y} the infinitesimal integration volume. In Eq.(2.8), the velocity field has been decomposed into its volume average $\mathbf{V}(\mathbf{x},\omega) := \langle\mathbf{v}\rangle_{\mathrm{Y}}$ and a perturbation $\tilde{\mathbf{v}}(\mathbf{y},\omega)$, itself implicitly defined at the fixed macropoint $\mathbf{x}$.

General homogenization techniques comprise the class of deterministic methods like volume averaging, multiscale asymptotics, mixture theories, and stochastic approaches based on ensemble averaging, whereby macroscale quantities are defined as mathematical expectations (Matheron, 1966; Gelhar et al., 1979; Dagan, 1979, 1989). As their name indicates, volume averaging methods rely on the seminal idea that macroscale variables are defined by spatial averaging; the method witnessed its first developments in the sixties, with (Whitaker, 1967; Slattery, 1967) as its main proponents. The volume averaging method proceeds by performing a spatial averaging of the governing partial differential equations, for a specific boundary volume problem; it involves the following main steps:

1. Definition of the averaging process.
2. Average equations and use an additive decomposition of the searched solution into an average plus perturbation - like in relation (2.8) - and use theorems to interchange spatial averaging and differential operators.
3. Make assumptions about the timescales and length scales of the physical processes, to simplify the problem and derive an approximate form of the perturbations.
4. Derive a closed form expression of the macroscopic boundary value problem obtained by volume averaging.

The averaging volume is selected as the smallest volume element such that the parameter fields (here the microscopic moduli and density) are quasi-stationary; this averaging volume is then selected as the representative volume element (RVE in short); in case of a periodic medium, it coincides with the notion of periodic unit cell. The perturbation of a field are supposed to encounter spatial and temporal variations of one order higher than those of its volume average. The field perturbation is dependent on both macroscopic and microscopic variables (the last one varying within the RVE), with an assumed periodicity over the microscopic variable.

The differences between the volume averaging method and asymptotic expansion method are exposed e.g. in (Davit et al., 2013); one important point is that volume averaging does not rely on an asymptotic expansion of the field versus a small scale parameter, so that no higher order terms beyond the field perturbation is computed. Contrary to that, multiscale asymptotic methods are more mathematical in spirit and introduce a clearer scaling of variables and parameters in terms of a small parameter (the ratio of the unit cell to a macroscopic characteristic dimension).

In volume averaging methods, the averaged variables do not depend on the microscopic variable - so they are function of the sole macroscopic variable -, whereas the limit asymptotic solution depends a priori on both micro and macroscale variables. An essential difference between both methods is related to periodicity: the medium is considered *a priori* to be periodic with multiscale asymptotics, whereas volume averaging method does not rely on this assumption a priori, but only a posteriori to calculate the effective parameters by selecting the RVE to coincide with the unit cell. Although both methods use a perturbative decomposition of the field, there are differences in the way the decomposition is done: asymptotic methods relies on a formal expansion of the fields as a power series of the small scale parameter, whereas volume averaging does not make any assumption on the structure of the perturbation. Moreover, as previously mentioned, the leading order terms are different.

All fields in Eq.(2.8) are function of the pulsation $\omega = 2\pi f$ in the Fourier domain (linearly related to the frequency f of motion of the material points). Note that the macroscopic displacement and velocity fields $\mathbf{U}(\mathbf{x},\omega), \mathbf{V}(\mathbf{x},\omega)$ represent the incident signal over the unit cell, depending on the macroscopic space and time (or frequency), while the microscopic fields (displacement, velocity) have their own dynamics. From a physical point of view, micropoints within the unit cell may vibrate with their own frequency, not necessarily identical to the overall frequency of the imposed strain over the unit cell, especially when the incident wavelength becomes comparable to the microstructural size: the assumed incident wave may indeed break down into smaller packets due to scattering phenomena so the planar nature of the wavefront could not be preserved any more in such a situation.

The displacement and velocity fluctuations are here by definition selected to have zero spatial average over the unit cell, thus using eq.(2.8) and an affine model for the homogeneous contribution to the microscopic displacement, the average displacement and velocity are linear in the average strain and strain rate respectively. This assumption is explicated by introducing the space of kinematically admissible fluctuations

$$\mathrm{V_K} := \left\{ \tilde{\mathbf{u}}(\mathbf{y}), \tilde{\mathbf{v}}(\mathbf{y}) \in \mathrm{H^1}(\mathrm{Y}) \middle| \left\langle \tilde{\mathbf{u}} \right\rangle_{\mathrm{Y}} = \mathbf{0} = \tilde{\mathbf{v}}(\mathbf{y}),\ \tilde{\mathbf{u}}(\mathbf{y},\omega) = \mathbf{0} \text{ on } \mathrm{S_u} \right\} \tag{2.9}$$

The homogeneous displacement describes the response of a (fictive) effective continuum that would behave exactly as a homogeneous strain medium, so that the introduced displacement and velocity fluctuations, the vectors $\tilde{\mathbf{u}}(\mathbf{y},\omega), \tilde{\mathbf{v}}(\mathbf{y},\omega)$, correct for the deviation of the real microscopic displacement within the heterogeneous composite from the displacement resulting from the homogeneous strain $\mathbf{E}(\mathbf{x},\omega)$ and average velocity $\langle \mathbf{v} \rangle_{\mathrm{Y}}(\mathbf{x},\omega)$ applied as kinematic loading over the unit cell, as will appear later on. Due to the condition of nil average of the velocity fluctuation, the effective velocity has been defined in Eq.(2.8) as the spatial average of the corresponding microscopic velocity.

Hill macrohomogeneity condition proven in **Appendix B** states the equality of the macroscopic energy density of the selected strain gradient continuum, the scalar valued function $\mathrm{H_M}(\mathbf{E},\mathbf{P})$, with the averaged microscopic strain energy density $\mathrm{h_\mu}(\boldsymbol{\varepsilon},\mathbf{p})$, both accounting for potential and kinetic energy contributions. Similarly, the volume average over the unit cell of the microscopic Lagrangian function $\mathrm{l_\mu}(\boldsymbol{\varepsilon},\mathbf{v})$ is equal to the macroscopic Lagrangian $\mathrm{L_M}(\mathbf{E},\mathbf{V})$.

Combining Hill macrohomogeneity condition with Euler's relation for homogeneous functions of degree two (the macroscopic and microscopic energy densities are selected as

quadratic functions of their respective kinematic arguments in the present context of linear elasticity) leads to the macroscopic constitutive law and dynamical equations of motion over the homogeneous domain $\mathrm{V}(\mathbf{x})$ pictured in Fig.1, referring to Eq.(2.3):

$$\begin{aligned}&\left\langle \mathrm{l}_\mu(\boldsymbol{\varepsilon},\mathbf{v})\right\rangle_{\mathrm{Y}} = \frac{1}{2}\left(\mathbf{P}.\mathbf{V}-\boldsymbol{\Sigma}:\mathbf{E}\right) = \mathrm{L}_{\mathrm{M}}(\mathbf{E},\mathbf{V}),\\ &\boldsymbol{\Sigma} := -\frac{\partial \mathrm{L}_{\mathrm{M}}(\mathbf{E},\mathbf{V})}{\partial \mathbf{E}},\ \ \mathbf{P} := -\frac{\partial \mathrm{L}_{\mathrm{M}}(\mathbf{E},\mathbf{V})}{\partial \mathbf{V}} \Rightarrow \mathrm{div}_{\mathrm{x}}\boldsymbol{\Sigma} - \frac{\mathrm{d}}{\mathrm{dt}}\mathbf{P} = \mathbf{0}\end{aligned} \tag{2.10}$$

wherein the bracket represents the volume averaging over the unit cell, viz $\left\langle (.)\right\rangle_{\mathrm{Y}} := \frac{1}{|\mathrm{Y}|}\int_{\mathrm{Y}}(.)\,\mathrm{dV_y}$.

Hill dynamical macrohomogeneity condition plays a central role in the present contribution, and has been written in terms of the Hamiltonian densities in Eq.(2.10), more explicitly stating the identity of the spatial average of the microscopic Lagrangian $\mathrm{l}_\mu(\boldsymbol{\varepsilon},\mathbf{v})$ to the macroscopic Lagrangian $\mathrm{L}_{\mathrm{M}}(\mathbf{E},\mathbf{V})$, in which the momentum has been expressed versus its conjugated variable, the average velocity. The proof of Hill dynamical macrohomogeneity condition is given in the **Appendix B**, thereby providing the elaboration of the macroscopic Lagrangian and Hamiltonian, and stating the following identity in the framework of a Cauchy effective medium:

$$\begin{aligned}&\left\langle l_\mu(\boldsymbol{\varepsilon},\mathbf{v})\right\rangle_Y := \frac{1}{2}\left\langle \rho\dot{\mathbf{u}}.\dot{\mathbf{u}} - \boldsymbol{\sigma}:\mathbf{u}\otimes\nabla_y\right\rangle_Y = \frac{1}{2}\mathbf{P}.\mathbf{V} - \frac{1}{2}\boldsymbol{\Sigma}^{dyn}:\mathbf{E} =: L_M(\mathbf{E},\mathbf{V})\\ &\mathbf{P} := \left\langle \rho\dot{\mathbf{u}}\right\rangle_Y,\ \mathbf{Q} := \left\langle \rho\dot{\mathbf{u}}\otimes\mathbf{y}\right\rangle_Y,\\ &\mathbf{E} := \left\langle \mathbf{U}\otimes\nabla_y\right\rangle_Y,\ \ \boldsymbol{\Sigma}^{dyn} := \left\langle \boldsymbol{\sigma}\right\rangle_Y + \left\langle \rho\ddot{\mathbf{u}}\otimes\mathbf{y}\right\rangle_Y\end{aligned} \tag{2.11}$$

with $\mathbf{P}$, $\boldsymbol{\Sigma}^{stat}, \boldsymbol{\Sigma}^{dyn}$ the effective momentum (a vector), the static and dynamical Cauchy stress tensors respectively, conjugated in the sense of power of internal forces to the macro velocity, strain and strain rate tensors successively. The macroscopic Lagrangian in Eq.(2.11) is defined as $\mathrm{L}_{\mathrm{M}}(\mathbf{E},\mathbf{V}) := \int_{\mathrm{Y}}\mathrm{l}_\mu(\boldsymbol{\varepsilon},\mathbf{v})\mathrm{dV_y}$, as explained in the **Appendix A** in the general context of dynamical field theory. Note that time integration by part has been done in the action integral, while we have extracted the temporal density of the Lagrangian to write Eq. (2.11) as explained in full generality in the **Appendix A**. A lower case and upper case notation is adopted here and in the sequel for the densities and their volume integral over the unit cell respectively. The dynamical macroscopic stress tensor $\boldsymbol{\Sigma}^{dyn}$ has been introduced in Eq.(2.11), wherein the last relation has been obtained using Hamilton's principle at the macroscopic level, with spatial integration done over the homogeneous volume element $\mathrm{V}(\mathbf{x})$, see Fig.1.

An extended stationarity principle of the action integral in Eq.(2.3) over all periodic fluctuations holds, with the macroscopic Lagrangian in space-frequency domain associated to the BVP written in Eq.(2.7), due to Parseval theorem (energy value does not depend on its representation – in time or frequency)

$$\mathrm{L}_{\mathrm{M}}(\mathbf{E},\mathbf{V}) = \underset{\tilde{\mathbf{u}},\tilde{\mathbf{v}}\in\mathrm{V_K}}{\mathrm{Min}}\ \frac{1}{2}\left\{\int_{\mathrm{Y}}\mathrm{dV_y}\rho\mathrm{i}\omega\mathbf{v}(\mathbf{y},\omega).\mathrm{i}\omega\mathbf{v}(\mathbf{y},\omega) - \mathbf{C}(\mathbf{y}):\mathbf{u}(\mathbf{y},\omega)\otimes\nabla_{\mathrm{y}}:\mathbf{u}(\mathbf{y},\omega)\otimes\nabla_{\mathrm{y}}\right\} \tag{2.12}$$

As a functional, $L_M(\mathbf{E},\mathbf{V})$ achieves a minimum for the solution of the BVP of Eq.(2.3) over all admissible displacement and velocity fluctuations, so that it holds using the additive decomposition of the displacement and velocity fields from Eq.(2.8) the following expression

$$L_M(\mathbf{E},\mathbf{V}) = \underset{\tilde{\mathbf{u}},\tilde{\mathbf{v}}\in V_K}{\text{Min}} \frac{1}{2}\left\{\begin{array}{l}\int_Y dV_y \rho i\omega\left(\mathbf{V}(\mathbf{x},\omega)+\tilde{\mathbf{v}}(\mathbf{y},\omega)\right).i\omega\left(\mathbf{V}(\mathbf{x},\omega)+\tilde{\mathbf{v}}(\mathbf{y},\omega)\right) - \\ \mathbf{C}(\mathbf{y}):\left(\mathbf{E}(\mathbf{x},\omega)+\tilde{\mathbf{u}}(\mathbf{y},\omega)\otimes\nabla_y\right):\left(\mathbf{E}(\mathbf{x},\omega)+\tilde{\mathbf{u}}(\mathbf{y},\omega)\otimes\nabla_y\right)\end{array}\right\} \tag{2.13}$$

The stationarity condition of the functional on the right-hand side of Eq.(2.13) delivers as a necessary condition a BVP to be satisfied by the optimal fluctuation associated to the real displacement field (in the absence of body forces):

$$\left|\begin{array}{l}\text{div}_y\left\{\mathbf{C}(\mathbf{y}):\left(\mathbf{E}(\mathbf{x},\omega)+\tilde{\mathbf{u}}(\mathbf{y},\omega)\otimes\nabla_y\right)\right\} - i\rho\omega\left(\mathbf{V}(\mathbf{x},\omega)+\tilde{\mathbf{v}}(\mathbf{y},\omega)\right)=\mathbf{0} \\ \tilde{\mathbf{u}}(\mathbf{y},\omega),\tilde{\mathbf{v}}(\mathbf{y},\omega)\ \text{Y-periodic} \\ \left\langle\tilde{\mathbf{u}}(\mathbf{y},\omega)\right\rangle_Y = 0 = \left\langle\tilde{\mathbf{v}}(\mathbf{y},\omega)\right\rangle_Y \\ \tilde{\mathbf{v}}(\mathbf{y},\omega) = i\omega\tilde{\mathbf{u}}(\mathbf{y},\omega) \\ \mathbf{u}(\mathbf{y},0)=\mathbf{0}=\mathbf{v}(\mathbf{y},0)\end{array}\right. \tag{2.14}$$

The last two equations in Eq.(2.14) define the initial conditions for the displacement and velocity fields; note that their spatial averaging $\mathbf{U}(\mathbf{x},t)$, $\mathbf{V}(\mathbf{x},t)$ have to satisfy consistent initial conditions.

Previous BVP rewrites in Laplace space using Eq.(2.14) considering the chosen nil initial conditions as:

$$\left|\begin{array}{l}\text{div}_y\left\{\mathbf{C}(\mathbf{y}):\left(\mathbf{E}(\mathbf{x},\omega)+\tilde{\mathbf{u}}(\mathbf{y},\omega)\otimes\nabla_y\right)\right\} - i\rho\omega\left(\left\langle\mathbf{v}(\omega)\right\rangle_Y+\tilde{\mathbf{v}}(\mathbf{y},\omega)\right)=\mathbf{0} \\ \tilde{\mathbf{u}}(\mathbf{y},\omega)\ \text{Y-periodic},\ \tilde{\mathbf{v}}(\mathbf{y},\omega)=i\omega\tilde{\mathbf{u}}(\mathbf{y},\omega)\end{array}\right. \tag{2.15}$$

The linearity of the solution – the fluctuation $\tilde{\mathbf{u}}(\mathbf{y},\omega)$ - of this BVP versus the prescribed kinematic macroscopic loading, the strain tensor $\mathbf{E}(\mathbf{x},\omega)$ and the average velocity $\mathbf{V}(\mathbf{x},\omega) := \langle\mathbf{v}\rangle_Y$ ensures the existence of four displacement and velocity localizators, respectively the third order tensors $\mathbf{H}^{EE}(\mathbf{y},\omega)$, $\mathbf{H}^{VE}(\mathbf{y},\omega)$, and the second order tensors $\mathbf{H}^{EV}(\mathbf{y},\omega)$, $\mathbf{H}^{VV}(\mathbf{y},\omega)$ - both frequency-dependent - , such that the displacement and velocity fluctuations write

$$\begin{array}{l}\tilde{\mathbf{u}}(\mathbf{y},\omega)=\mathbf{H}^{EE}(\mathbf{y},\omega):\mathbf{E}(\mathbf{x},\omega)+\mathbf{H}^{EV}(\mathbf{y},\omega).\mathbf{V}(\mathbf{x},\omega) \\ \Rightarrow \tilde{\mathbf{v}}(\mathbf{y},\omega)=\mathbf{H}^{VE}(\mathbf{y},\omega):\mathbf{E}(\mathbf{x},\omega)+\mathbf{H}^{VV}(\mathbf{y},\omega).\mathbf{V}(\mathbf{x},\omega)\equiv i\omega\left(\mathbf{H}^{EE}(\mathbf{y},\omega):\mathbf{E}(\mathbf{x},\omega)+\mathbf{H}^{EV}(\mathbf{y},\omega).\mathbf{V}(\mathbf{x},\omega)\right)\end{array} \tag{2.16}$$

Note that the velocity being the time derivative of the displacement, the second relation in (2.16) is a mere consequence of the first one. Observe further that the microscopic fields (displacement, velocity) depend on time through the frequency parameter ω. Thereby, the microscopic displacement becomes the sum of an average displacement evaluated over the unit cell and a fluctuation depending on the average velocity. As all appear later on, this will entail that the effective stress depends on the average velocity. A similar localization was obtained in (Nassar, 2015; Nassar et al., 2016) but using the body force as the driving term for such unusual velocity-

dependent effects appearing in the homogenized constitutive law. Inserting Eq.(2.14) into the unit cell BVP Eq.(2.13) then leads to a BVP in complex space for the strain and average velocity localizators

$$\begin{aligned}&-\mathrm{div}_{\mathrm{y}}\left\{\mathbf{C}(\mathbf{y}):\left(\mathbf{E}+\left\{\mathbf{H}^{\mathrm{EE}}(\mathbf{y},\omega):\mathbf{E}+\mathbf{H}^{\mathrm{EV}}(\mathbf{y},\omega).\mathbf{V}(\mathbf{x},\omega)\right\}\otimes\nabla_{\mathrm{y}}\right)\right\}\\&-\mathrm{i}\rho\omega\left(\mathbf{V}(\mathbf{x},\omega)+\mathbf{H}^{\mathrm{VE}}(\mathbf{y},\omega):\mathbf{E}+\mathbf{H}^{\mathrm{VV}}(\mathbf{y},\omega).\mathbf{V}(\mathbf{x},\omega)\right)=\mathbf{0}\end{aligned}\qquad(2.17)$$

The static localizator $\mathbf{H}^{\mathrm{E}}(\mathbf{y})$ therein is first determined in conditions of a nil imposed strain rate - at zero frequency, clearly corresponding to a static situation - thus it solves the first order unit cell BVP:

$$-\mathrm{div}_{\mathrm{y}}\left\{\mathbf{C}(\mathbf{y}):\left(\mathbf{I}_4+\mathbf{H}^{\mathrm{EE}}(\mathbf{y},\omega)\otimes\nabla_{\mathrm{y}}\right)\right\}=\mathbf{0}\qquad(2.18)$$

In a second step, the velocity localizators $\mathbf{H}^{\mathrm{EV}}(\mathbf{y},\omega),\mathbf{H}^{\mathrm{VE}}(\mathbf{y},\omega),\mathbf{H}^{\mathrm{VV}}(\mathbf{y},\omega)$ are evaluated as the solution of the BVP of Eq.(2.18). It is further convenient to introduce the strain localization operator, the fourth order tensor $\mathbf{A}^{\mathrm{EE}}(\mathbf{y},\omega)$ relating the microscopic strain to the macro strain, given from the displacement localizator by the following relations:

$$\mathbf{A}^{\mathrm{EE}}(\mathbf{y},\omega):=\mathbf{I}_4+\mathbf{H}^{\mathrm{EE}}(\mathbf{y},\omega)\otimes\nabla_{\mathrm{y}}\Rightarrow\boldsymbol{\varepsilon}(\mathbf{y},\omega)=\mathbf{A}^{\mathrm{EE}}(\mathbf{y},\omega):\mathbf{E}(\mathbf{x},\omega)\qquad(2.19)$$

wherein $\mathbf{I}_4$ denotes the fourth order identity tensor. The presence of the displacement and velocity fluctuating terms, the set of fluctuations $\tilde{\mathbf{u}}(\mathbf{y},\omega),\tilde{\mathbf{v}}(\mathbf{y},\omega)$ is descriptive of the influence of microinertia in the dynamical microstructural response, reflected through the kinetic energy contribution $\mathrm{k}_{\mu}\left(\tilde{\mathbf{v}}(\mathbf{y},\omega)\right):=\frac{1}{2}\rho(\mathbf{y})\tilde{\mathbf{v}}(\mathbf{y},\omega).\tilde{\mathbf{v}}(\mathbf{y},\omega)$ of the microscopic Lagrangian density. In contrast to the macroscopic velocity defined in Eq.(2.8), $\mathbf{V}(\mathbf{x},\omega):=\left\langle\mathbf{v}(\omega)\right\rangle_{\mathrm{Y}}$, the microscopic fluctuation $\tilde{\mathbf{v}}(\mathbf{y},\omega):=\mathbf{v}(\mathbf{y},\omega)-\mathbf{V}(\mathbf{x},\omega)$ quantifies the motion of micropoints within the unit cell (see Fig.1) around their center of gravity (moving with the macroscopic velocity), thereby characterizing microinertia effects.

2.2. Homogeneous contribution to the displacement

The local homogeneous displacement field describing a heterogeneous medium that would obey exactly the postulated effective medium is obtained using Hill macrohomogeneity condition: the average Cauchy stress tensor is obtained exploiting Hill dynamical macrohomogeneity condition in Eq.(2.11) and the definition of the microscopic strain energy density as a potential for the microscopic Cauchy stress: using the definition of the effective Cauchy stress and first order momentum obtained in relation Eq.(B30) of the **Appendix B** leads to a set of integral relations for the microscopic velocity and strain tensors versus the macro velocity and strain (note that the time derivative present in Euler operator commutes with spatial integration therein). Solving these equations to express the microscopic velocity and strain fields in terms of the macroscopic fields imposed as frequency-kinematic controls over the unit cell, $\left(\mathbf{E}(\mathbf{x},\omega),\mathbf{V}(\mathbf{x},\omega)\right)$, allows identifying the so-called homogenous part of the microscopic velocity and strain fields:

$$v_i(\mathbf{y},\omega)=V_i(\mathbf{x},\omega)+V_{i,j}(\mathbf{x},\omega)\,y_j+i\omega E_{ij}(\mathbf{x},\omega)\,y_j\qquad(2.20)$$

$$\varepsilon_{ij}(\mathbf{y},\omega)=E_{ij}(\mathbf{x},\omega) \tag{2.21}$$

In the performed derivations, the macroscopic kinematic variables are considered as parameters (since they do not depend on the microscale), thus the partial derivatives in previous equations commute with microscopic volume integration done over the RVE. Note that the wording 'homogeneous' used for the so-called homogeneous solution applies to the macroscale but not to the microscale, since the obtained microscopic kinematics depends on both microscopic and macroscopic spatial variables. Its formulation leads by spatial derivation of the microscopic field to the macroscopic kinematic variables.

The obtained localization relation (2.20) highlights the dependency of the microscopic velocity field to the macro strain tensor. This dependency will induce a homogenized response relating the macrostress and momentum to the macro velocity and strain fields, evaluated in the next section.

2.3. Effective dynamical response of the homogeneous substitution medium

The functional defined on the right-hand side of (2.12) is regular in the macrostrain $\mathbf{E}(\mathbf{x},\omega)$ and average velocity $\mathbf{V}(\mathbf{x},\omega)$ - playing the role of mere parameters in the integrand of bounded nature – thus partial derivative and integration commute, so that exploitation of the effective constitutive law, Eq.(2.11), decomposition of the fluctuation in Eq.(2.8) and permutation of minimization and partial derivative entails the average stress and momentum (the dependency on frequency has been dropped to simplify the notations), noting the minus sign in the definition of the stress tensor:

$$\begin{aligned}
\boldsymbol{\Sigma} &:= -\frac{\partial \mathrm{L_M}(\mathbf{E},\mathbf{V})}{\partial \mathbf{E}} = -\frac{\partial}{\partial \mathbf{E}} \underset{\tilde{\mathbf{u}},\tilde{\mathbf{v}}\in \mathrm{V_K}}{\mathrm{Min}} \frac{1}{2}\left\{ \begin{array}{l} \int\limits_{\mathrm{Y}} \mathrm{dV_y} \rho \mathrm{i}\omega\left(\mathbf{V}+\mathbf{H}^{\mathrm{VE}}:\mathbf{E}+\mathbf{H}^{\mathrm{VV}}.\mathbf{V}\right).\mathrm{i}\omega\left(\mathbf{V}+\mathbf{H}^{\mathrm{VE}}:\mathbf{E}+\mathbf{H}^{\mathrm{VV}}.\mathbf{V}\right)- \\ \mathbf{C}(\mathbf{y}):\left(\mathbf{A}^{\mathrm{E}}:\mathbf{E}\right):\left(\mathbf{A}^{\mathrm{E}}:\mathbf{E}\right) \end{array} \right\} \\
&= -\underset{\tilde{\mathbf{u}},\tilde{\mathbf{v}}\in \mathrm{V_K}}{\mathrm{Min}} \frac{\partial}{\partial \mathbf{E}} \frac{1}{2}\left\{ \begin{array}{l} \int\limits_{\mathrm{Y}} \mathrm{dV_y} \rho \mathrm{i}\omega\left(\mathbf{V}+\mathbf{H}^{\mathrm{VE}}:\mathbf{E}+\mathbf{H}^{\mathrm{VV}}.\mathbf{V}\right).\mathrm{i}\omega\left(\mathbf{V}+\mathbf{H}^{\mathrm{VE}}:\mathbf{E}+\mathbf{H}^{\mathrm{VV}}.\mathbf{V}\right)- \\ \mathbf{C}(\mathbf{y}):\left(\mathbf{A}^{\mathrm{E}}:\mathbf{E}\right):\left(\mathbf{A}^{\mathrm{E}}:\mathbf{E}\right) \end{array} \right\} \\
&= -\int\limits_{\mathrm{Y}} \left\{ \rho \mathrm{i}\omega\left(\mathbf{V}+\mathbf{H}^{\mathrm{VE}}:\mathbf{E}+\mathbf{H}^{\mathrm{VV}}.\mathbf{V}\right).\left(\mathbf{H}^{\mathrm{VE}}:\mathbf{I}_4\right)-\left(\mathbf{A}^{\mathrm{E}}\right)^{\mathrm{T}}:\mathbf{C}:\mathbf{A}^{\mathrm{E}}:\mathbf{E} \right\} \mathrm{dV_y} = \\
&\left\{-\left(\mathbf{A}^{\mathrm{E}}\right)^{\mathrm{T}}:\mathbf{C}:\mathbf{A}^{\mathrm{E}}+\rho\mathbf{H}^{\mathrm{VE}}.\left(\mathbf{H}^{\mathrm{VE}}:\mathbf{I}_4\right)^{\mathrm{T}}\right\}:\mathbf{E}+\rho\left\{\left(\mathbf{I}_2+\mathbf{H}^{\mathrm{VV}}\right).\left(\mathbf{H}^{\mathrm{VE}}:\mathbf{I}_4\right)^{\mathrm{T}}\right\}.\mathbf{V},
\end{aligned} \tag{2.22}$$

$$\begin{aligned}
\mathbf{P} &:= \frac{\partial \mathrm{L_M}(\mathbf{E},\mathbf{V})}{\partial \mathbf{V}} = \frac{\partial}{\partial \mathbf{V}} \underset{\tilde{\mathbf{u}},\tilde{\mathbf{v}}\in \mathrm{V_K}}{\mathrm{Min}} \frac{1}{2}\left\{ \begin{array}{l} \int\limits_{\mathrm{Y}} \mathrm{dV_y} \mathrm{i}\omega\rho\left(\mathbf{V}+\mathbf{H}^{\mathrm{VE}}:\mathbf{E}+\mathbf{H}^{\mathrm{VV}}.\mathbf{V}\right).\mathrm{i}\omega\left(\mathbf{V}+\mathbf{H}^{\mathrm{VE}}:\mathbf{E}+\mathbf{H}^{\mathrm{VV}}.\mathbf{V}\right)- \\ \mathbf{C}:\left(\mathbf{A}^{\mathrm{E}}:\mathbf{E}\right):\left(\mathbf{A}^{\mathrm{E}}:\mathbf{E}\right) \end{array} \right\} = \\
&= \underset{\tilde{\mathbf{u}},\tilde{\mathbf{v}}\in \mathrm{V_K}}{\mathrm{Min}} \frac{\partial}{\partial \mathbf{V}} \frac{1}{2}\left\{ \begin{array}{l} \int\limits_{\mathrm{Y}} \mathrm{dV_y} \mathrm{i}\omega\rho\left(\mathbf{V}+\mathbf{H}^{\mathrm{VE}}:\mathbf{E}+\mathbf{H}^{\mathrm{VV}}.\mathbf{V}\right).\mathrm{i}\omega\left(\mathbf{V}+\mathbf{H}^{\mathrm{VE}}:\mathbf{E}+\mathbf{H}^{\mathrm{VV}}.\mathbf{V}\right)- \\ \mathbf{C}:\left(\mathbf{A}^{\mathrm{E}}:\mathbf{E}\right):\left(\mathbf{A}^{\mathrm{E}}:\mathbf{E}\right) \end{array} \right\} \\
&= \int\limits_{\mathrm{Y}} \mathrm{dV_y} \rho\omega^2\left(\mathbf{V}+\mathbf{H}^{\mathrm{VE}}:\mathbf{E}+\mathbf{H}^{\mathrm{VV}}.\mathbf{V}\right).\left(\mathbf{I}_2+\mathbf{H}^{\mathrm{VV}}\right) \\
&= \left\{\int\limits_{\mathrm{Y}} \mathrm{dV_y} \rho\omega^2\left(\mathbf{I}_2+\mathbf{H}^{\mathrm{VV}}\right)^{\mathrm{T}}.\mathbf{H}^{\mathrm{VE}}\right\}:\mathbf{E}+\left\{\int\limits_{\mathrm{V_y}} \mathrm{dV_y} \rho\omega^2\left(\mathbf{I}_2+\mathbf{H}^{\mathrm{VV}}\right).\left(\mathbf{I}_2+\mathbf{H}^{\mathrm{VV}}\right)^{\mathrm{T}}\right\}.\mathbf{V}
\end{aligned} \tag{2.23}$$

Since the macroscopic strain and velocity play the mere role as parameters appearing within the integrands of previous expressions (2.22) and (2.23), minimization and derivation can be switched, so that the integrals in these equations are written for the optimal fluctuations, and partial derivatives is taken for the achieved optimal macroscopic Lagrangian.

Note that the averaged strain and velocity are not independent since it holds the relation

$$\mathrm{i}\omega\left\langle\boldsymbol{\varepsilon}\right\rangle_{\mathrm{Y}}=\mathrm{i}\omega\left(\left\langle\mathrm{grad}_{\mathrm{y}}\otimes^{\mathrm{S}}\mathbf{u}\right\rangle_{\mathrm{Y}}+\mathrm{i}\mathbf{k}\otimes^{\mathrm{S}}\left\langle\mathbf{u}\right\rangle_{\mathrm{Y}}\right)=\mathrm{i}\mathbf{k}\otimes^{\mathrm{S}}\left\langle\mathbf{v}\right\rangle_{\mathrm{Y}} \tag{2.24}$$

The term $\mathrm{i}\mathbf{k}\otimes^{\mathrm{S}}$ in previous equation is the Fourier counterpart of the (symmetrized) spatial gradient in physical space. In Eq.(2.20), we have used the periodicity condition of the microstrain, so that $\left\langle\mathrm{grad}_{\mathrm{y}}\otimes^{\mathrm{S}}\mathbf{u}\right\rangle_{\mathrm{Y}}=\mathbf{0}$. One way to keep the independency of the variables $\left\langle\boldsymbol{\varepsilon}\right\rangle_{\mathrm{Y}},\left\langle\mathbf{v}\right\rangle_{\mathrm{Y}}$ is by recoursing to an eigenstrain $\boldsymbol{\gamma}$ as in (Nassar et al., 2015, 2016), so that the microscopic constitutive law writes

$$\boldsymbol{\sigma}=\mathbf{C}:\left(\boldsymbol{\varepsilon}-\boldsymbol{\gamma}\right) \tag{2.25}$$

One can conveniently redefine the average strain such that $\boldsymbol{\gamma}$ is incorporated, viz.

$$\mathbf{E}:=\left\langle\left(\boldsymbol{\varepsilon}-\boldsymbol{\gamma}\right)\right\rangle_{\mathrm{Y}} \tag{2.26}$$

Previous expressions of the average stress and momentum allows identifying the effective dynamical tensors in the matrix format of the effective constitutive law:

$$\begin{aligned}&\begin{pmatrix}\boldsymbol{\Sigma}\\ \mathbf{P}\end{pmatrix}=\begin{pmatrix}\mathbf{C}^{\Sigma\Sigma}\left(\omega\right) & \mathbf{S}^{\Sigma\mathrm{P}}\left(\omega\right)\\ \mathbf{S}^{\mathrm{P}\Sigma}\left(\omega\right) & \boldsymbol{\rho}^{\mathrm{H}}\left(\omega\right)\end{pmatrix}.\begin{pmatrix}\mathbf{E}\left(\omega\right)\\ \mathbf{V}\left(\omega\right)\end{pmatrix},\\ &\mathbf{V}\left(\mathbf{x},\omega\right):=\left\langle\mathbf{v}\left(\omega\right)\right\rangle_{\mathrm{Y}}=\mathrm{i}\omega\mathbf{E}\left(\mathbf{x};\omega\right)\cdot\mathbf{x}\end{aligned} \tag{2.27}$$

with effective moduli expressing as the following unit cell averaging:

$$\left|\begin{aligned}&\mathbf{C}^{\Sigma\Sigma}\left(\mathrm{k},\omega\right)=\left\langle\left(\mathbf{A}^{\mathrm{E}}\right)^{\mathrm{T}}:\mathbf{C}:\mathbf{A}^{\mathrm{E}}-\rho\omega^{2}\mathbf{H}^{\mathrm{VE}}.\left(\mathbf{H}^{\mathrm{VE}}:\mathbf{I}_{4}\right)^{\mathrm{T}}\right\rangle_{\mathrm{Y}}\equiv-\omega^{2}\left\langle\rho\mathbf{H}^{\mathrm{VE}}:\mathbf{H}^{\mathrm{VE}}+\rho\mathbf{H}^{\mathrm{VE}}.\left(\mathbf{H}^{\mathrm{VE}}\right)^{\mathrm{T}}\right\rangle_{\mathrm{Y}}\\ &\mathbf{S}^{\Sigma\mathrm{P}}\left(\mathrm{k},\omega\right)=\omega^{2}\left\langle\rho\left(\mathbf{I}_{2}+\mathbf{H}^{\mathrm{VV}}\right).\left(\mathbf{H}^{\mathrm{VE}}:\mathbf{I}_{4}\right)^{\mathrm{T}}\right\rangle_{\mathrm{Y}}\equiv-\omega^{2}\left\langle\rho\left(\mathbf{I}_{2}+\mathbf{H}^{\mathrm{VV}}\right).\left(\mathbf{H}^{\mathrm{VE}}\right)^{\mathrm{T}}\right\rangle_{\mathrm{Y}}\\ &\mathbf{S}^{\mathrm{P}\Sigma}\left(\mathrm{k},\omega\right)=\omega^{2}\left\langle-\rho\left(\mathbf{I}_{2}+\mathbf{H}^{\mathrm{VV}}\right)^{\mathrm{T}}.\mathbf{H}^{\mathrm{VE}}\right\rangle_{\mathrm{Y}}\\ &\boldsymbol{\rho}^{\mathrm{H}}\left(\mathrm{k},\omega\right)=-\left\langle\rho\omega^{2}\left(\mathbf{I}_{2}+\mathbf{H}^{\mathrm{VV}}\right).\left(\mathbf{I}_{2}+\mathbf{H}^{\mathrm{VV}}\right)^{\mathrm{T}}\right\rangle_{\mathrm{Y}}\equiv-\omega^{2}\left\langle\rho\right\rangle_{\mathrm{Y}}\mathbf{I}_{2}-\omega^{2}\left\langle\rho\mathbf{H}^{\mathrm{VV}}+\rho\left(\mathbf{H}^{\mathrm{VV}}\right)^{\mathrm{T}}-\rho\mathbf{H}^{\mathrm{VV}}.\left(\mathbf{H}^{\mathrm{VV}}\right)^{\mathrm{T}}\right\rangle_{\mathrm{Y}}\end{aligned}\right. \tag{2.28}$$

All effective moduli in Eq.(2.28) are frequency and wavelength-dependent through the frequency-dependent localization operators therein. Observe that the mass matrix $\boldsymbol{\rho}^{\mathrm{H}}\left(\mathrm{k},\omega\right)$, a second order tensor, is no more isotropic after averaging, as it is the sum of an isotropic contribution (supported by the average density, with $\mathbf{I}_{2}$ denoting the second order identity tensor) and an anisotropic term traducing the dynamic anisotropy of the effective medium. The coupling tensors $\mathbf{S}^{\Sigma\mathrm{P}},\mathbf{S}^{\mathrm{P}\Sigma}$ in Eq.(2.28) have the meaning that a strain generates a momentum and conversely the average velocity generates a stress. It is straightforward to check that the

dynamical effective stiffness tensor in Eq.(2.28) is symmetrical, a consequence of the existence of an energy density (the Hamiltonian) at the macroscopic level.

When the effective constitutive law is mapped back to the real domain using the inverse Fourier transform - the inverse of a product becomes a convolution integral -, it gives rise to a hereditary type response as to the time component (the spatial part of the response remains local according to our modeling framework), viz. it holds that the stress and momentum are given by the following convolution integrals (integration is done over the real set R representing the time axis):

$$\begin{aligned}\boldsymbol{\Sigma}(\mathbf{x},t) &= \int_R \mathbf{C}^{\Sigma\Sigma}(\mathbf{x},t-t') : \mathbf{E}(\mathbf{x},t-t') + \mathbf{S}^{\Sigma P}(\mathbf{x},t-t').\mathbf{V}(t')\,dt' \\ \mathbf{P}(\mathbf{x},t) &= \int_R \mathbf{S}^{P\Sigma}(\mathbf{x},t-t') : \mathbf{E}(\mathbf{x},t-t') + \boldsymbol{\rho}^{H}(\mathbf{x},t-t').\mathbf{V}(t')\,dt'\end{aligned} \tag{2.29}$$

Since the effective response of the dynamical Cauchy continuum is limited to small frequencies, one may further take a time Taylor series expansion of the nonlocal kernels in Eq.(2.29), functions $\mathbf{C}^{\Sigma\Sigma}(\mathbf{x},t-t'),\mathbf{S}^{\Sigma P}(\mathbf{x},t-t'),\mathbf{S}^{P\Sigma}(\mathbf{x},t-t'),\boldsymbol{\rho}^{H}(\mathbf{x},t-t')$, to identify their characteristic internal times, reflecting the dynamical characteristic times of the underlying microstructure. Thereby, we advocate an alternative to the enrichment of the Cauchy effective continuum by additional DOFs, considering instead a spatially local behavior but a nonlocal in time response.

A few words related to the comparison of the obtained nonlocal in time dynamical formulation are in order. Auriault and Bonnet (1985) study the dynamical response of periodic composites using asymptotic homogenization; the impact on the dynamical response of strong discontinuities of the properties of composite constituents is analyzed, considering a scaling of the ratio of the two-phase moduli versus the small-scale parameter of the asymptotic method. The obtained macroscopic response is that of a homogeneous effective material with a tensor-valued frequency-dependent density. The classical quasi-static formulation is recovered in the limit of vanishing frequencies, with a scalar-valued effective density. This result is similar to our dynamical Cauchy effective model developed in this section, since the mass matrix $\boldsymbol{\rho}^{H}(k,\omega)$, a second order tensor, is no more isotropic at high frequencies after averaging, as shown in Eq.(2.28), including an anisotropic term traducing the dynamic anisotropy of the effective medium. The dynamical response obtained in Auriault and Bonnet (1985) for constituents having a strong contrast of properties has a long memory described by a convolution integral, as in the nonlocal in time response obtained in Eq.(2.28), having the form of a time convolution integral. These authors obtain for the specific case of stratified materials an analytical solution of the dynamical response. Rohan et al. (2009) analyze the dispersion of acoustic waves in elastic composites for soft inclusions embedded into a stiffer matrix using asymptotic homogenization. The obtained limit homogenized model exhibits band gaps due to the chosen scaling of the microscopic elastic properties of ellipsoidal shaped inclusions versus the small-scale parameter. The authors introduce the notions of weak and strong band gaps depending on the sign of the eigenvalues of the mass tensor. As shown later on in this contribution, the nonlocal in space and time formulation to be developed also exhibits band gaps, in line with those works. The elastodynamic response of composite materials showing a high contrast of properties is analyzed in Smyshlaev (2009); both situations of isolating and inter-connected inclusions is analyzed, showing in the last situation that the number of propagating modes is dependent on the direction of wave propagation. The homogenized dynamical behavior also shows in this last work nonlocal temporal effect, which may further extend to a spatial nonlocality for mutually

connected inclusions like fibers.

The obtained nonlocal response of the effective continuum is in line with physical situations in which Cauchy medium is dispersive, like in conditions of a macroscopically inhomogeneous behavior or a finite dimension of the support of wave propagation, for instance for plates or rods having a varying cross-section. Such a nonlocal in time constitutive model may be adequate to model optical branches, as underlined in (Rosi and Auffray, 2016). Note that truncating the time-dependency of previous kernels to the first order leads to the two time scale models developed e.g. in (Fish and Chen, 2001; Chen and Fish, 2000).

As a final step, the dynamical hyperbolic PDE's of motion are recovered at the macroscopic level and in the time domain, using Maxwell-Betti reciprocity relations (the constitutive tensors enjoy index symmetry properties) and the mean field Lagrangian

$$\begin{aligned} &\mathrm{L_M}\left(\mathbf{V},\mathbf{E}\right)=\frac{1}{2}\left(\mathbf{P}.\mathbf{V}-\boldsymbol{\Sigma}:\mathbf{E}\right)\Rightarrow \mathrm{S}:=\int_t\int_{\mathrm{V_y}}\mathrm{L_M}\left(\mathbf{V},\mathbf{E}\right)\mathrm{dtdV_y}: \\ &\delta\mathrm{S}=0: \quad -\frac{\mathrm{d}}{\mathrm{dt}}\left(\frac{\partial \mathrm{L_M}\left(\mathbf{V},\mathbf{E}\right)}{\partial\mathbf{V}}\right)-\mathrm{div_x}\left(\frac{\partial \mathrm{L_M}\left(\mathbf{V},\mathbf{E}\right)}{\partial\mathbf{E}}\right)=\mathbf{0}\Rightarrow\frac{\mathrm{d}\mathbf{P}}{\mathrm{dt}}+\mathrm{div_x}\boldsymbol{\Sigma}=\mathbf{0} \end{aligned} \tag{2.30}$$

Since the spatial enrichment must pair the time enrichment of the effective dynamical response for the dynamical model to be consistent, we consider as an extension of previous dynamical model a strain gradient in space and nonlocal in time effective model that we establish based on dynamical homogenization.

3. Strain gradient dynamical homogenization

Homogenized models based on classical Cauchy-type elasticity theory are not able to provide realistic predictions of many effects arising from small scale, amongst of them wave dispersion. Classical theories based upon the sole first order displacement gradient lack indeed internal length parameters, characteristic of the underlying microstructure. This explains the success of gradient-enriched theories in capturing microstructural effect on the macroscopic behavior of materials, by including high-order gradients associated to internal lengths representative of the microstructure. Many theories based on an enrichment of the classical elasticity framework by higher order gradients have been proposed in the past to overcome deficiencies of classical elasticity (Aifantis, 1992, 1999; Askes and Aifantis, 2009) theories in describing both static and dynamic phenomena, including size effects, and wave dispersion in dynamics. Since the early works in the 1960s by (Toupin, 1962; Koiter, 1964; Mindlin, 1964, 1965), there has been an abundant literature devoted to the topic.

We subsequently aim to describe the dynamical behavior of heterogeneous materials close to the origin of the dispersion diagram, but extending the range of validity of the previous formulation to wavelengths that become comparable to the unit cell size, thus to larger wavelengths than those strictly allowed by the Cauchy effective medium. Moreover, the subsequent developed nonlocal in time (but local in space) strain gradient dynamical formulation aims to describes the dynamics at medium and high frequencies, thereby extending the range of validity of the low frequency – low wavelengths purely local strain gradient models.

As for the Cauchy dynamical formulation of previous section, we will perform the Laplace transform of the time-dependent BVP to formulate a BVP in space-frequency domain.

3.1. Averaging relations and extended dynamical Hill macrohomogeneity condition

We extend the elaboration of the microscopic displacement and velocity fields given in Eq.(2.8) by the consideration of a higher order kinematics at the unit cell level, that will intervene in the linkage between the micro-displacement and velocity fields and their macroscopic counterparts. Similar to Cauchy dynamical homogenization (section 2), the micro-displacement and velocity fields are decomposed into homogeneous and fluctuating parts as in Eq.(2.8), with the homogeneous contribution expressed versus the macroscopic velocity vector, strain and strain gradient tensors. The determination of this relation will be done in subsection 3.5.

We extend the elaboration of the microscopic displacement and velocity fields given in Eq.(2.8) to the consideration of a higher order kinematics at the unit cell level, viz. using the frequency-representation of the fields:

$$\left|\begin{array}{l}\mathbf{u}(\mathbf{y},\omega)=\mathbf{U}(\mathbf{x},\omega)+\tilde{\mathbf{u}}(\mathbf{y},\omega),\\ \mathbf{u}^{\hom}(\mathbf{y},\omega)=\mathbf{E}\left(\mathbf{x},\omega\right)\cdot\mathbf{y}+\frac{1}{2}\mathbf{K}\left(\mathbf{x},\omega\right):\left(\mathbf{y}\otimes\mathbf{y}\right)\\ \left\langle\tilde{\mathbf{u}}\right\rangle_{\mathrm{Y}}=0\Rightarrow\mathbf{U}(\mathbf{x},\omega):=\left\langle\mathbf{u}\right\rangle_{\mathrm{Y}}(\mathbf{x},\omega)=\mathbf{E}\left(\mathbf{x},\omega\right)\cdot\mathbf{x}+\mathbf{K}\left(\mathbf{x},\omega\right):\mathbf{G}_2\\ \mathbf{u}(\mathbf{y},\omega)\otimes\nabla_{\mathrm{y}}=\mathbf{E}\left(\mathbf{x},\mathrm{t}\right)+\mathbf{K}\left(\mathbf{x},\omega\right).\mathbf{y}\Rightarrow\left\langle\mathbf{u}(\mathbf{y},\omega)\otimes\nabla_{\mathrm{y}}\right\rangle_{\mathrm{Y}}=\mathbf{E}\left(\mathbf{x},\omega\right)+\mathbf{K}\left(\mathbf{x},\omega\right).\mathbf{x}\end{array}\right. \tag{3.1}$$

with $\mathbf{K}\left(\mathbf{x},\omega\right):=\left(\mathbf{U}\left(\mathbf{x},\omega\right)\otimes^{\mathrm{S}}\nabla_{\mathrm{x}}\right)\otimes\nabla_{\mathrm{x}}$ the frequency-dependent strain gradient tensor and $\mathbf{G}_2:=\int_{\mathrm{Y}}\left(\mathbf{y}\otimes\mathbf{y}\right)\mathrm{dV}_{\mathrm{y}}$ - arising by taking the unit cell spatial averaging - the quadratic moment of inertia tensor. Set of relations (3.1) entail the following additive decomposition of the microscopic velocity as the sum of its average and a periodic fluctuation:

$$\left|\begin{array}{l}\mathbf{v}(\mathbf{y},\omega)=\mathbf{V}(\mathbf{x},\mathrm{t})+\tilde{\mathbf{v}}(\mathbf{y},\omega)\\ \left\langle\tilde{\mathbf{v}}\right\rangle_{\mathrm{Y}}=0\Rightarrow\mathbf{V}(\mathbf{x},\omega):=\left\langle\mathbf{v}\right\rangle_{\mathrm{Y}}(\mathbf{x},\omega)=\dot{\mathbf{E}}\left(\mathbf{x},\omega\right)\cdot\mathbf{x}+\dot{\mathbf{K}}\left(\mathbf{x},\omega\right):\mathbf{G}_2,\end{array}\right. \tag{3.2}$$

The effective Hamiltonian of the strain gradient dynamical continuum is the sum of the internal deformation energy and the kinetic energy, itself based on the momentum (vector) and the hypermomentum tensor $\mathbf{Q}$ (a second order tensor), respectively conjugated to the velocity and velocity gradient. The internal energy involves Cauchy stress and the hyperstress tensor as work conjugate to the strain $\mathbf{E}(\mathbf{x},\omega)$ and strain gradient tensor $\mathbf{K}(\mathbf{x},\omega):=\mathbf{E}(\mathbf{x},\omega)\otimes\nabla_{\mathrm{x}}$ respectively, so that the effective Lagrangian writes (omitting the dependency upon frequency and spatial position), see the derivations in **Appendix B**:

$$\mathrm{L}_{\mathrm{M}}\left(\mathbf{E},\mathbf{K},\mathbf{V},\mathbf{V}\otimes\nabla_{\mathrm{x}}\right)=\frac{1}{2}\left(\mathbf{P}.\mathbf{V}+\mathbf{Q}:\left(\mathbf{V}\otimes\nabla_{\mathrm{x}}\right)-\boldsymbol{\Sigma}^{\mathrm{stat}}:\mathbf{E}-\mathbf{S}^{\mathrm{stat}}\therefore\mathbf{K}-\boldsymbol{\Sigma}^{\mathrm{dyn}}:\dot{\mathbf{E}}-\mathbf{S}^{\mathrm{dyn}}\therefore\dot{\mathbf{K}}\right)\equiv\mathrm{L}_{\mathrm{M}}\left(\mathbf{x},\omega\right)$$

(3.3)

A Lagrangian is obtained in the space-frequency domain (last relation) when all the fields are made frequency-dependent. Thereby, the dynamical macrohomogeneity condition sets an identity of the macroscopic Lagrangian density of the effective continuum to the average of the corresponding microscopic Lagrangian density, here extended to the consideration of strain gradient and hypermomentum contributions:

$$\left\langle \mathrm{l}_{\mu}\left(\boldsymbol{\varepsilon},\mathbf{v}\right)\right\rangle_{\mathrm{Y}}=\frac{1}{2}\left(\mathbf{P}.\mathbf{V}+\mathbf{Q}:\left(\mathbf{V}\otimes\nabla_{\mathrm{x}}\right)-\boldsymbol{\Sigma}:\mathbf{E}-\mathbf{S}\therefore\mathbf{K}\right) \tag{3.4}$$

The gradient velocity tensor $\mathbf{V}\otimes\nabla_{\mathrm{x}}$ therein describes macroinertia contributions to the dynamics. The strain gradient contribution proves relevant when the strict scale separation does no more hold; the same holds in the time domain, so when the frequency of the loading is no more negligible compared to the unit cell frequency, microinertia contributions are expected, as well as space-time couplings, both appearing in the homogenized dynamical constitutive law.

When writing Eqs.(3.3) and (3.4), Hill dynamical macrohomogeneity condition established in the **Appendix B** expressed in the form of relation (B31) has been used, wherein the macroscopic Lagrangian has been constructed by upscaling the microscopic one. It states the identity of the spatial average of the microscopic Lagrangian (the energy) and the macroscopic Lagrangian:

$$\begin{aligned}
&\left\langle l_{\mu}\left(\boldsymbol{\varepsilon},\mathbf{p}\right)\right\rangle_{Y}:=\frac{1}{2}\left\langle \rho\dot{\mathbf{u}}.\dot{\mathbf{u}}-\boldsymbol{\sigma}:\mathbf{u}\otimes\nabla_{y}\right\rangle_{Y}=\frac{1}{2}\mathbf{P}.\mathbf{V}-\frac{1}{2}\boldsymbol{\Sigma}^{dyn}:\mathbf{E}-\frac{1}{2}\mathbf{S}^{dyn}\therefore\mathbf{K}=:L_{M}\left(\mathbf{E},\mathbf{K},\mathbf{V},\mathbf{V}\otimes^{S}\nabla_{x},\left(\mathbf{V}\otimes^{S}\nabla_{x}\otimes\nabla_{x}\right)\right)\\
&\mathbf{P}:=\left\langle \rho\dot{\mathbf{u}}\right\rangle_{Y},\ \mathbf{Q}:=\left\langle \rho\dot{\mathbf{u}}\otimes\mathbf{y}\right\rangle_{Y},\\
&\mathbf{E}:=\left\langle \mathbf{U}\otimes\nabla_{y}\right\rangle_{Y},\ \mathbf{K}:=\left\langle \mathbf{U}\otimes^{S}\nabla_{y}\right\rangle_{Y}\otimes\nabla_{x}\\
&\boldsymbol{\Sigma}^{dyn}:=\left\langle \boldsymbol{\sigma}\right\rangle_{Y}+\left\langle \rho\ddot{\mathbf{u}}\otimes\mathbf{y}\right\rangle_{Y},\ \mathbf{S}^{dyn}:=\left\langle \boldsymbol{\sigma}\otimes\boldsymbol{\xi}\right\rangle_{Y}+\frac{1}{2}\left\langle \rho\dot{\mathbf{u}}\otimes\mathbf{y}\otimes\mathbf{y}\right\rangle_{Y}
\end{aligned} \tag{3.5}$$

Note that integration by part in time has been done at both micro and macro levels. A similar Hill dynamical macrohomogeneity condition has been further written relating the microscopic and effective (macroscopic) Lagrangian functions, Eqs.(B29) and (B30).

The dynamical stress and hyperstress tensors, $\boldsymbol{\Sigma}^{dyn},\mathbf{S}^{dyn}$ have been expressed in Eq.(3.5), their elaboration provided in **Appendix B**. It holds moreover the kinematic relations

$$\begin{aligned}
&\mathbf{K}\left(\mathbf{x},\omega\right):=\mathbf{E}\left(\mathbf{x},\omega\right)\otimes\nabla_{\mathrm{x}}\\
&\mathbf{E}\left(\mathbf{x},\omega\right)=\mathbf{U}(\mathbf{x},\omega)\otimes^{\mathrm{S}}\nabla_{\mathrm{x}}\ \wedge\ \mathbf{V}(\mathbf{x},\omega)=\mathrm{i}\omega\mathbf{U}(\mathbf{x},\omega)\Rightarrow\mathrm{i}\omega\mathbf{E}\left(\mathbf{x},\omega\right)=\mathbf{V}(\mathbf{x},\omega)\otimes^{\mathrm{S}}\nabla_{\mathrm{x}}\\
&\Rightarrow\mathrm{i}\omega\mathbf{K}\left(\mathbf{x},\omega\right):=\mathrm{i}\omega\mathbf{E}\left(\mathbf{x},\omega\right)\otimes\nabla_{\mathrm{x}}\equiv\left(\mathbf{V}(\mathbf{x},\omega)\otimes^{\mathrm{S}}\nabla_{\mathrm{x}}\right)\otimes\nabla_{\mathrm{x}}
\end{aligned} \tag{3.6}$$

showing that the mean velocity is not independent from the first and second velocity gradients; such a kinematic constraints will be incorporated into the Lagrangian in the next subsection as an additional term involving a Lagrange multiplier.

3.2. Homogeneous contribution to the microscopic displacement and velocity fields

The local homogeneous displacement field describing a heterogeneous medium that would obey exactly the postulated effective medium is obtained using Hill macrohomogeneity condition: the average Cauchy stress and hyperstress tensors are obtained exploiting Eq.(3.5) and the definition of the microscopic strain energy density as a potential for the microscopic Cauchy stress: in a first step and for the first gradient part of the dynamical constitutive law, using the definition of the effective Cauchy stress and first order momentum obtained in relation (B30) of the **Appendix B** leads to a set of integral relations for the microscopic velocity and strain tensors versus the macro velocity and strain associated to the Cauchy part of the macroscopic response (note that the time derivative present in Euler operator commutes with spatial integration therein). Similarly, for the higher gradient part of the dynamical constitutive laws, using the definition of the macroscopic hyperstress and hypermomentum obtained in relation (B31) of the **Appendix B** in conjunction with the extended dynamical Hill macrohomogeneity condition leads

to a system of integral relations for the microscopic velocity and strain. Solving these equations to express the microscopic velocity and strain fields in terms of the macro-fields imposed as frequency-kinematic controls over the unit cell, $(\mathbf{E},\mathbf{K},\mathbf{V})(\mathbf{x},\omega)$ allows identifying the so-called homogenous part of the microscopic velocity and strain fields, **as detailed in the Appendix C**:

$$v_i(\mathbf{y},\omega) = V_i(\mathbf{x},\omega) + V_{i,j}(\mathbf{x},\omega)\, y_j + i\omega E_{ij}(\mathbf{x},\omega)\, y_j + i\omega K_{ijk}(\mathbf{x},\omega)\, y_j y_k \tag{3.7}$$

$$\varepsilon_{ij}(\mathbf{y},\omega) = E_{ij}(\mathbf{x},\omega) + \mathrm{K}_{ijk}(\mathbf{x},\omega)\, \mathrm{y}_k \tag{3.8}$$

In the performed derivations, the macroscopic kinematic variables are considered as parameters (since they do not depend on the microscale), thus the partial derivatives in previous equations commute with microscopic volume integration done over the RVE. The localization relation (3.7) highlights the dependency of the microscopic velocity field to the macro strain and strain gradient tensors.

Similar computations leading to the expression of the microscopic homogeneous displacement versus the macroscopic strain and strain gradient tensor have been done for the static situation in (Ganghoffer and Reda, 2021).

Straightforward computations then lead to the final expression of the homogeneous in space macroscopic velocity field as the average of the microscopic velocity field, considering its expression successively in the time and frequency domains:

$$\begin{aligned} &\mathbf{V}(\mathbf{x},\mathrm{t}) := \langle \mathbf{v} \rangle_{\mathrm{Y}} = \dot{\mathbf{E}}(\mathbf{x},\mathrm{t}) \cdot \mathbf{x} + \dot{\mathbf{K}}(\mathbf{x},\mathrm{t}) : \mathbf{G}_2 \\ &\Rightarrow \mathbf{V}(\mathbf{x},\omega) = \left(\mathbf{V}(\mathbf{x},\omega) \otimes^{\mathrm{S}} \nabla_{\mathrm{x}}\right) \cdot \mathbf{x} + \left(\mathbf{V}(\mathbf{x},\omega) \otimes^{\mathrm{S}} \nabla_{\mathrm{x}} \otimes \nabla_{\mathrm{x}}\right) : \mathbf{G}_2 = \mathrm{i}\omega \mathbf{E}(\mathbf{x},\omega) \cdot \mathbf{x} + \mathrm{i}\omega \mathbf{K}(\mathbf{x},\omega) : \mathbf{G}_2 \end{aligned} \tag{3.9}$$

recalling that $\mathbf{G}_2$ is the moment of inertia tensor within the unit cell.

3.3. Homogenized dynamical strain gradient constitutive law

An extended minimization principle over all Y-periodic kinematic fluctuations holds, so that one can write using the effective Lagrangian at macroscopic level and in Fourier domain, incorporating therein the kinematic relation between the macro velocity and its first and second spatial gradients obtained in Eq.(3.6):

$$\begin{aligned} &\mathrm{L_M}\left(\mathbf{E},\mathbf{K},\mathbf{V},\mathbf{V} \otimes^{\mathrm{S}} \nabla_{\mathrm{x}}, \left(\mathbf{V} \otimes^{\mathrm{S}} \nabla_{\mathrm{x}} \otimes \nabla_{\mathrm{x}}\right), \mathbf{\Lambda}\right) = \\ &\underset{\tilde{\mathbf{u}},\tilde{\mathbf{v}} \in \mathrm{K}}{\mathrm{Min}} \frac{1}{2} \left\{ \begin{array}{l} \int_{\mathrm{Y}} \mathrm{d}V_{\mathrm{y}} \rho \left(\mathbf{V}(\mathbf{x},\omega) + \tilde{\mathbf{v}}(\mathbf{y},\omega)\right).\left(\mathbf{V}(\mathbf{x},\omega) + \tilde{\mathbf{v}}(\mathbf{y},\omega)\right) - \\ \left(\mathbf{E}((\mathbf{x},\omega)) + \mathbf{K}(\mathbf{x},\omega).\mathbf{x} + \tilde{\mathbf{u}}(\mathbf{y},\omega) \otimes \nabla_{\mathrm{y}}\right) : \mathbf{C}(\mathbf{y}) : \left(\mathbf{E}(\mathbf{x},\omega) + \mathbf{K}(\mathbf{x},\omega).\mathbf{x} + \tilde{\mathbf{u}}(\mathbf{y},\omega) \otimes \nabla_{\mathrm{y}}\right) + \\ \frac{\mathbf{\Lambda}}{|\mathrm{Y}|}.\left(\mathbf{V}(\mathbf{x},\omega) - \left(\mathbf{V}(\mathbf{x},\omega) \otimes^{\mathrm{S}} \nabla_{\mathrm{x}}\right) \cdot \mathbf{x} - \left(\mathbf{V}(\mathbf{x},\omega) \otimes^{\mathrm{S}} \nabla_{\mathrm{x}} \otimes \nabla_{\mathrm{x}}\right) : \mathbf{G}_2\right) \end{array} \right\} \end{aligned} \tag{3.10}$$

The stationarity condition of the action functional built from the Lagrangian of Eq.(3.10) is done at fixed frequency (considered as a parameter) with respect to the fluctuations; it delivers as a necessary condition a BVP to be satisfied by the optimal fluctuation $\tilde{\mathbf{u}}(\mathbf{y},\omega), \tilde{\mathbf{v}}(\mathbf{y},\omega)$ associated to the real displacement field (in the absence of body forces):

$$
\left|\begin{array}{l}
\mathrm{div}_{\mathrm{y}}\left\{\mathbf{C}(\mathbf{y}):\left(\mathbf{E}(\mathbf{x},\omega)+\mathbf{K}(\mathbf{x},\omega).\mathbf{x}+\tilde{\mathbf{u}}(\mathbf{y},\mathrm{t})\otimes\nabla_{\mathrm{y}}\right)\right\}-\mathrm{i}\rho\omega\left(\mathbf{V}(\mathbf{x},\omega)+\tilde{\mathbf{v}}(\mathbf{y},\omega)\right)=\mathbf{0} \\
\mathbf{V}(\mathbf{x},\omega):=\left\langle\mathbf{v}\right\rangle_{\mathrm{Y}}=\mathrm{i}\omega\mathbf{E}(\mathbf{x},\omega)\cdot\mathbf{x}+\mathrm{i}\omega\mathbf{K}(\mathbf{x},\omega):\mathbf{G}_2 \\
\tilde{\mathbf{u}}(\mathbf{y}),\tilde{\mathbf{v}}(\mathbf{y})\ \text{Y-periodic} \\
\mathbf{u}(\mathbf{y},\mathrm{t}=0)=\mathbf{0}=\mathbf{v}(\mathbf{y},\mathrm{t}=0)
\end{array}\right. \tag{3.11}
$$

Previous BVP writes in abstract operator format

$$
\mathrm{D}(\mathbf{y},\omega)\left\{\tilde{\mathbf{u}}(\mathbf{y});\ \mathbf{E}(\mathbf{x},\omega),\mathbf{K}(\mathbf{x},\omega),\mathbf{V}(\mathbf{x},\omega)\right\}=0
$$

wherein $\mathrm{D}(\mathbf{y},\omega)$ is a second order differential in space but algebraic in frequency operator acting on the fluctuation $\tilde{\mathbf{u}}(\mathbf{y})$ and with $\mathbf{E}(\mathbf{x},\omega),\mathbf{K}(\mathbf{x},\omega),\mathbf{V}(\mathbf{x},\omega)$ entering as parameters. The linearity of this BVP versus the macroscopic loading $\mathbf{E}(\mathbf{x},\omega),\mathbf{K}(\mathbf{x},\omega),\mathbf{V}(\mathbf{x},\omega)$ entails the existence of displacement and velocity localizators such that

$$
\begin{array}{l}
\tilde{\mathbf{u}}(\mathbf{y},\omega)=\mathbf{H}^{\mathrm{EE}}(\mathbf{y},\omega):\mathbf{E}(\mathbf{x},\omega)+\mathbf{H}^{\mathrm{EK}}(\mathbf{y},\omega):\mathbf{K}(\mathbf{x},\omega)+\mathbf{H}^{\mathrm{EV}}(\mathbf{y}).\mathbf{V}(\mathbf{x},\omega) \\
\Rightarrow\tilde{\mathbf{v}}(\mathbf{y},\omega)=\mathbf{H}^{\mathrm{VE}}(\mathbf{y}):\mathbf{E}(\mathbf{x},\omega)+\mathbf{H}^{\mathrm{VK}}(\mathbf{y},\omega):\mathbf{K}(\mathbf{x},\omega)+\mathbf{H}^{\mathrm{VV}}(\mathbf{y},\omega).\mathbf{V}(\mathbf{x},\omega) \\
\mathbf{V}(\mathbf{x},\omega)=\mathrm{i}\omega\mathbf{E}(\mathbf{x},\omega).\mathbf{x}+\mathrm{i}\omega\mathbf{K}(\mathbf{x},\omega):\mathbf{G}_2(\mathbf{x})
\end{array} \tag{3.12}
$$

Inserting expressions (3.12) into (3.10) delivers the Lagrangian, wherein the last kinematic relation in Eq.(3.12) is prescribed via a Lagrange multiplier (the space and frequency are skipped as arguments for the sake of simplification of the notations), as detailed in the **Appendix D**. The dynamical strain gradient constitutive law follows from Hill macrohomogeneity condition, Eq.(3.5), wherein minimization and partial derivatives with respect to the macroscopic kinematic variables has been done (using similar argumentation as for the first gradient situation previously exposed)

Remark: the kinematic constraint (3.9) entails the emergence of a second order momentum not present initially as an argument of the effective Lagrangian in Eq.(3.10).

On the constraint set (3.9), the last term on the right hand side of relations (3.12) and (D1) vanishes, thus the constitutive law can be compactly written in matrix format in frequency domain:

$$
\begin{array}{l}
\begin{pmatrix}\boldsymbol{\Sigma}\\ \mathbf{S}\\ \mathbf{P}\end{pmatrix}=\begin{pmatrix}\mathbf{C}_\omega^{\Sigma\Sigma} & \mathbf{C}_\omega^{\Sigma\mathrm{S}} & \mathbf{C}_\omega^{\Sigma\mathrm{P}}\\ \mathbf{C}_\omega^{\mathrm{S}\Sigma} & \mathbf{C}_\omega^{\mathrm{SS}} & \mathbf{C}_\omega^{\mathrm{SP}}\\ \mathbf{C}_\omega^{\mathrm{P}\Sigma} & \mathbf{C}_\omega^{\mathrm{PS}} & \boldsymbol{\rho}_\omega^{\mathrm{H}}\end{pmatrix}.\begin{pmatrix}\mathbf{E}\\ \mathbf{K}\\ \mathbf{V}\end{pmatrix}+\begin{pmatrix}\mathbf{0}\\ \mathbf{0}\\ \boldsymbol{\Lambda}\end{pmatrix} \\
\mathbf{Q}=-\boldsymbol{\Lambda}^{\mathrm{S}}\left(\mathbf{E},\mathbf{K},\mathbf{V},\mathbf{V}\otimes\nabla_{\mathrm{x}}\right) \\
\mathbf{R}=-\boldsymbol{\Lambda}.\mathbf{G}_2
\end{array} \tag{3.13}
$$

The last relation in (3.13) then follows from Eq.(D7). It is important to note that all effective static and dynamical moduli in Eq.(3.13) are frequency-dependent (indicated by the subscript ω). The Lagrange multiplier can be determined e.g. from the initial conditions satisfied by the momentum: assuming e.g. no initial strain and strain gradient, it holds the relation

$$\mathbf{P}_0 := \mathbf{P}\left(t=0\right) = \boldsymbol{\rho}_{\omega}^{H}.\mathbf{V}_0 + \boldsymbol{\Lambda} \Rightarrow \boldsymbol{\Lambda} = \mathbf{P}_0 - \boldsymbol{\rho}_{\omega}^{H}.\mathbf{V}_0 \tag{3.14}$$

The constitutive model in Eq.(3.13) and Eq.(3.14) can be directly expressed in terms of the set of kinematic variables $\left(\mathbf{E}(\mathbf{x},\omega),\mathbf{K}(\mathbf{x},\omega)\right)$ and in the space-frequency domain when replacing the velocity $\mathbf{V}(\mathbf{x},\omega)$ by the strain and strain rate gradient terms (in frequency domain) using the kinematic coupling in Eq.(3.9):

$$\begin{aligned}
\boldsymbol{\Sigma} &= \mathbf{C}_{\omega}^{\Sigma\Sigma} : \mathbf{E} + \mathbf{C}_{\omega}^{\Sigma S} \therefore \mathbf{K} + i\omega\mathbf{C}_{\omega}^{\Sigma P}.\left(\mathbf{E}(\mathbf{x},\omega)\cdot\mathbf{x} + \mathbf{K}(\mathbf{x},\omega) : \mathbf{G}_2\right) \\
\mathbf{S} &= \mathbf{C}_{\omega}^{S\Sigma} : \mathbf{E} + \mathbf{C}_{\omega}^{SS} \therefore \mathbf{K} + i\omega\mathbf{C}_{\omega}^{SP}.\left(\mathbf{E}(\mathbf{x},\omega)\cdot\mathbf{x} + \mathbf{K}(\mathbf{x},\omega) : \mathbf{G}_2\right) \\
\mathbf{P} &= \mathbf{C}_{\omega}^{P\Sigma} : \mathbf{E} + \mathbf{C}_{\omega}^{PS} \therefore \mathbf{K} + i\omega\boldsymbol{\rho}_{\omega}^{H}.\left(\mathbf{E}(\mathbf{x},\omega)\cdot\mathbf{x} + \mathbf{K}(\mathbf{x},\omega) : \mathbf{G}_2\right) + \boldsymbol{\Lambda}
\end{aligned} \tag{3.15}$$

3.4. Homogenized strain gradient constitutive law formulated in time domain

When formulated back in the time domain, using the inverse Fourier transform, the resulting constitutive law proves to be nonlocal in time, as it expresses as a convolution integral of the form

$$\begin{aligned}
\boldsymbol{\Sigma}(\mathbf{x},t) &= \int \mathbf{C}_{\omega}^{\Sigma\Sigma}(\mathbf{x},t-t') : \mathbf{E}(\mathbf{x},t-t') + \mathbf{C}_{\omega}^{\Sigma S}(\mathbf{x},t-t') \therefore \mathbf{K}(\mathbf{x},t-t') + \mathbf{C}_{\omega}^{\Sigma P}(\mathbf{x},t-t').\mathbf{V}(t')dt' \\
\mathbf{S}(\mathbf{x},t) &= \int \mathbf{C}_{\omega}^{S\Sigma}(\mathbf{x},t-t') : \mathbf{E}(\mathbf{x},t-t') + \mathbf{C}_{\omega}^{SS}(\mathbf{x},t-t') \therefore \mathbf{K}(\mathbf{x},t-t') + \mathbf{C}_{\omega}^{SP}(\mathbf{x},t-t').\mathbf{V}(t')dt' \\
\mathbf{P}(\mathbf{x},t) &= \int \mathbf{C}_{\omega}^{P\Sigma}(\mathbf{x},t-t') : \mathbf{E}(\mathbf{x},t-t') + \mathbf{C}_{\omega}^{PS}(\mathbf{x},t-t') : \mathbf{K}(\mathbf{x},t-t') + \boldsymbol{\rho}^{H}(\mathbf{x},t-t').\mathbf{V}(t')dt' + \boldsymbol{\Lambda}
\end{aligned} \tag{3.16}$$

The dynamical equation of motion in time domain is classically obtained from the stationarity principle of the functional built from the Lagrangian (integrating over time and the homogeneous domain $\mathbf{V}(\mathbf{x})$ the effective Lagrangian) as the following relation satisfied by the effective stress $\boldsymbol{\tau}$ modeling internal (classical and higher gradient) forces and the classical and higher order momenta:

$$\begin{aligned}
&\mathrm{div}_x\boldsymbol{\tau} = \dot{\mathbf{P}} - \mathrm{div}_x\dot{\mathbf{Q}} \\
&\boldsymbol{\tau} := \boldsymbol{\Sigma} - \mathrm{div}_x\mathbf{S}
\end{aligned} \tag{3.17}$$

Assuming the hypermomentum is linearly related to the velocity gradient via the relation $\mathbf{V}\otimes\nabla_x \equiv \dot{\mathbf{E}}$, leads using $(3.15)_3$ to the following more specific form of the dynamical equation of motion:

$$\mathrm{div}_x\left(\boldsymbol{\Sigma} - \mathrm{div}_x\mathbf{S}\right) + \boldsymbol{\beta}^{H} : \mathrm{div}_x\ddot{\mathbf{E}} = \mathbf{C}_{\omega}^{P\Sigma} : \dot{\mathbf{E}} + \mathbf{C}_{\omega}^{PS} \therefore \dot{\mathbf{K}} + \boldsymbol{\rho}_{\omega}^{H}.\left(\ddot{\mathbf{E}}\cdot\mathbf{x} + \ddot{\mathbf{K}} : \mathbf{G}_2\right) + \left(\dot{\boldsymbol{\Lambda}} \equiv \mathbf{0}\right) \tag{3.18}$$

The term $\dot{\boldsymbol{\Lambda}} \equiv \mathbf{0}$ in (3.18) vanishes when the Lagrange multiplier is identified from an initial condition like the one formulated in Eq.(3.14). The formulated strain gradient model with microinertia effects is descriptive of behaviors occurring at low and medium frequencies and short wavelengths; it extends the predictive capacity of Cauchy formulation which neglects both space and time higher order effects, and is non dispersive.

3.5. Dynamical behavior of inclusion based composites based on the dynamical strain gradient effective medium

We use the dynamical first and second gradient stress tensors evaluated in Section 3.2 and 3.3 to compute some of the dynamical characteristics of heterogeneous composite media recoursing to the formulated dynamical strain gradient effective continuum, considering a general harmonic wave.

Following the methodology exposed in section 3, the unit cell of the periodic medium is subjected to the kinematic loading in the frequency domain, defined by the set $\{\mathbf{E}(\mathbf{x},\omega),\mathbf{K}(\mathbf{x},\omega),\mathbf{V}(\mathbf{x},\omega)\}$. The variational formulation for the strain gradient effective medium is considered, wherein the displacement and velocity fluctuations express using now explicitly the kinematic constraint in Eq.(3.6):

$$\begin{aligned}
&\mathbf{V}(\mathbf{x},\omega)=\mathrm{i}\omega\mathbf{U}(\mathbf{x},\omega)\rightarrow\mathbf{U}(\mathbf{x},\omega)=\mathbf{E}(\mathbf{x},\omega)\cdot\mathbf{x}+\mathbf{K}(\mathbf{x},\omega):\mathbf{G}_2\\
&\tilde{\mathbf{u}}(\mathbf{y},\omega)=\left(\mathbf{H}^{\mathrm{EE}}(\mathbf{y},\omega)+\mathrm{i}\omega\mathbf{H}^{\mathrm{EV}}(\mathbf{y})\right):\mathbf{E}(\mathbf{x},\omega)+\left(\mathbf{H}^{\mathrm{EK}}(\mathbf{y},\omega)+\mathrm{i}\omega\mathbf{K}(\mathbf{x},\omega)\right):\mathbf{G}_2:\mathbf{K}(\mathbf{x},\omega)\\
&\Rightarrow\tilde{\mathbf{v}}(\mathbf{y},\omega)=\mathrm{i}\omega\left(\mathbf{H}^{\mathrm{VE}}(\mathbf{y},\omega)+\mathbf{H}^{\mathrm{VV}}(\mathbf{y},\omega)\otimes\mathbf{x}\right):\mathbf{E}(\mathbf{x},\omega)+\mathrm{i}\omega\left(\mathbf{H}^{\mathrm{VK}}(\mathbf{y},\omega)+\dot{\mathbf{K}}(\mathbf{x},\omega):\mathbf{G}_2\right)\therefore\mathbf{K}(\mathbf{x},\omega)
\end{aligned}\tag{3.19}$$

The dispersion relation is obtained by incorporating the constitutive law of Eq.(3.13) into the dynamical equation of motion of the effective (dynamical) medium, combining the two equations of Eq.(3.17), rewritten fully in $\mathrm{k}-\omega$ domain in the harmonic regime:

$$\mathrm{i}\mathbf{k}.\boldsymbol{\Sigma}+\mathbf{k}.\mathbf{k}.\mathbf{S}=\mathrm{i}\omega\mathbf{P}+\omega\mathbf{k}.\mathbf{Q},\tag{3.20}$$

$$\left|\begin{aligned}
&\boldsymbol{\Sigma}=\mathbf{C}_\omega^{\Sigma\Sigma}:\mathbf{E}+\mathbf{C}_\omega^{\Sigma S}\therefore\mathbf{K}+\mathbf{S}_\omega^{\Sigma P}.\left(\mathrm{i}\omega\mathbf{E}\cdot\mathbf{x}+\mathrm{i}\omega\mathbf{K}:\mathbf{G}_2\right)\\
&\mathbf{S}=\mathbf{C}_\omega^{S\Sigma}:\mathbf{E}+\mathbf{C}_\omega^{SS}\therefore\mathbf{K}+\mathbf{C}_\omega^{SP}.\left(\mathrm{i}\omega\mathbf{E}\cdot\mathbf{x}+\mathrm{i}\omega\mathbf{K}:\mathbf{G}_2\right)\\
&\mathbf{P}=\mathbf{S}_\omega^{P\Sigma}:\mathbf{E}+\mathbf{C}_\omega^{\Sigma S}\therefore\mathbf{K}+\boldsymbol{\rho}_\omega^{\mathrm{H}}.\left(\mathrm{i}\omega\mathbf{E}\cdot\mathbf{x}+\mathrm{i}\omega\mathbf{K}:\mathbf{G}_2\right)\\
&\mathbf{Q}=\mathrm{i}\omega\boldsymbol{\beta}^{\mathrm{H}}:\mathbf{E}
\end{aligned}\right.$$

Combining these expressions and expressing the kinematic relation $\mathbf{K}(\mathbf{x},\omega):=\mathbf{E}(\mathbf{x},\omega)\otimes\nabla_{\mathrm{x}}$ leads to the following nonlinear dispersion relation (including quadratic frequency terms):

$$\mathrm{i}\mathbf{k}.\boldsymbol{\Sigma}+\mathbf{k}.\mathbf{k}.\mathbf{S}-\mathrm{i}\boldsymbol{\beta}^{\mathrm{H}}\mathrm{k}\omega^2\mathbf{E}=\mathrm{i}\omega\mathbf{S}_\omega^{P\Sigma}:\mathbf{E}+\mathrm{i}\omega\mathbf{C}_\omega^{\Sigma S}\therefore\mathbf{K}-\omega^2\boldsymbol{\rho}_\omega^{\mathrm{H}}.\left(\mathbf{E}\cdot\mathbf{x}+\mathbf{K}:\mathbf{G}_2\right)=0\tag{3.21}$$

The effective dynamical strain gradient constitutive law from Eq.(3.13) is specified for 2D periodic voided unit cells with a square geometry, with a void volume fraction of 30 %, the void being embedded into a surrounding matrix, as shown in Fig 2.

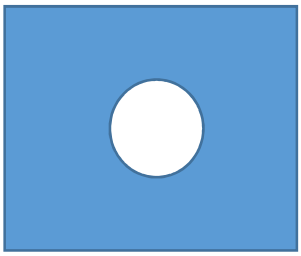

Figure 2: Periodic unit cell of the composite of linear size L with a voided inclusion

The chosen properties of the matrix obeying an isotropic linear elastic model are given in Table 2; these properties are those of a fictitious material in the class of polymers.

Property	Matrix
Elastic modulus	1400 MPa
Poisson's coefficient	0.25
Density	5 kg/m^3

Table 2. Mechanical parameters for the matrix

Computations are done with the open source finite element code Freefem++ relying on the weak form of the established dynamical BVP. We mesh the unit cell domain in Fig.2 with 20 elements along each side, and automatic meshing is then done with triangular elements. The constants matrices $\mathbf{C}_\omega^{\Sigma S}, \mathbf{C}_\omega^{S\Sigma}$ will vanish in the case of centro-symmetric composite material, reflecting the chosen example. The matrices $\mathbf{C}_\omega^{\Sigma P}, \mathbf{C}_\omega^{SP}$ also vanish due to the independency of the microscopic displacement upon the macroscopic velocity V in Eq. (3.8). The constitutive law then takes the following simplified form:

$$\begin{pmatrix} \mathbf{\Sigma} \\ \mathbf{S} \\ \mathbf{P} \end{pmatrix} = \begin{pmatrix} \mathbf{C}_\omega^{\Sigma\Sigma} & 0 & 0 \\ 0 & \mathbf{C}_\omega^{SS} & 0 \\ \mathbf{C}_\omega^{P\Sigma} & \mathbf{C}_\omega^{PS} & \boldsymbol{\rho}_\omega^{H} \end{pmatrix} . \begin{pmatrix} \mathbf{E} \\ \mathbf{K} \\ \mathbf{V} \end{pmatrix} \tag{3.22}$$

Note that the coupling between the so called microscopic velocity and the strain and strain gradient tensors appearing in the homogeneous velocity expressed in Eq.(3.8) is reflected in the existing couplings at the macroscale occurring in Eq.(3.22) between $\mathbf{E}, \mathbf{K}$ and the macroscopic momentum $\mathbf{P}$. The values of the coefficients of the first and second gradient rigidity matrices, respectively $\mathbf{C}_\omega^{\Sigma\Sigma}$ and $\mathbf{C}_\omega^{SS}$, are independent of the frequency (since the static and the dynamic behavior at the micro scale are decoupled) and they are given as follows, adopting here and in the sequel a fixed Cartesian basis:

$$\begin{pmatrix} \Sigma_{11} \\ \Sigma_{22} \\ \sqrt{2}\Sigma_{12} \end{pmatrix} = \begin{pmatrix} 1214.2 & 369.9 & 0 \\ 369.9 & 1214.2 & 0 \\ 0 & 0 & 525.9 \end{pmatrix} \begin{pmatrix} E_{11} \\ E_{22} \\ \sqrt{2}E_{12} \end{pmatrix} \tag{3.23}$$

$$\begin{pmatrix} S_{111} \\ S_{121} \\ S_{221} \\ S_{222} \\ S_{122} \\ S_{112} \end{pmatrix} = \begin{pmatrix} 84.38 & 0 & 84.37 & 35.73 & 0 & 71.17 \\ 1.97 & 112.51 & 8.57 & 1.67 & 86.12 & 7.23 \\ 39.57 & 0 & 113.86 & 64.57 & 0 & 64.53 \\ 35.76 & 0 & 71.23 & 84.36 & 0 & 84.35 \\ 1.67 & 86.16 & 7.26 & 1.97 & 112.49 & 8.56 \\ 64.61 & 0 & 64.61 & 39.56 & 0 & 113.78 \end{pmatrix} \begin{pmatrix} K_{111} \\ K_{121} \\ K_{221} \\ K_{222} \\ K_{122} \\ K_{112} \end{pmatrix} \tag{3.24}$$

The variation of the first component of the momentum P_1 versus the frequency of incident waves is pictured in Fig.3 for different boundary conditions applied over the unit cell boundary triggering the corresponding macroscopic kinematic deformation mode.

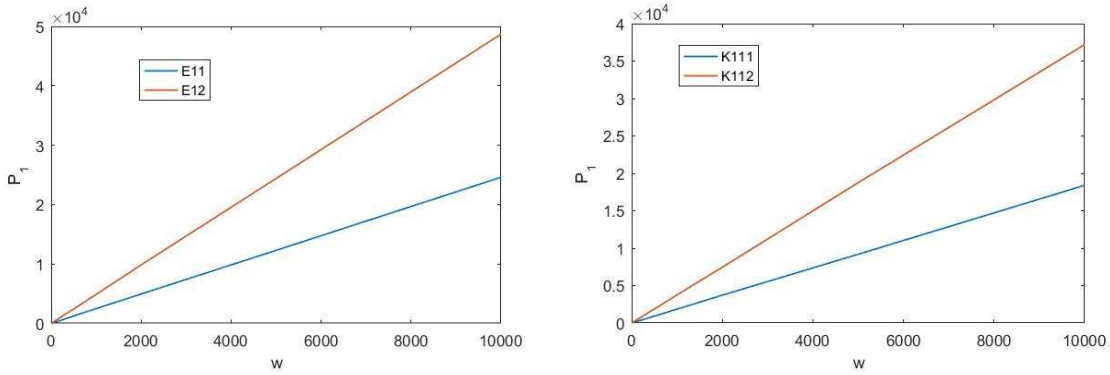

Figure 3: Variation of the momentum component P_1 versus frequency for an imposed macroscopic deformation E_{11} and E_{12} and gradient of deformation K_{111} and K_{112}

In contrast to the previous behavior, the momentum component P_1 does not vary versus the strain component E_{22}, but it does vary versus the horizontal velocity V_1. A symmetric plot is obtained for the momentum component P_2. The variation of the frequency versus the incident wave angle is plotted in Fig.4 for different wave number values.

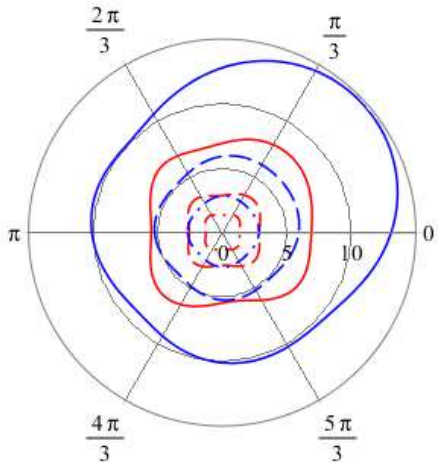

Figure 4: Polar plot of the frequency versus the incident angle for longitudinal waves (blue line) and shear waves (red line) for different wavenumbers: kL=1 (continuous line), kL=0.5 (dashed line) and kL=0.25 (dashed-dotted line)

While the polar plot reflects the square symmetry of the unit cell for high wave lengths (the iso-frequency plot has a square shape reflecting the tetragonal symmetry of the unit cell), the initial anisotropy breaks down when increasing the wavenumber, leading to an irregular non-symmetrical shape of the iso-frequency line. The predictions of the local and nonlocal strain gradient homogenized media are next compared on the iso-frequency polar plot of Fig.5.

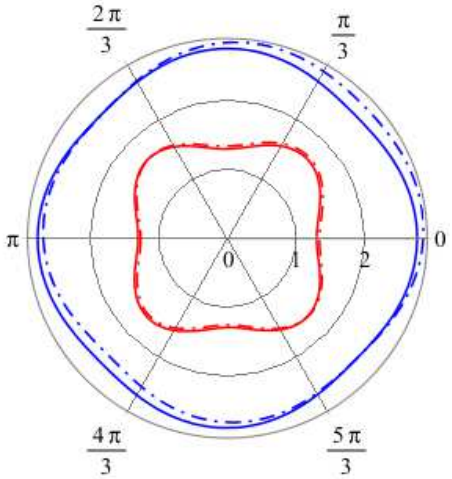

Figure 5: Frequency plot versus the incident wave angle for longitudinal and shear waves (blue and red lines respectively) for the effective local SG medium (solid line) and nonlocal SG effective media (dashed line)

Both local and nonlocal strain gradient effective media are dispersive, since the phase velocity of propagating waves depends on wavelength. Most importantly, the purely local strain gradient continuum shows a square symmetrical iso-frequency plot, whereas the square symmetry breaks down for the nonlocal strain gradient continuum (Fig.5). The effect of nonlocality remains nevertheless limited, even very small in the case of shear waves.

To conclude this section, the proposed dynamical homogenization methodology relying on a variational Hamiltonian type formulation of equilibrium bypasses the need to recourse to the body force loading to derive such a velocity dependent constitutive model as in (Nassar et al., 2015, 2016) as the average velocity dependency instead follows from the very structure of the dynamical equation of motion using the proposed additive decomposition of the microscopic velocity into its spatial average and a periodic fluctuation.

We next extend previous framework restricted to long wavelengths to the general situation of high frequency and short wavelengths by exploiting the properties of Floquet-Bloch transform in order to derive a nonlocal in space and time effective medium of Willis type and evaluate its effective properties.

4. Derivation of a spatio-temporal nonlocal dynamical homogenized behavior

The improvement of the predictions of the quasi-static homogenization theory is essential for modeling the macroscopic elastodynamic behavior of heterogeneous materials in a broad sense, and especially of metamaterials. Metamaterials are man-made materials designed on purpose to reach an unusual exceptional behavior not encountered by more classical materials, regarding their optical, electromagnetic, acoustic or elastic behavior. Such improvements of the quasi-static, low frequency limit, aim to capture important phenomena like dispersion effects, optimal modes and band gaps. To capture those effects, the prevailing strict assumptions made on the range of frequencies and wavelengths needed for scale separation to hold have to be modified. Willis theory has been a new approach to bypass such a scale separation to be able to describe the dynamical response of composite materials at high frequencies and short wavelengths.

As nonlocal effects arise at the macroscopic level after homogenization of a heterogeneous material has been performed, a few words about micromechanics are in order. Dynamical homogenization has specific features that are not encountered in statics, and dynamical homogenization theories were flourishing in the last two decades, with their outcomes depending on assumptions made related to the involved length scales and frequencies, see (Nassar et al., 2016) and references therein. A distinction between random media and periodic materials is in order, since incident waves are little sensitive to the details of the microstructure for the former (it feels only the averaged effects for large wavelengths compared to the typical size of heterogeneities); in contrast, for periodic media, scattered waves have specific directions of propagation, and the wave solution of the microscopic equations of motion includes a whole spectrum of smaller fluctuations, thereby leading to a macroscopic equation of motion that differs in form from the initial microscopic dynamical equation. Several mathematical theories have been elaborated since more than four decades, introducing specific notions of convergence of the dynamical equations of motion, such as G-, H-, or two-scale convergence (Braides, 2002; Allaire, 1992) and references therein.

The problem considered in the sequel is the dynamical homogenization of a periodical heterogeneous medium, and its replacement by a homogeneous medium over which effective fields are defined and an effective elastodynamic behavior is evaluated such that the most salient features of the dynamics of the initial medium are captured. In order to reach this goal, we will use the Floquet-Bloch transform of the fields to fully exploit the periodicity and simplify the formulation of the boundary value problem. Floquet-Bloch (FB in short) theory is a methodology to analyze the behavior of systems having a periodic spatial structure. Floquet's seminal paper treated the solution of 1D partial differential equations with periodic coefficients (Floquet, 1883). The corresponding theory of wave propagation in mechanical systems deserves the name Floquet-Bloch theory, or more simply, Floquet theory. The chief interest of FB theory is to reduce the calculation of wave propagation in the so-called unit cell of the structure, associated to specific boundary conditions – called Bloch conditions – issued from FB theory and elastodynamics.

4.1. Floquet-Bloch writing of the dynamical equilibrium

In order to set the stage and following (Nassar et al., 2015, 2016), we consider the reciprocal lattice Y^* of the direct lattice Y (Fig. 6). A plane wave of the form $e^{i\boldsymbol{\xi}.\mathbf{x}}$ is R-periodic (periodic over the lattice R) if:

$$\forall \boldsymbol{\xi} \in E^*, \forall \mathbf{r} \in Y,\ \boldsymbol{\xi}.\mathbf{r} \in 2\pi\mathbf{Z}$$

Figure 6: the direct diamond chiral lattice with the primitive unit cell Y, the reciprocal lattice Y^* and the first Brillouin zone T^* colored in blue (Reda et al., 2016)

The plane wave expansion of a spatially varying E-periodic function $h(\mathbf{x})$, such that:

$$\forall \mathbf{x} \in \Omega,\ \forall \mathbf{r} \in Y,\ h(\mathbf{x}) = h\left(\mathbf{x}+\mathbf{r}\right), Y = \sum_{j=1}^{d} \mathbf{Z} b_j \text{ , is defined by}$$

$$h(\mathbf{x}) = \sum_{\xi \in R^*} \tilde{\mathbf{h}}_\xi e^{i\xi.\mathbf{x}},\ \ \tilde{\mathbf{h}}_\xi = \frac{1}{|Y|}\int_Y h(\mathbf{x}) e^{-i\xi.\mathbf{x}} dx \tag{4.1}$$

The first Brillouin zone T^* of the reciprocal lattice E^* is defined as the set of wavenumbers closer to the null wavenumber than to any other wavenumber:

$$Y^* = \left\{ k \in E^* \middle| \forall \xi \in E^* / \{0\}, \|k\| < \|k - \xi\| \right\} \subset E^* \tag{4.2}$$

This zone separates short from long wavelengths: all k close to $\forall \xi \in E^* / \{0\}$ define rapidly in space oscillating fields, whereas all k close to the nil wavenumber define slowly spatially varying fields; this is the case for wavenumbers within the first Brillouin zone T^*. Note that the first Brillouin zone is isomorphic to the quotient space E^* / Y^*, which entails the decomposition $E^* = T^* + Y^*$, with the meaning of a clear separation of wavelengths into short ones within the reciprocal lattice R^* and large wavelengths in the first Brillouin zone T^*. Previous decomposition results from the implication

$$\mathbf{k} \in T^* \Rightarrow \left(\mathbf{k}+\boldsymbol{\xi}\right) \notin E^*,\ \forall \boldsymbol{\xi} \in E^* / \{0\} \tag{4.3}$$

The Floquet-Bloch wave expansion is then elaborated using the Fourier expansion of the FB component $\tilde{\mathbf{u}}_k(\mathbf{x})$, viz.

$$\tilde{\mathbf{u}}_k(\mathbf{x}) = \sum_{\xi \in R^*} \tilde{\mathbf{u}}_{k+\xi}(\mathbf{x}) e^{i\xi.\mathbf{x}},\ \tilde{\mathbf{u}}_{k+\xi} = \frac{1}{|Y|}\int_Y \tilde{\mathbf{u}}_k(\mathbf{x}) e^{i\xi.\mathbf{x}} dx \tag{4.4}$$

as

$$\mathbf{u}(\mathbf{x}) = \int_{E^*} \tilde{\mathbf{u}}_k(\mathbf{x}) e^{i\mathbf{k}.\mathbf{x}} dk = \int_{Y^*+R^*} \tilde{\mathbf{u}}_k(\mathbf{x}) e^{i\mathbf{k}.\mathbf{x}} dk = \int_{y^*+R^*} \sum_{\xi \in R^*} \tilde{\mathbf{u}}_{k+\xi}(\mathbf{x}) e^{i\xi.\mathbf{x}} e^{i\mathbf{k}.\mathbf{x}} dk = \int_{y^*} \tilde{\mathbf{u}}_k(\mathbf{x}) e^{i\mathbf{k}.\mathbf{x}} dk \tag{4.5}$$

wherein we have introduced the Floquet-Bloch transform of the displacement field:

$$\forall \mathbf{k} \in Y^*,\ \forall \mathbf{x} \in \Omega,\ \tilde{\mathbf{u}}_k\left(\mathbf{x}\right) = \sum_{\xi \in R^*} \tilde{\mathbf{u}}_{k+\xi} e^{-i\xi.\mathbf{x}} \tag{4.6}$$

A Floquet-Bloch component $\tilde{\mathbf{u}}_k\left(\mathbf{x}\right)$ is Y-periodic due its definition as a Fourier series.

We first take the Floquet-Bloch transform of the initial BVP and use of Parseval theorem (Gazalet et al., 2013) for the writing of the Lagrangian density associated to the obtained algebraic problem, simplifying all subsequent writings by the phase factor $e^{i\mathbf{k}.\mathbf{x}}$, thereby defining successively the microscopic strain tensor, velocity, momentum and Hooke's type linear constitutive law:

$$\forall \mathbf{k} \in \mathrm{Y}^{*},\ \ \tilde{\boldsymbol{\varepsilon}}_{\mathrm{k}} = \left(\mathrm{grad}_{\mathrm{y}} + \mathrm{i}\mathbf{k}\right) \otimes^{\mathrm{S}} \tilde{\mathbf{u}}_{\mathrm{k}},\ \ \tilde{\mathbf{v}}_{\mathrm{k}} = \mathrm{i}\omega \tilde{\mathbf{u}}_{\mathrm{k}},\ \ \tilde{\mathbf{p}}_{\mathrm{k}} = \rho \tilde{\mathbf{v}}_{\mathrm{k}}$$
$$\tilde{\boldsymbol{\sigma}}_{\mathrm{k}} = \mathbf{C} : \tilde{\boldsymbol{\varepsilon}}_{\mathrm{k}} \tag{4.7}$$

Using these definitions, the balance of linear momentum writes:

$$\left(\mathrm{div}_{\mathrm{y}} + \mathrm{ik}\right) \tilde{\boldsymbol{\sigma}}_{\mathrm{k}} = \mathrm{i}\omega \tilde{\mathbf{p}}_{\mathrm{k}} \Rightarrow \mathrm{ik} \left\langle \tilde{\boldsymbol{\sigma}}_{\mathrm{k}} \right\rangle_{\mathrm{Y}} = \mathrm{i}\omega \left\langle \tilde{\mathbf{p}}_{\mathrm{k}} \right\rangle_{\mathrm{Y}} \tag{4.8}$$

The virtual work theorem in the static case can be written in terms of the Floquet-Bloch components using Parseval theorem and Plancherel equality (Nassar et al., 2015), stating that the difference between the work of internal forces and inertia forces vanishes in the present absence of body forces:

$$\forall \mathrm{k} \in \mathrm{Y}^{*},\ \int_{\mathrm{Y}} \left(\tilde{\boldsymbol{\sigma}}_{\mathrm{k}} : \tilde{\boldsymbol{\varepsilon}}_{\mathrm{k}} - \tilde{\mathbf{p}}_{\mathrm{k}} . \tilde{\mathbf{v}}_{\mathrm{k}} \right) = 0 \tag{4.9}$$

4.2. Variational principle for the displacement fluctuation in reciprocal space

The Lagrangian density to be integrated over the unit cell expressed in Eq.(2.3) writes in terms of the Floquet-Bloch components of the displacement and velocity as:

$$\mathrm{l}_{\mu}\left(\tilde{\mathbf{u}}_{\mathrm{k}}, \tilde{\mathbf{v}}_{\mathrm{k}}\right) = \frac{1}{2}\left(\tilde{\mathbf{p}}_{\mathrm{k}} . \tilde{\mathbf{v}}_{\mathrm{k}} - \left(\mathrm{grad}_{\mathrm{y}} + \mathrm{i}\mathbf{k}\right) \otimes \tilde{\mathbf{u}}_{\mathrm{k}} : \mathbf{C} : \left(\mathrm{grad}_{\mathrm{y}} + \mathrm{i}\mathbf{k}\right) \otimes \tilde{\mathbf{u}}_{\mathrm{k}} \right) \tag{4.10}$$

The Lagrangian density has been expressed in the Floquet-Bloch space in the last relation.

The decomposition of the microscopic displacement into an average and a spatially varying and periodic fluctuation done in section 2 entails a similar decomposition of its Floquet-Bloch components in a spatially long range term (representing the average) - depending on the macroscopic variable - and a spatially rapidly oscillating contribution $\hat{\tilde{\mathbf{u}}}_{\mathrm{k}}$:

$$\begin{aligned}
&\mathbf{u}(\mathbf{y}) = \mathbf{U}(\mathbf{x}, \mathrm{t}) + \hat{\mathbf{v}}(\mathbf{y}),\ \left\langle \tilde{\mathbf{v}} \right\rangle_{\mathrm{Y}} = 0 \rightarrow \left\langle \mathbf{u} \right\rangle_{\mathrm{Y}} = \mathbf{U}(\mathbf{x}, \mathrm{t}) \\
&\tilde{\boldsymbol{\varepsilon}}(\mathbf{y}) = \mathbf{E}(\mathbf{x}, \mathrm{t}) + \hat{\tilde{\boldsymbol{\varepsilon}}}(\mathbf{y}) \equiv \left(\mathrm{grad}_{\mathrm{y}} + \mathrm{i}\mathbf{k}\right) \otimes \tilde{\mathbf{u}}_{\mathrm{k}}(\mathbf{y}) \\
&\Rightarrow \hat{\tilde{\boldsymbol{\varepsilon}}}_{\mathrm{k}} = \left(\mathrm{grad}_{\mathrm{y}} + \mathrm{i}\mathbf{k}\right) \otimes \hat{\tilde{\mathbf{u}}}_{\mathrm{k}} \\
&\Rightarrow \mathbf{v}(\mathbf{y}) = \mathbf{V}(\mathbf{x}, \mathrm{t}) + \hat{\mathbf{v}}(\mathbf{y}, \mathrm{t}),\ \left\langle \hat{\mathbf{v}} \right\rangle_{\mathrm{Y}} = 0 \Rightarrow \left\langle \mathbf{v} \right\rangle_{\mathrm{Y}} = \mathbf{V}(\mathbf{x}, \mathrm{t})
\end{aligned} \tag{4.11}$$

The induced decomposition of the same fields after taking the Floquet-Bloch transform writes:

$$\begin{aligned}
&\tilde{\mathbf{u}}_{\mathrm{k}}\left(\mathbf{y}; \mathbf{x}\right) = \tilde{\mathbf{U}}_{\mathrm{k}}\left(\mathbf{x}\right) + \tilde{\tilde{\mathbf{u}}}_{\mathrm{k}}(\mathbf{y}),\ \tilde{\mathbf{v}}_{\mathrm{k}}\left(\mathbf{y}; \mathbf{x}\right) = \tilde{\mathbf{V}}_{\mathrm{k}}\left(\mathbf{x}\right) + \tilde{\tilde{\mathbf{v}}}_{\mathrm{k}}(\mathbf{y}) \\
&\Rightarrow \tilde{\mathbf{p}}_{\mathrm{k}}\left(\mathbf{y}; \mathbf{x}\right) = \tilde{\mathbf{P}}_{\mathrm{k}}\left(\mathbf{x}\right) + \tilde{\tilde{\mathbf{p}}}_{\mathrm{k}}\left(\mathbf{y}; \mathbf{x}\right)
\end{aligned} \tag{4.12}$$

In Eq.(4.12), the fluctuations are denoted with an overhead hat, so that the vectors therein $\hat{\tilde{\mathbf{u}}}_{\mathrm{k}}(\mathbf{y})$, $\hat{\tilde{\boldsymbol{\varepsilon}}}_{\mathrm{k}}(\mathbf{y})$, $\hat{\tilde{\mathbf{v}}}_{\mathrm{k}}(\mathbf{y})$, $\hat{\tilde{\mathbf{p}}}_{\mathrm{k}}\left(\mathbf{y}\right)$ successively denote the displacement, strain, velocity and momentum periodic fluctuations in Floquet-Bloch representation.

As a consequence, the action integral is stationary with respect to the displacement and velocity fluctuations, so it holds the following stationarity condition, wherein the Lagrangian is made dependent on the displacement and velocity fluctuations:

$$\delta\left\{\int_{Y} l_{\mu}\left(\hat{\tilde{\mathbf{u}}}_k,\ \hat{\tilde{\mathbf{v}}}_k\right)\right) dV_y\Big\} = 0,\ \ k \in Y^{*} \tag{4.13}$$

Inserting the additive kinematic decomposition of Equ.(4.12) into the previous Lagrangian functional of Equ.(4.10) delivers the stationarity condition:

$$\begin{aligned} & l_{\mu}\left(\hat{\tilde{\mathbf{u}}}_k,\ \hat{\tilde{\mathbf{v}}}_k\right)\right) = \frac{1}{2}\left(\left(\tilde{\mathbf{P}}_k(\mathbf{x}) + \hat{\tilde{\mathbf{p}}}_k\right).\left(\tilde{\mathbf{V}}_k + \hat{\tilde{\mathbf{v}}}_k\right) - \left(\text{grad}_y + \text{ik}\right) \otimes \left(\tilde{\mathbf{U}}_k(\mathbf{x}) + \hat{\tilde{\mathbf{u}}}_k\right) : \mathbf{C} : \left(\text{grad}_y + \text{ik}\right) \otimes \left(\tilde{\mathbf{U}}_k(\mathbf{x}) + \hat{\tilde{\mathbf{u}}}_k\right)\right) \\ & \Rightarrow \underset{\tilde{\mathbf{u}}_k, \tilde{\mathbf{v}}_k}{\text{Min}}\ S[\tilde{\mathbf{u}}_k] := \int_{Y} l_{\mu}(\tilde{\mathbf{u}}_k, \tilde{\mathbf{v}}_k)\, dx,\ k \in Y^{*} \end{aligned} \tag{4.14}$$

Previous minimization principle rewrites using the definition of velocity and momentum and the previous decomposition of the microscopic variables in Eqs.(4.7), (4.12), in which both arguments of the Lagrangian density, the fluctuation vectors $\left(\hat{\tilde{\mathbf{u}}}_k, \hat{\tilde{\mathbf{v}}}_k\right)$, are considered as independent DOF's:

$$\begin{aligned} & l_{\mu}\left(\hat{\tilde{\mathbf{u}}}_k, \hat{\tilde{\mathbf{v}}}_k\right) = \frac{1}{2}\left(\rho\left(\tilde{\mathbf{V}}_k + \hat{\tilde{\mathbf{v}}}_k\right).\left(\tilde{\mathbf{V}}_k + \hat{\tilde{\mathbf{v}}}_k\right) - \left(\text{grad}_y + \text{i}\mathbf{k}\right) \otimes \left(\tilde{\mathbf{U}}_k + \hat{\tilde{\mathbf{u}}}_k\right) : \mathbf{C} : \left(\text{grad}_y + \text{i}\mathbf{k}\right) \otimes \left(\tilde{\mathbf{U}}_k + \hat{\tilde{\mathbf{u}}}_k\right)\right) \\ & \tilde{\mathbf{v}}_k = \text{i}\omega\tilde{\mathbf{u}}_k,\ \ \tilde{\mathbf{p}}_k = \rho\tilde{\mathbf{v}}_k = \text{i}\rho\omega\tilde{\mathbf{u}}_k,\ \tilde{\boldsymbol{\varepsilon}}_k = \left(\text{grad}_y + \text{i}\mathbf{k}\right) \otimes^{S} \left(\tilde{\mathbf{U}}_k + \hat{\tilde{\mathbf{u}}}_k\right),\ \tilde{\mathbf{E}}_k = \text{i}\mathbf{k} \otimes^{S} \tilde{\mathbf{U}}_k \\ & \Rightarrow \underset{\tilde{\mathbf{u}}_k, \tilde{\mathbf{v}}_k}{\text{Min}}\ S[\tilde{\mathbf{u}}_k] := \int_{t_1}^{t_2} \int_{Y} l_{\mu}(\tilde{\mathbf{u}}_k, \tilde{\mathbf{v}}_k)\, dV_y \end{aligned} \tag{4.15}$$

The stationarity condition of the action integral delivers the following necessary condition the Euler equation for a given state of Floquet-Bloch homogeneous components $\left(\tilde{\mathbf{U}}_k(\mathbf{x}), \tilde{\mathbf{V}}_k(\mathbf{x})\right)$ over the unit cell:

$$\begin{aligned} & \delta S\left[\hat{\tilde{\mathbf{u}}}_k, \hat{\tilde{\mathbf{v}}}_k\right] = 0 \Rightarrow \\ & \text{i}\omega\rho\left(\tilde{\mathbf{V}}_k + \hat{\tilde{\mathbf{v}}}_k\right).\delta\hat{\tilde{\mathbf{v}}}_k - \mathbf{C} : \hat{\tilde{\boldsymbol{\varepsilon}}}.\delta\hat{\tilde{\mathbf{u}}}_k = \mathbf{0},\ \ \forall\left(\delta\hat{\tilde{\mathbf{u}}}_k, \delta\hat{\tilde{\mathbf{v}}}_k\right) \text{ s.t. } \delta\hat{\tilde{\mathbf{v}}}_k = \text{i}\omega\delta\hat{\tilde{\mathbf{u}}}_k \\ & \hat{\tilde{\boldsymbol{\varepsilon}}} = \left(\text{grad}_y + \text{i}\mathbf{k}\right) \otimes \left(\tilde{\mathbf{U}}_k + \hat{\tilde{\mathbf{u}}}_k\right) \end{aligned} \tag{4.16}$$

Note that the variations $\left(\delta\hat{\tilde{\mathbf{u}}}_k, \delta\hat{\tilde{\mathbf{v}}}_k\right)$ are considered as independent when deriving the Euler equations as the necessary stationarity condition of the action integral $S\left[\hat{\tilde{\mathbf{u}}}_k, \hat{\tilde{\mathbf{v}}}_k\right]$; this is similar to Lagrangian mechanics that considers a priori the degrees of freedom and their temporal derivative as independent degrees of freedom. However, the Euler equations account for their dependency, as reflected by the presence of the time derivative in the Euler operator.

Eq.(4.16) stands for the dynamical equations of motion in the wavelength-frequency domain for the Floquet-Bloch components of the displacement and velocity fields. Note that previous algebraic equation is written in the complex plane.

The linearity of previous algebraic condition with respect to the kinematic loading over the unit cell, the set $\left(\tilde{\mathbf{E}}_k, \tilde{\mathbf{V}}_k\right)$ at the macroscale, entails the existence of four localization operators

$\left(\tilde{\mathbf{H}}^{uE}(\mathbf{y}),\tilde{\mathbf{H}}^{uV}(\mathbf{y}),\tilde{\mathbf{H}}^{vE}(\mathbf{y}),\tilde{\mathbf{H}}^{vV}(\mathbf{y})\right)$, respectively tensors of orders (4, 2, 4, 2), such that the set of fluctuations $\left(\tilde{\tilde{\mathbf{u}}}_k,\tilde{\tilde{\mathbf{v}}}_k\right)$ writes versus the controlled loading:

$$\begin{aligned}
&\hat{\tilde{\mathbf{u}}}_k(\mathbf{y})=\tilde{\mathbf{H}}^{uE}(\mathbf{y}).\tilde{\mathbf{E}}_k(\mathbf{x})+\tilde{\mathbf{H}}^{uV}.\tilde{\mathbf{V}}_k(\mathbf{x})\\
&\hat{\tilde{\mathbf{v}}}_k(\mathbf{y})=\tilde{\mathbf{H}}^{vE}(\mathbf{y}).\tilde{\mathbf{E}}_k(\mathbf{x})+\tilde{\mathbf{H}}^{vV}(\mathbf{y}).\tilde{\mathbf{V}}_k(\mathbf{x})\\
&\hat{\tilde{\mathbf{v}}}_k(\mathbf{y})=i\omega\tilde{\tilde{\mathbf{u}}}_k(\mathbf{y})\Rightarrow\tilde{\mathbf{H}}^{vE}(\mathbf{y})=i\omega\tilde{\mathbf{H}}^{uE}(\mathbf{y}),\ \tilde{\mathbf{H}}^{vV}(\mathbf{y})=i\omega\tilde{\mathbf{H}}^{uV}(\mathbf{y})
\end{aligned}\tag{4.17}$$

Let recall that the macrostrain incorporates the eigenstrain as defined in Eq.(2.23). Inserting these decompositions into the previous Euler equations gives

$$\left\{\begin{aligned}
&i\rho\omega\left(\tilde{\mathbf{V}}_k(\mathbf{x})+\tilde{\mathbf{H}}_k^{uV}(\mathbf{y}).\tilde{\mathbf{E}}_k(\mathbf{x})+\tilde{\mathbf{H}}_k^{vV}(\mathbf{y}).\tilde{\mathbf{V}}_k(\mathbf{x})\right).\delta\hat{\tilde{\mathbf{v}}}_k-\\
&\mathbf{C}:\left(\text{grad}_y+i\mathbf{k}\right)\otimes\left(\tilde{\mathbf{U}}_k(\mathbf{x})+\tilde{\mathbf{H}}_k^{uV}(\mathbf{y}).\tilde{\mathbf{E}}_k(\mathbf{x})+\tilde{\mathbf{H}}_k^{vV}(\mathbf{y}).\tilde{\mathbf{V}}_k(\mathbf{x})\right).\delta\hat{\tilde{\mathbf{u}}}_k
\end{aligned}\right\}=\mathbf{0},\ \ \forall\left(\delta\hat{\tilde{\mathbf{u}}}_k,\delta\hat{\tilde{\mathbf{v}}}_k\right)\in V$$

(4.18)

The previous equation written in complex space provides two algebraic equations for the unknown, the two localization operators $\tilde{\mathbf{H}}^{uE}(\mathbf{y})$, $\tilde{\mathbf{H}}^{uV}(\mathbf{y})$, for the two virtual controlled kinematic loads at the macroscale $\left\{\tilde{\mathbf{E}}_k(\mathbf{x}),\tilde{\mathbf{V}}_k(\mathbf{x})\right\}$.

4.3. Effective dynamical moduli

The effective dynamical response is obtained from the Lagrangian density representing the dynamical energy expressed versus the Floquet-Bloch components of the fields using Parseval theorem, in conjunction with Hill dynamical macrohomogeneity condition for the Lagrangian, as proven in the **Appendix B**:

$$L_M\left(\tilde{\mathbf{E}}_k,\tilde{\mathbf{V}}_k\right):=\frac{1}{2}\left(-\tilde{\boldsymbol{\Sigma}}_k:\tilde{\mathbf{E}}_k(\mathbf{x})+\tilde{\mathbf{P}}_k.\tilde{\mathbf{V}}_k\right)\Rightarrow\underset{\hat{\tilde{\mathbf{u}}},\hat{\tilde{\mathbf{v}}}}{\text{Min}}\ \frac{1}{2}\left\{\int_Y dV_y\left\{-\tilde{\boldsymbol{\sigma}}:\left(\tilde{\mathbf{E}}_k-\langle\tilde{\boldsymbol{\gamma}}\rangle_Y+\hat{\tilde{\boldsymbol{\varepsilon}}}_k\right)+\tilde{\mathbf{P}}_k.\left(\tilde{\mathbf{V}}_k+\tilde{\tilde{\mathbf{v}}}_k\right)\right\}\right\}\tag{4.19}$$

in which $\left(\tilde{\boldsymbol{\Sigma}}_k,\tilde{\mathbf{V}}_k,\tilde{\mathbf{P}}_k\right)$ are the macroscopic effective stress, velocity and momentum. Inserting the previous expression of the displacement and velocity localizators of Eq.(4.17) in the minimization principle of Eq.(4.19) and using the microscopic constitutive law for the stress and momentum from Eq.(4.7) results in Eq.(4.19) relating the macroscopic Lagrangian to the average of the microscopic Lagrangian in Floquet-Bloch representation, wherein the dynamical Hill macrohomogeneity conditions has been used:

$$\begin{aligned}
&\tilde{\boldsymbol{\Sigma}}_k=\left\{\int_Y\tilde{\mathbf{A}}_k^{\varepsilon E}(\mathbf{y})^T:\mathbf{C}:\tilde{\mathbf{A}}_k^{\varepsilon E}(\mathbf{y})dV_y\right\}:\tilde{\mathbf{E}}_k(\mathbf{x})+\left\{\int_Y\tilde{\mathbf{A}}_k^{\varepsilon E}(\mathbf{y})^T:\mathbf{C}:\tilde{\mathbf{H}}_k^{vE}(\mathbf{y})dV_y\right\}.\tilde{\mathbf{V}}_k\\
&\tilde{\mathbf{P}}_k=\left\{\int_Y\rho(\mathbf{y})\left(\mathbf{I}_2+\tilde{\mathbf{H}}_k^{vV}(\mathbf{y})\right)^T.\tilde{\mathbf{H}}_k^{vE}(\mathbf{y})dV_y\right\}:\tilde{\mathbf{E}}_k(\mathbf{x})+\left\{\int_Y\rho(\mathbf{y})\left(\mathbf{I}_2+\tilde{\mathbf{H}}_k^{vV}(\mathbf{y})\right)^T.\left(\mathbf{I}_2+\tilde{\mathbf{H}}_k^{vV}(\mathbf{y})\right)dV_y\right\}.\tilde{\mathbf{V}}_k\\
&\tilde{\mathbf{A}}_k^{\varepsilon E}(\mathbf{y}):=\mathbf{I}_4+i\mathbf{k}\otimes\tilde{\mathbf{H}}_k^{uE}(\mathbf{y})\\
&\tilde{\mathbf{H}}_k^{vE}(\mathbf{y}):=i\omega\tilde{\mathbf{H}}_k^{uE}(\mathbf{y}),\ \tilde{\mathbf{H}}_k^{vV}(\mathbf{y}):=i\omega\tilde{\mathbf{H}}_k^{uV}(\mathbf{y})
\end{aligned}\tag{4.20}$$

Relations (4.20) expressing the homogenized dynamical constitutive law can be rewritten in condensed matrix format as follows, highlighting the effective moduli:

$$\begin{pmatrix} \tilde{\boldsymbol{\Sigma}}_k \\ \tilde{\mathbf{P}}_k \end{pmatrix} = \begin{pmatrix} \mathbf{C}_{k,\omega}^{\Sigma\Sigma} & \mathbf{S}_{k,\omega}^{\Sigma P} \\ \mathbf{S}_{k,\omega}^{P\Sigma} & \boldsymbol{\rho}_{k,\omega}^{H} \end{pmatrix} . \begin{pmatrix} \tilde{\mathbf{E}}_k \\ \tilde{\mathbf{V}}_k \end{pmatrix},$$

$$\begin{aligned} \mathbf{C}_{k,\omega}^{\Sigma\Sigma} &= \int_Y \tilde{\mathbf{A}}_k^{\varepsilon E}(\mathbf{y})^T : \mathbf{C} : \tilde{\mathbf{A}}_k^{\varepsilon E}(\mathbf{y}) dV_y \\ \mathbf{S}_{k,\omega}^{\Sigma P} &= \int_Y \tilde{\mathbf{A}}_k^{\varepsilon E}(\mathbf{y})^T : \mathbf{C} : \tilde{\mathbf{A}}_k^{\varepsilon E}(\mathbf{y}) dV_y \\ \mathbf{S}_{k,\omega}^{P\Sigma} &= \int_Y \rho(\mathbf{y}) \left(\mathbf{I}_2 + \tilde{\mathbf{H}}_k^{vV}(\mathbf{y}) \right) . \tilde{\mathbf{H}}_k^{vE}(\mathbf{y}) dV_y \\ \boldsymbol{\rho}_{k,\omega}^{H} &= \int_Y \rho(\mathbf{y}) \left(\mathbf{I}_2 + \tilde{\mathbf{H}}_k^{vV}(\mathbf{y}) \right)^T . \left(\mathbf{I}_2 + \tilde{\mathbf{H}}_k^{vV}(\mathbf{y}) \right) dV_y \end{aligned} \tag{4.21}$$

in which all effective moduli are both wavelength and frequency-dependent. Observe that the overall dynamical stiffness matrix assembling the submatrices from Eq.(4.21) has to be symmetrical due to the existence of a macroscopic energy density.

Going back to physical space leads to a non-local in both space and time dynamical constitutive model relating the average stress and momentum to the average velocity and strain by a space-time convolution integral. The effective stress and momentum are finally obtained in direct space by integrating their Floquet Bloch components over the wavenumbers that belong to the Brillouin zone and over all frequencies, so that it holds

$$\begin{pmatrix} \boldsymbol{\Sigma} \\ \mathbf{P} \end{pmatrix} = \int_\omega d\omega \int_{T^*} \begin{pmatrix} \tilde{\boldsymbol{\Sigma}}_k \\ \tilde{\mathbf{P}}_k \end{pmatrix} (\mathbf{x}) e^{i\mathbf{k}.\mathbf{x}} dk \tag{4.22}$$

Note that the localizators play in some the sense the role of Green's functions but at the macroscale, since they correspond to the microscopic response of the unit cell under a prescribed macroscopic unit loading localized at fixed macroscopic position. The dynamical homogenization conditions have been discussed in (Nassar et al., 2015); they consist of the satisfaction of Hill macrohomogeneity condition, the restriction to the first Brillouin zone, and the existence of an upper bound for the frequency of freely propagating waves, setting a relation between frequency and wavelength.

The effective dynamical constitutive law then writes back in space-time domain as a convolution integral of the form

$$\begin{aligned} \boldsymbol{\Sigma}(\mathbf{x},t) &= \int_{Y x \mathbf{R}} \mathbf{C}^{\Sigma\Sigma}(\mathbf{x},t-t') : \mathbf{E}(\mathbf{x},t-t') + \mathbf{S}^{\Sigma P}(\mathbf{x},t-t') . \mathbf{V}(t') dt' \\ \mathbf{P}(\mathbf{x},t) &= \int_{Y x \mathbf{R}} \mathbf{S}^{P\Sigma}(\mathbf{x},t-t') : \mathbf{E}(\mathbf{x},t-t') + \boldsymbol{\rho}^{H}(\mathbf{x},t-t') . \mathbf{V}(t') dt' \end{aligned} \tag{4.23}$$

4.4. Application to periodic composites

The effective dynamical constitutive law from Eq.(4.21) is specified for the 2D periodic voided unit cells shown in Fig.2, for a void volume fraction of 30 %, and adopting the mechanical parameters from Table 2. For a plane wave without attenuation in the x-y plane, the propagation

constants along the x and y directions are k_1 and k_2. For a plane wave without attenuation in the Cartesian coordinate system (in 2D), the propagation constants along the x and y directions are

$$\mathrm{k}_1 = \varepsilon_1 = |\mathrm{k}|\cos(\beta),\ \mathrm{k}_2 = \varepsilon_2 = |\mathrm{k}|\sin(\beta) \tag{4.24}$$

The effective Cauchy and strain gradient moduli given in Eq.(4.21) are plotted as a function of the wavenumber k and for a specific wave propagation β. We introduce for this purpose the dimensionless wavenumber K=kL, in which L is the unit cell length (it has a square geometry) pictured in Fig.1.

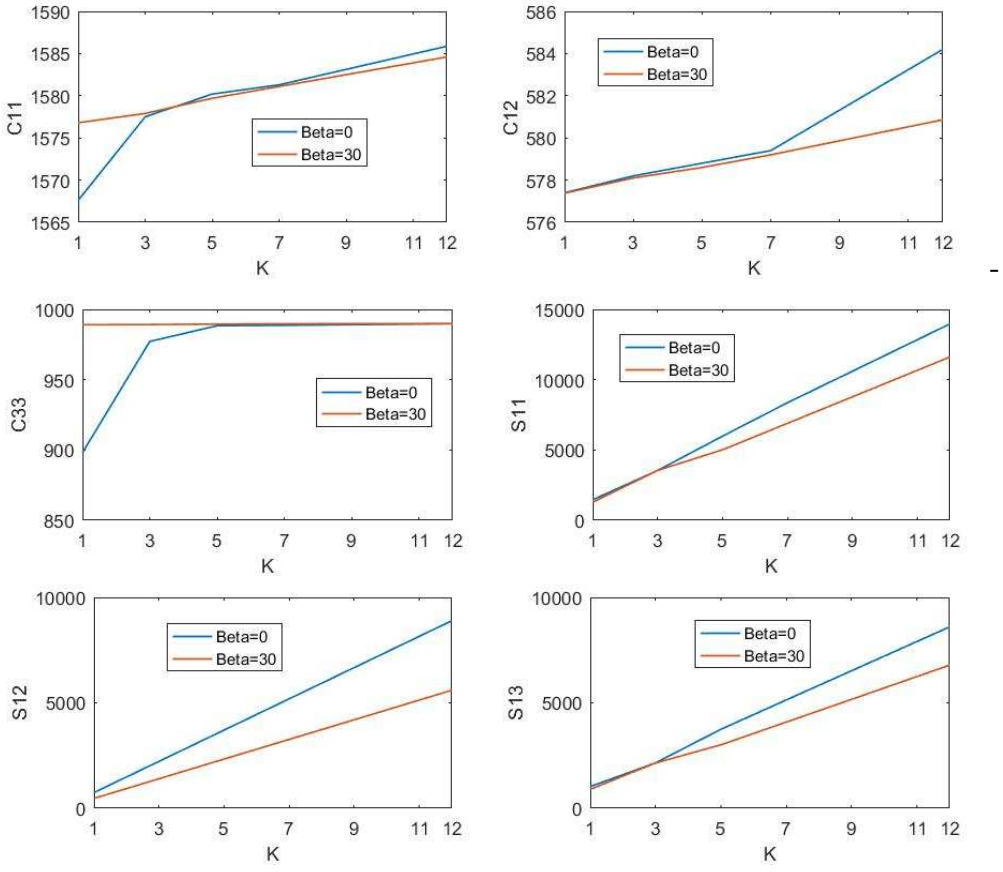

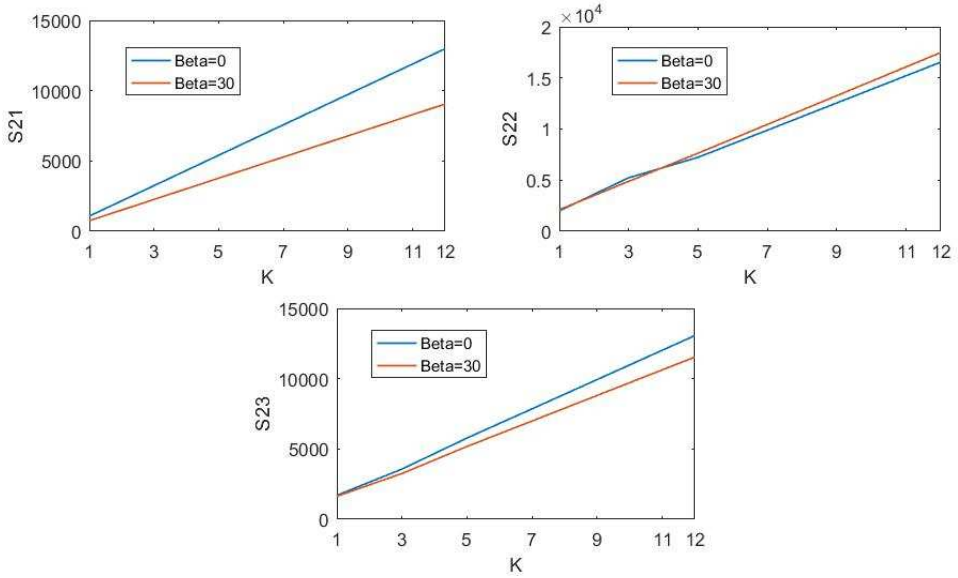

Figure 7: Dynamical effective properties in function of dimensionless wavenumber K for two incident angles β and for a frequency $\omega = 10.000$ Hz

We observe from Fig.7 that the effective Cauchy moduli C_{ij} vary very little versus the normalized wavenumber - about one per cent - so that they can be considered as constant; the effective coupling moduli S_{ij} of the tensor $\mathbf{S}^{P\Sigma}_{k,\omega}$ experience a linear variation versus wavenumber, so they can reasonably be approximated by a first polynomial in the wavenumber k. These moduli traduce the existing coupling between the macroscopic velocity and macroscopic stress.

4.5. Phase velocity plots for the nonlocal effective composite

The phase velocity of propagating waves is obtained from the vanishing condition of the impedance of the homogenized dynamical equations of motion in Fourier-Floquet-Bloch space, viz. rewriting the constitutive Eqs.(4.21) into the form

$$\left| \begin{array}{l} \tilde{\boldsymbol{\Sigma}}_k = \mathbf{C}^{\Sigma\Sigma}_{k,\omega} : \tilde{\mathbf{E}}_k + i\omega \mathbf{S}^{\Sigma P}_{k,\omega} . \tilde{\mathbf{U}}_k \\ \tilde{\mathbf{P}}_k = \left(\mathbf{S}^{P\Sigma}_{k,\omega} : \tilde{\mathbf{E}}_k + i\omega \boldsymbol{\rho}^{H}_{k,\omega} . \tilde{\mathbf{U}}_k \right) \end{array} \right. \tag{4.25}$$

The effective moduli therein are evaluated from Eq.(4.21), wherein the localizators are computed by solving the unit cell problems Eq.(4.18). The homogenized dynamical equations of motion are obtained by taking the spatial averaging of its microscopic counterpart and using the definition of the macroscopic stress and momentum from Eq. (4.8):

$$\mathrm{div}_y \tilde{\boldsymbol{\sigma}}_k + i\mathbf{k}.\tilde{\boldsymbol{\sigma}}_k = i\omega \tilde{\mathbf{p}}_k \Rightarrow i\mathbf{k}.\left\langle \tilde{\boldsymbol{\sigma}}_k \right\rangle_Y = i\omega \left\langle \tilde{\mathbf{p}}_k \right\rangle_Y \Rightarrow \mathbf{k}.\tilde{\boldsymbol{\Sigma}}_k = \omega \tilde{\mathbf{P}}_k \tag{4.26}$$

Inserting therein the previous effective constitutive law from Eq. (4.25) delivers in turn:

$$\begin{array}{l} \mathbf{k}.\mathbf{C}^{\Sigma\Sigma}_{k,\omega} : \tilde{\mathbf{E}}_k + i\omega \mathbf{k}.\mathbf{S}^{\Sigma P}_{k,\omega}.\tilde{\mathbf{U}}_k = i\omega \left(\mathbf{S}^{P\Sigma}_{k,\omega} : \tilde{\mathbf{E}}_k + i\omega \boldsymbol{\rho}^{H}_{k,\omega}.\tilde{\mathbf{U}}_k \right) \\ \tilde{\mathbf{E}}_k = i\mathbf{k} \otimes^S \tilde{\mathbf{U}}_k \\ \Rightarrow \left\{ i\mathbf{k}.\mathbf{C}^{\Sigma\Sigma}_{k,\omega}.\mathbf{k} + i\omega \mathbf{k}.\mathbf{S}^{\Sigma P}_{k,\omega} + \omega i \frac{1}{2} \left(\mathbf{S}^{P\Sigma}_{k,\omega} + \left(\mathbf{S}^{P\Sigma}_{k,\omega} \right)^T \right).\mathbf{k} - \omega^2 \boldsymbol{\rho}^{H}_{k,\omega} \right\}.\tilde{\mathbf{U}}_k = \mathbf{0} \end{array} \tag{4.27}$$

in which the transpose of the third order tensor $\mathbf{S}^{P\Sigma}_{k,\omega}$ is taken over the last two indices, so that $\left(\mathbf{S}^{P\Sigma}_{k,\omega}\right)^{T}_{ijk} = \left(\mathbf{S}^{P\Sigma}_{k,\omega}\right)_{ikj}$. The necessary condition for previous system of algebraic equations showing a cubic form in the frequency to have non-trivial solutions is the vanishing of its determinant (denoted with two bars), viz.

$$D(k,\omega) := \left| i\mathbf{k}.\mathbf{C}^{\Sigma\Sigma}_{k,\omega}.\mathbf{k} + i\omega\mathbf{k}.\mathbf{S}^{\Sigma P}_{k,\omega} + \omega i\frac{1}{2}\left(\mathbf{S}^{P\Sigma}_{k,\omega} + \left(\mathbf{S}^{P\Sigma}_{k,\omega}\right)^{T}\right).\mathbf{k} - \omega^2\boldsymbol{\rho}^{H}_{k,\omega}\right| = 0 \qquad (4.28)$$

These last relations constitute the dispersion relations, which is here exploited to evaluate the phase velocity. Adopting a constant value of the homogenized Cauchy moduli and a linear approximation of strain gradient homogenized moduli (as inferred from Fig.7), we compute the phase velocity versus the normalized wavenumber, represented in Fig. 8. Eq. (4.28) leads to two real solutions and two complex conjugated solutions, the imaginary part of which being negligible; this entails a double root of Eq.(4.28), thus two acoustic branches and one optical branch are obtained.

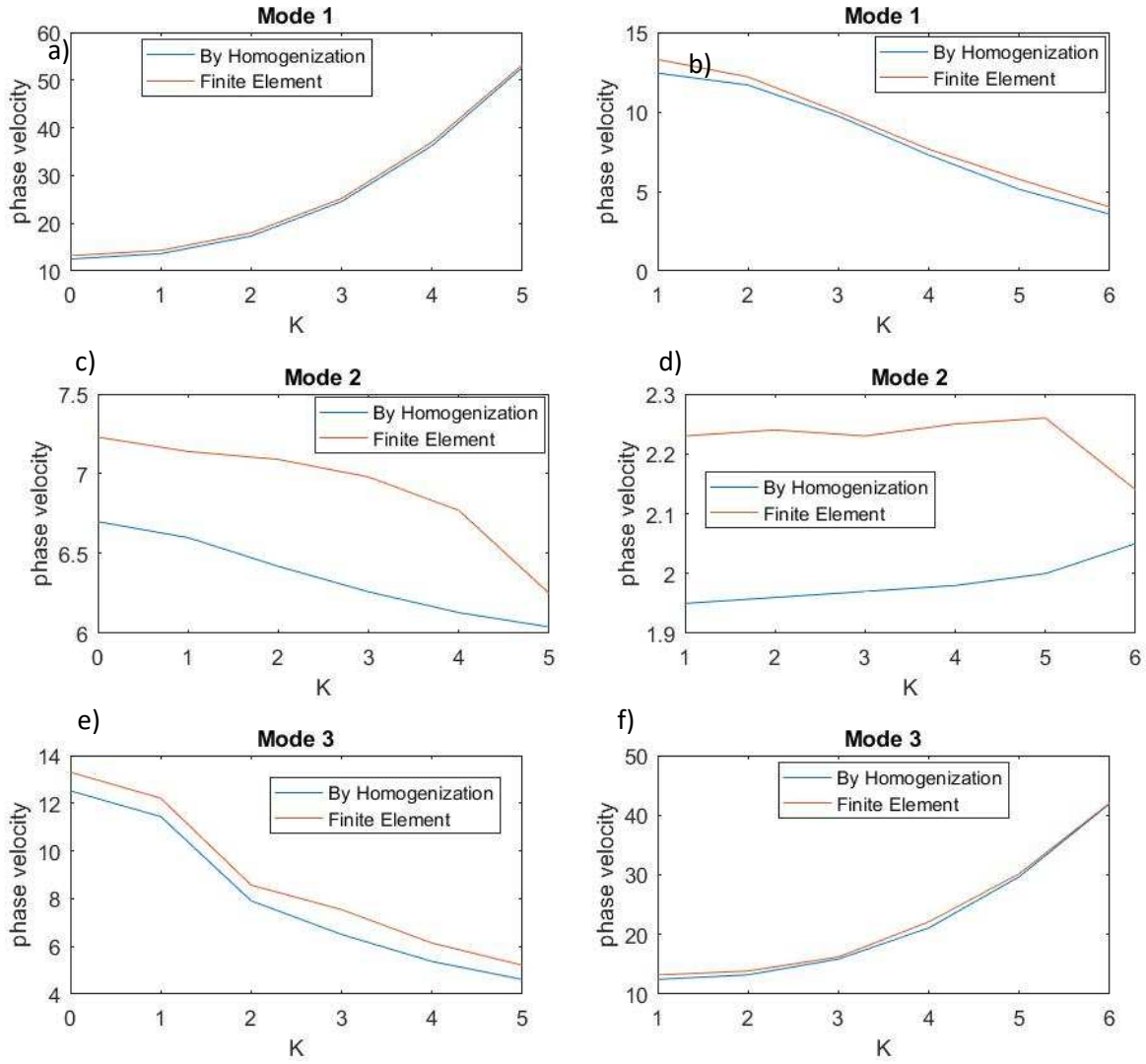

Figure 8: Normalized phase velocity in function of dimensionless wavenumber K for two incident angles, predicted by the nonlocal homogenized model and the reference Floquet-Bloch

solution. $\beta = 0°$ (subplots a,c,e). $\beta = 30°$ (subplots b,d,f). The phase velocity is normalized by the longitudinal phase velocity of the matrix constituent.

The phase velocity predictions are compared with the full solutions obtained using Floquet-Bloch theorem, computed over the unit cell of Fig.2, which defines the reference solution to assess the accuracy of the predictions of the effective nonlocal model. The plots of Fig.8 show that the propagating modes 1 and 3 are well predicted by the dynamical homogenized model, whereas a difference of about 10% appears for mode 2 between the phase velocity predicted by the homogenized model and the phase velocity derived from the reference solution obtained using Floquet-Bloch theorem. These differences are attributed to the performed interpolation of the effective moduli versus wavenumber using in the calculation of phase velocities.

Moreover, the phase velocity of Fig.8 shows a clear separation between the three modes, underlining the existence of band gaps, as shown in Fig.9. For the nonlocal model, a full band gap is evidenced on Fig.9 depending on the range of incident wave vector orientations (band gaps are present for $\beta = 30°$, but not for $\beta = 0°$, a value for which crossing of two branches occurs.

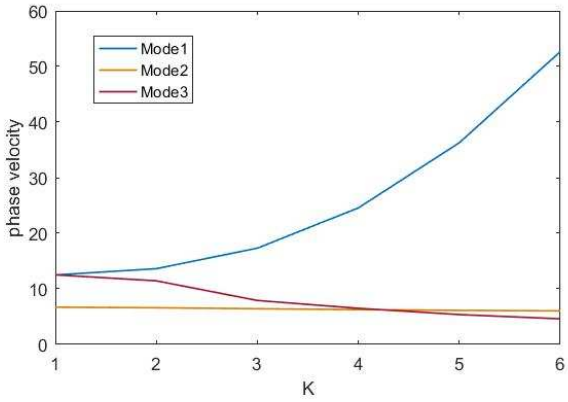

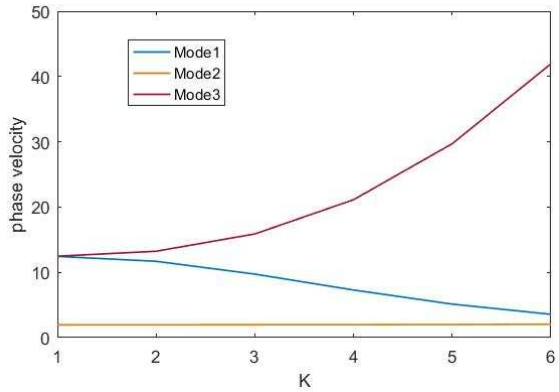

Figure 9: Normalized phase velocity in function of dimensionless wavenumber K for two incident angles $\beta = 0°$ (left) and $\beta = 30°$ (right) predicted by the nonlocal homogenized model

Inspection of Fig.10 leads to conclude that the two acoustic modes 1 and 2 represents the phase velocities of the longitudinal and shear modes that prevail for the Cauchy and second gradient media.

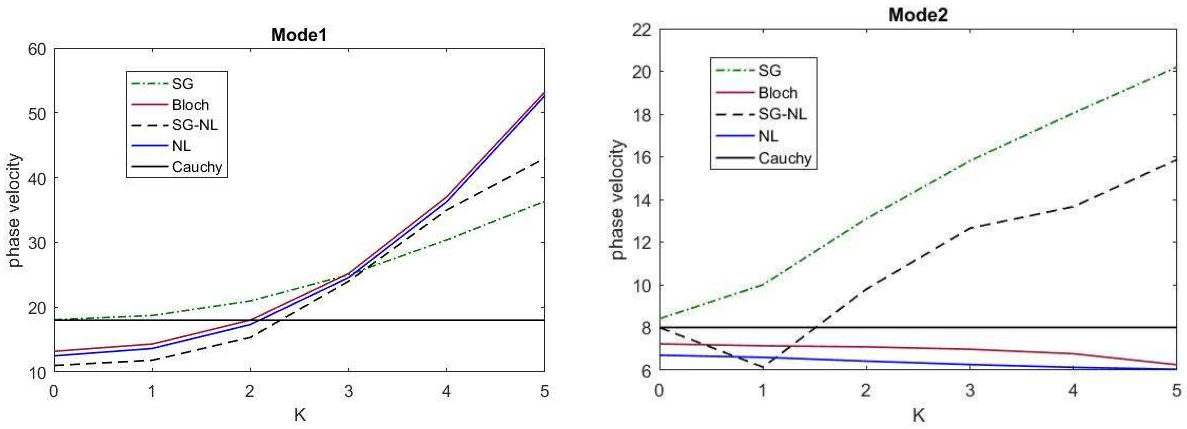

Figure 10: Comparison of the normalized phase velocity versus the dimensionless wavenumber $K = kL$ for the incident angle $\beta = 0°$ for the different effective media.

Mode 3 in Fig.8 represents the phase velocity plot for the optical branch reached solely by the nonlocal medium and that cannot be obtained by classical Cauchy type homogenization in which the displacement is the sole degree of freedom. The second gradient nonlocal solution is far from the Bloch solution at low wavelengths for both modes, whereas the nonlocal solution is very close to Bloch solution and it thus predicts much better the dispersive behavior of the initial heterogeneous medium as shown in Fig.10.

In the low frequency region (so for low values of the wavenumber K), the phase velocity for the local and nonlocal second gradient media is very close to the predictions of Floquet-Bloch solution and the nonlocal medium for both modes 1 and 2. As the wave number increases, a noticeable difference between modes appears; this reflects the fact that the second gradient medium predictions are limited to low frequencies (up to wavenumber values $K = 2.5$, corresponding to wavelengths more than three times larger than the unit cell size). In contrast to this, the nonlocal medium exhibits a larger interval of validity in terms of frequencies, since its predictions are in excellent agreement with the reference Floquet-Bloch type prediction up to normalized wavenumber values K=4.

Waves can propagate under the tripe condition enunciated in (Nassar, 2015): i) Hill macrohomogeneity condition (see the **Appendix B** for the details of the derivation) is satisfied, ii) the wavelength is at least twice the unit cell size, and iii) the square of the phase velocity has to be bounded above by the ratio of the maximum eigenvalue of the microscopic elasticity tensor $\lambda_I(\mathbf{y})$, normalized by the microscopic density $\rho(\mathbf{y})$, so that the following condition has to hold:

$$c_p{}^2 \leq \max_{\mathbf{y}\in Y,I}\left(\frac{\lambda_I(\mathbf{y})}{\rho(\mathbf{y})}\right) \tag{4.29}$$

This last condition sets an inverse relation between the frequency of propagating waves and the allowed wavelengths. Based on the mechanical parameters listed in Table 2 for both matrix and fiber, we shall note that the square of the normalized phase velocities should be bounded by the maximum value 506, which is the case considering the range of phase velocities exhibited in Fig. 10.

4.6. Discussion

Local generalized continua provide a good description of the dynamics and dispersion relations only over a small window of wavelengths. The classical Long-Wavelength (LW) and Low-Frequency (LF) homogenization theories (Bensoussan et al., 1978; Sanchez-Palencia, 1980) deliver a homogeneous substitution Cauchy medium missing all dispersive effects and all internal resonances, thus all optical modes. Extending this theory, the higher-order LW-LF asymptotic homogenization approaches (Andrianov et al., 2008; Boutin and Auriault, 1993) lead to homogenized strain-gradient continua that can model well dispersive behaviors and size effects but that are valid only near the acoustic branches whatever the order of the employed asymptotic approximations. High-frequency asymptotic approaches (Antonakakis et al., 2014; Boutin et al., 2014; Craster et al., 2010; Nolde et al., 2011) succeed in capturing high-frequency optical modes but are still valid only in the vicinity of some finite frequency. In contrast to these, the high-contrast asymptotic approaches (Auriault and Bonnet, 1985; Auriault and Boutin, 2012; Smyshlyaev, 2009) have a wide frequency validity domain encompassing an infinite number of optical branches; the corresponding effective behavior is nonlocal in time. The non-asymptotic theory developed by Willis (1997, 2011) yields the entire dispersion curve.

The extended theories constructed in the present contribution have some domain of validity; higher-grade continua lack internal degrees of freedom, with the consequence that optical branches cannot be captured. In the long wavelength, low frequency limit, the dispersion relation becomes linear, thus dispersive effects do vanish. In the low frequency regime, the phase velocity for the local and nonlocal second gradient media is well predicted considering the Floquet-Bloch solution for both modes 1 and 2. As the wave number increases, a noticeable difference between modes appears; this reflects the fact that the second gradient medium predictions are limited to low frequencies (and for wavelengths at least three times larger the unit cell size). The nonlocal medium exhibits a larger interval of validity in terms of frequencies, with predictions in excellent agreement with Floquet-Bloch solution up to normalized wavenumber values K=4.

The panel of developed dynamical homogenized models has been benchmarked in terms of their capability to predict the phase velocity versus normalized wavenumber. Cauchy and second gradient media predict two acoustic modes corresponding to longitudinal and shear waves. The nonlocal in time (but local in space) strain gradient dynamical formulation describes the dynamics at medium and high frequencies, thereby extending the range of validity of the low frequency – low wavelengths purely local strain gradient models; it nevertheless can only capture acoustic branches. The nonlocal medium enables to access the optical mode thanks to the nonlocality in time and space inherent to its formulation, having the advantage of relying on a kinematic description solely based on the displacement, and not involving additional degrees of freedom (like e.g. the micromorphic medium). The effect of nonlocality appears to be more pronounced for longitudinal waves in comparison to shear waves. Band gaps appear between the acoustic and optical modes within a certain range of orientations of the incident wave vector, considering the separation of the phase velocity plots shown in Fig.9. The second gradient nonlocal solution proves to be far from Bloch solution at low wavelengths, whereas the nonlocal solution is very close to Bloch solution and it thus predicts much better the dispersive behavior of the initial heterogeneous medium.

The structure of waves has been restricted to harmonic Bloch type waves in this contribution. Preservation of the form of the incident waves in conditions of wavelength comparable to the microstructure size and / or frequency close to the resonance frequencies of the microstructure may be questionable. Therefore, consideration of more general wave types remains as an important perspective of development of the present work.

5. Conclusion

In this contribution, we have derived nonlocal dynamical models of heterogeneous periodic materials of Willis type, enlarged to the medium frequencies and / or short wavelengths regimes, using a variational formulation and a Fourier (in the time domain) or Fourier-Floquet-Bloch transform of the initial elastodynamics boundary value problem. The formulation of a dynamical energy equivalence based on the Lagrangian building the Hamilton formulation of dynamical equilibrium and the established dynamical Hill macrohomogeneity condition plays a central role in the elaboration of the homogenized dynamical behavior. The weak form of the unit cell dynamical equilibrium has been formulated from Hamilton principle, in which the Lagrangian has been expressed in terms of the Floquet components of the displacement and velocity fields. These components are formulated using localization operators, leading to a constitutive law in integro-differential format when expressed in space-time domain. The resulting effective constitutive law has the peculiarity of introducing a velocity-dependent effective stress. The effective properties in Floquet-Bloch domain have been computed from a variational formulation, and they have been further used to evaluate the phase velocity versus wavenumber of propagating waves in voided composites.

More specific dynamical models involving locality in space (thus valid for long wavelengths) but nonlocality in time have been formulated as specific cases, including a Cauchy type formulation and an enhanced strain gradient homogenized model. These generalized continuum models have the capability to extend the predictability of the standard, strongly local, Cauchy formulation that restricts to the edge of the first Brillouin zone. The exhibited material symmetry manifested in the polar frequency plots of the purely local in time strain gradient effective medium breaks down for the nonlocal strain gradient continuum. The nonlocal dynamical model is very close to Bloch predictions and it thus predicts much better the dispersive behavior of heterogeneous media; moreover, the nonlocal model predicts full band gaps, depending on the orientations of the incident wave vector.

The established dynamical homogenization formulations provide the basis for the development of a numerical platform to compute the effective properties of architectured materials including metamaterials) and composites exhibiting such nonlocal behaviors reflecting at the macrolevel the dynamical response of their underlying microstructure.

References

Achenbach, J.D., 2003. Reciprocity in elastodynamics, pp. 91–93. Cambridge, UK: University of Cambridge.

Aifantis E, 1992. On the role of gradients in the localization of deformation and fracture. Int. J. Engng Sci., 30:1279-1299.

Aifantis E., 1999. Strain gradient interpretation of size effects. Int. J. Fract., 95:299-314.Allaire, G., 1992. Homogenization and two-scale convergence. SIAM Journal on Mathematical Analysis 23, 1482–1518.

Allaire, G., Conca C., 1998. Bloch wave homogenization and spectral asymptotic analysis, J. Math. Pures. Appl. 77, 153-208.

Allaire, G., Piatnitski, A., 2005. Homogenisation of the Schrödinger equation and effective mass theorems, Commun. Math. Phys. 258, 1-22.

Andrianov, I.V., Bolshakov, V.I., Danishevs'kyy, V.V., Weichert, D., 2008. Higher order asymptotic homogenization and wave propagation in periodic composite materials. Proceedings of the Royal Society A, 464(2093), 1181–1201. https://doi.org/10.1098/rspa.2007.0267.
Andrianov, I.V., Awrejcewicz, J., Danishevs'kyy, V.V., Weichert, D., 2011. Wave propagation in periodic composites: higher-order asymptotic analysis versus plane-wave expansion method. Journal of Computational and Nonlinear Dynamics 6(1), 011015-1 - 011015-8.DOI: 10.1115/1.4002389.
Andrianov, I., Awrejcewicz, J., Weichert, D., 2010. Improved Continuous Models for Discrete Media. Mathematical Problems in Engineering, http://dx.doi.org/10.1155/2010/986242.
Antonakakis, T., Craster, R.V., Guenneau, S., 2014. Homogenisation for elastic photonic crystals and dynamic anisotropy. J. Mech. Phys. Solids, 71, 84-96.
Auriault, J.L., Boutin, C., 2012. Long wavelength inner-resonance cut-off frequencies in elastic composite materials. Int. J. Solids Struct., 49(23–24), 3269-3281.
Askes H, Aifantis E., 2009. Gradient elasticity and flexural wave dispersion in carbon nanotubes. Phys. Rev. B, 80:195412.
Askes, H., Aifantis, E., 2011. Gradient elasticity in statics and dynamics: An overview of formulations, length scale identification procedures, finite element implementations and new results. Int. J. Solids Struct., 48(13),1962-1990.
Auriault, J., Bonnet, G., 1985. Dynamique des composites élastiques périodiques. Arch. Mech., 37, 269–284.
Ayad, M., Karathanasopoulos, N., Reda, H., Ganghoffer, J.F., Lakiss, H. 2019. On the role of second gradient constitutive parameters in the static and dynamic analysis of heterogeneous media with micro-inertia effects Int. J. Solids Struct. DOI: 10.1016/j.ijsolstr.2019.10.017
Bacigalupo, A., Gambarotta, L., 2010. Strain-gradient computational homogenization of heterogeneous materials with periodic microstructure. ZAMM Z. Angew. Math. Mech. 90, 796–811. https://doi.org/10.1016/j.ijsolstr.2012.07.002.
Bacigalupo, A. 2014a. Second-order homogenization of periodic materials based on asymptotic approximation of the strain energy: formulation and validity limits. Materials Science. arXiv:1401.7855.
Bacigalupo, A., Gambarotta, L., 2014b. Second-gradient homogenized model for wave propagation in heterogeneous periodic media. Int. J. Solids Struct., 51(5) 1052-1065.https://doi.org/10.1016/j.ijsolstr.2013.12.001.
Bensoussan, A., Lions, J.L., Papanicolaou, G., 1978. Asymptotic analysis for periodic structures. North-Holland Publishing Company.
Berezovski, A., Engelbrecht, J., Salupere, A., Tamm, K., Peets, T., Berezovski, M., 2013. Dispersive waves in microstructured solids. Int. J. Solids Struct., 50(11–12) 1981-1990.doi: https://doi.org/10.1016/j.ijsolstr.2013.02.018.
Birman, M. S., Suslina, T. A., 2006. Homogenization of a multidimensional periodic elliptic operat
or in a neighborhood of the edge of an internal gap, J. Math. Sciences 136, 3682-3690.
Boutin, C., Auriault, J.L., 1993. Rayleigh scattering in elastic composite materials. International Journal of Engineering Science, 31(12) 1669-1689. https://doi.org/10.1016/0020-7225(93)90082-6.
Boutin, C., 1996. Microstructural effects in elastic composites. Int. J. Solids Struct., 33 (7) 1023-105.
Boutin, C., Hans, S., Chesnais, C., 2010. Dynamics of reticulated structures. Mechanics of generalized continua. Springer, New York, PP.131-141. Advances in Mechanics and Mathematics, Volume 21.
Boutin, C. Rallu, A., Hans, S., 2014. Large scale modulation of high frequency waves in periodic elastic composites. J. Mech. Phys. Solids, 70, 362-381.

Braides, A., 2002. Gamma-convergence for beginners. Oxford lecture series in mathematics and its applications, Oxford University Press.
Chesnais, C., Boutin, C., & Hans, S., 2015. Wave propagation and non-local effects in periodic frame materials: Generalized continuum mechanics. Math. Mech. Solids, 20(8), 929–958. https://doi.org/10.1177/1081286513511092
Chen, W., Fish, J., 2000. A dispersive model for wave propagation in periodic heterogeneous media based on homogenization with multiple spatial and temporal scales. J. Applied Mech., 68(2), 153-161. doi:10.1115/1.1357165.
Colquitt, D. J., 2018. Composite dynamic models for periodically heterogeneous media. 14–16. https://doi.org/10.1177/1081286518776704
Cohen-Tanoundji, C, Dupont Roc, J., Grynberg, G., 1987. Photons et atomes. Introduction à l'électrodynamique quantique. Interédition / Edition du CNRS.
Craster, R.V.,Kaplunov, J., Pichugin, A.V., 2010. High-frequency homogenization for periodic media. Proc. Royal Soc. A, 466, 2341–2362. https://doi.org/10.1098/rspa.2009.0612.
Dagan G. The generalization of Darcy's law for nonuniform flows. Water Resour. Res. 1979;15(1):1–7.
Dagan, G., 1989. Flow and Transport in Porous Formations. Heidelberg, Berlin, New York: Springer-Verlag.
Davit, Y., Bell, C., G. Byrne, H., Chapman, L.A. C., Kimpton, L.S., Lang, Georgina E., Leonard, K.H. L., Oliver, J.M., Pearson, N.C. and Shipley, R.J., Waters, S.L., Whiteley, J.P. Wood, B.D. Quintard, M., 2013. Homogenization via formal multiscale asymptotics and volume averaging: How do the two techniques compare? Advances in Water Resources, vol. 62 (part B). pp. 178-206. ISSN 0309-1708.
Drugan, W.J., Willis, J.R. 1996. A micromechanics-based nonlocal constitutive equation and estimates of representative volume element size for elastic composites. J. Mech. Phys. Solids. Volume 44, Issue 4, 497-524.
Eringen, A.C., Edelen, D.G.B., 1972. On nonlocal elasticity, Int. J. Engng Sci., 10, 3, 233-248.
Erofeyev, V. I., 2003. Wave Processes in Solids with Microstructure. World Scientific, 2003.
Fafalis, D., Filopoulos, S., Tsamasphyros, G., 2012. On the capability of generalized continuum theories to capture dispersion characteristics at the atomic scale. Eur. J. Mech/ A/Solids, 36, 25–37. doi:10.1016/j.euromechsol.2012.02.004.
Fish, J., Chen, W., 2001. Higher-order homogenization of initial/boundary-value problem, J. Eng. Mech. 127, 1223-1230.
Floquet, G., 1883. Sur les équations différentielles linéaires à coefficients périodiques. Annales de l'Ecole Normale Supérieure 12, 47–88.
Ganghoffer, J.F., Reda, H., 2021. A Variational approach of homogenization of heterogeneous materials toward second gradient continua. Mech. Mat., 103743.
Gazalet, J., Dupont, S., Kastelik, J.C., Rolland, Q., Djafari-Rouhani, B., 2013. A tutorial survey on waves propagating in periodic media: electronic, photonic and phononic crystals. Perception of the Bloch theorem in both real and Fourier domains. Wave motion, 50, 619-654.
Gelhar, L.W., Gutjahr, A.L., Naff, R.L., 1979. Stochastic Analysis of Macrodispersion in a Stratified Aquifer. Water Resour. Res., 15(6):1387–97.
Guenneau, S., Craster, R., Antonakakis, T., Cherednichenko, K., Cooper, S., 2013. Homogenization Techniques for Periodic Structures. E. Popov. Gratings: Theory and Numeric Applications, AMU (PUP), pp.11.1-11.31.https://hal.archives-ouvertes.fr/hal-00785718.
Hoefer, M. A., Weinstein, M. I., 2011. Defect modes and homogenization of periodic Schrödinger operators, SIAM J. Math. Anal. 43, 971-996.
Huang, Z.G., 2011. Analysis of Acoustic Wave in Homogeneous and Inhomogeneous Media Using Finite Element Method. Acoustic Waves - From Microdevices to Helioseismology, Marco G. Beghi, IntechOpen.DOI: 10.5772/18792.

Karathanasopoulos, N., Reda, H., & Ganghoffer, J.-F., 2019. The role of non-slender inner structural designs on the linear and non-linear wave propagation attributes of periodic, two-dimensional architectured materials. J. Sound Vibrations, 455, 312–323. https://doi.org/10.1016/J.JSV.2019.05.011.
Koiter, W.T., 1964. Couple-stresses in the theory of elasticity: I and II. K. Ned. Akad. Wet. (R.Neth.Acad.ArtsSci.) B; 67:17–44.

Matheron, G., 1966. Genèse et signification énergétique de la loi de Darcy. Rev Inst. Français du Pétrole. 21(11):1697–706.
Mencik, J.M., Duhamel, D.A., 2015. Wave-based model reduction technique for the description of the dynamic behavior of periodic structures involving arbitrary-shaped substructures and large-sized finite element models. Finite Elements in Analysis and Design, Elsevier, 101(2015)1-14. https://doi.org/10.1016/j.finel.2015.03.003
Milton GW, Willis JR. 2007. On modifications of Newton's second law and linear continuum elastodynamics. Proc. R. Soc. A 463. (doi:10.1098/rspa.2006.1795)
Mindlin, R.D., 1964. Micro-structure in linear elasticity. Arch. Rat. Mech. Anal., 16(1), 51–78. https://doi.org/10.1007/BF00248490.
Mindlin, R., 1965. Second gradient of strain and surface-tension in linear elasticity. International Journal of Solids and Structures, 1(4), 417-438.https://doi.org/10.1016/0020-7683(65)90006-5.
Mindlin, R.D., 1972. Elasticity, piezoelectricity and crystal lattice dynamics. J. Elasticity, 2(4), 217–282.https://doi.org/10.1007/BF00045712.
Nassar, H., He, Q.C., Auffray, N., 2015. Willis elastodynamic homogenization theory revisited for periodic media. J. Mech. Phys. Solids, 77, 158-178.
Nassar, H., He, Q.C., Auffray, N., 2016. A generalized theory of elastodynamic homogenization for periodic media. Int. J. SolidsStruct., 84, 139-146.
Nemat-Nasser, S., Srivastava, A., 2011. Overall dynamic constitutive relations of layered elastic composites. Journal of the Mechanics and Physics of Solids 59(10), 1953-1965.Doi: 10.1016/j.jmps.2011.07.008.
Nemat-Nasser, S., Willis, J. R., Srivastava, A., Amirkhizi, A. V., 2011. Homogenization of periodic elastic composites and locally resonant sonic materials, Phys. Rev. B 83, 104103.
Nolde, E., Craster, R.V., Kaplunov, J., 2011. High frequency homogenization for structural mechanics. J. Mech. Phys. Solids, 59(3), 651-671.
Norris, A.N., Shuvalov, A.L., Kutsenko, A.A., 2012. Analytical formulation of three-dimensional dynamic homogenization for periodic elastic systems. Proc. R. Soc. A 468, 1629–1651. (doi:10.1098/rspa.2011.0698).
Oliver, J.M., Pearson, N.C., Shipley, R.J., Waters, S.L., Whiteley, J.P., Wood, B.D., Quintard, M. Homogenization via formal multiscale asymptotics and volume averaging: How do the two techniques compare? (2013) Advances in Water Resources, vol. 62 (part B). pp. 178-206. ISSN 0309-1708.
Panasenko, G.,2005. Multi-scale Modelling for Structures and Composites, Springer Netherlands, 2005.
Papargyri-Beskou, S., Polyzos, D., Beskos. D.E., 2009. Wave dispersion in gradient elastic solids and structures: a unified treatment. International Journal of Solids and Structures 46 (21), 3751-3759.https://doi.org/10.1016/j.ijsolstr.2009.05.002.
Pinnola, F.P., Ali Faghidian, S., Barretta, R., Marotti de Sciarra, F., 2020a. Variationally consistent dynamics of nonlocal gradient elastic beams. Int. J. Engng Sci., 149, art. no. 103220.
Pinnola, F.P., Vaccaro, M.S., Barretta, R., Marotti de Sciarra, F., 2020b. Random vibrations of stress-driven nonlocal beams with external damping. Meccanica, 56 (6), 1329-1344.
Reda, H., Ganghoffer, J.F., Lakiss, H., 2016. Micropolar dissipative models for the analysis of 2D dispersive waves in periodic lattices. J. Sound Vibr., 392. DOI: 10.1016/j.jsv.2016.12.007

Reda, H., Karathanasopoulos, N., Ganghoffer, J. F., Lakiss, H., 2018. Influence of first to second gradient coupling energy terms on the wave propagation of three-dimensional non-centrosymmetric architectured materials. Int. J. of Engng Sci., 128, 151–164. https://doi.org/10.1016/J.IJENGSCI.2018.03.014.
Reda, H., Karathanasopoulos, N., Ganghoffer, J. F., & Lakiss, H., 2018b. Wave propagation characteristics of periodic structures accounting for the effect of their higher order inner material kinematics. J. Sound Vib., 431, 265–275. https://doi.org/10.1016/J.JSV.2018.06.006
Reda, H., Karathanasopoulos, N., Elnady K., Ganghoffer, J. F., & Lakiss, H., 2018c. The role of anisotropy on the static and wave propagation characteristics of two-dimensional architectured materials under finite strains, Mat. Design, 147, 134-145, 2018, https://doi.org/10.1016/j.matdes.2018.03.039
Roca, D., Lloberas-Valls, O., Cante, J., Oliver, J., 2017. A computational multiscale homogenization framework accounting for inertial effects: Application to acoustic metamaterials modelling. Comput. Meth. Applied Mech. Engrg. DOI: https://doi.org/10.1016/j.cma.2017.10.025
Rohan, E., Miara, B., Seifrt, F., 2009. Numerical simulation of acoustic band gaps in homogenized elastic composites. Int. J. Eng. Sci., 47(4), 573–594.
Rosi, G., Auffray, N., 2016. Anisotropic and dispersive wave propagation within strain-gradient framework. Wave motion, 63, 120-134.
Rosi, G., Placidi, L., Auffray, N., 2018. On the validity range of strain-gradient elasticity: a mixed static-dynamic identification procedure. Eur. J. Mech. –A/ Solids, 69, 179-191.
Sieck, C.F., Alù, A., Haberman, M.R., 2015 Dynamic homogenization of acoustic metamaterials with coupled field response. Phys. Procedia 70, 275–278. (doi:10.1016/j.phpro.2015.08.153).
Silva, P.B. Mencik, J.M., Arruda, J.R.F., 2015. Wave finite element-based superelements for forced response analysis of coupled systems via dynamic substructuring. Int. J. Num. Meth. Eng. 107, 453-476. https://doi.org/10.1002/nme.5176
Slattery, J.C., 1967. Flow of Viscoelastic Fluids Through Porous Media. AIChE J. 1967;13:1066–71.
Smyshlyaev, V. P., 2009. Propagation and localization of elastic waves in highly anisotropic periodic composites via two-scale homogenization. Mech. Mater., 41, 434–447.
Smyshlyaev, V.P., Cherednichenko, K.D., 2000. On rigorous derivation of strain gradient effects in the overall behaviour of periodic heterogeneous media. Journal of the Mechanics and Physics of Solids 48(6):1325-1357. DOI: 10.1016/S0022-5096(99)00090-3.
Srivastava A, Nemat-Nasser S. 2011. Overall dynamic properties of three-dimensional periodic elastic composites. Proc. R. Soc. A 468, 269–287 (doi:10.1098/rspa.2011.0440).
Srivastava, A., 2015. Causality and passivity in elastodynamics. Proc. R. Soc. A 471, 20150256. (doi:10.1098/rspa.2015.0256).
Suiker, A. S. J., Metrikine, A. V., & de Borst, R., 2001. Comparison of wave propagation characteristics of the Cosserat continuum model and corresponding discrete lattice models. Int. J. Solids Struct., 38(9), 1563–1583. https://doi.org/10.1016/S0020-7683(00)00104-9.
Sun, C.T., Huang, G.L., 2006. Modeling Heterogeneous Media with Microstructures of Different Scales. J. Applied Mech., 74(2), 203–209. doi:10.1115/1.2188536.
Toupin, R.A., 1962. Elastic materials with couple-stresses. Arch. Rat. Mech. Anal., 11, 385–414.
Wang, J., & Chen, W., 2019. Abnormal wave propagation behaviors in two-dimensional mass – spring structures with nonlocal effect. https://doi.org/10.1177/1081286519853606.
Wang, Z.-P., Sun, C.T., 2002. Modelling micro-inertia in heterogeneous materials under dynamic loading. Wave Motion, 36(4), 473–485. DOI: 10.1016/S0165-2125(02)00037-9.
Willis, J.R., 1981. Variational principles for dynamic problems for inhomogeneous elastic media.
Wave Motion 3, 1–11. (doi:10.1016/0165-2125(81)90008-1).

Willis JR. 1997. Dynamics of composites. In Continuum micromechanics, pp. 265–290. CISM Lecture Notes, 495. New York, NY: Springer.
Willis, J.R., 2011. Effective constitutive relations for waves in composites and metamaterials. Proceedings of the Royal Society A: Mathematical, Physical and Engineering Sciences, 467, 1865-1879.
Whitaker, S., 1967. Diffusion and dispersion in porous media. AICHE J. 1967;13:420–7.
Zhikov, V.V., 2000. On an extension of the method of two-scale convergence and its applications. Sbornik: Mathematics, 191(7), 973-1014.DOI:10.1070/SM2000v191n07ABEH000491.

Appendix A: Lagrange and Hamilton equations for a dynamical field theory

The notion of functional derivative is useful each time a law of physics is formulated by a variational principle (Cohen-Tanoundji, 1993): for a dynamical system, the Lagrangian L_M that intervenes as a temporal density of the action integral $S\left[A_j(\mathbf{x},t)\right]$ is itself a functional of the fields $\left(A_i, \dot{A}_j, \partial_i A_j\right)$, considering here vector fields in a first gradient theory for the sake of clarity of the presentation:

$$S\left[A_j(\mathbf{x},t)\right] := \int_{t_i}^{t_f} L_M\left(A_i, \dot{A}_j, \partial_i A_j\right) dt, \quad L_M\left(A_i, \dot{A}_j, \partial_i A_j\right) := \int_D l\left(A_i, \dot{A}_j, \partial_i A_j\right) dV \tag{A1}$$

Introducing therein the Lagrangian spatio-temporal density $l\left(A_i, \dot{A}_j, \partial_i A_j\right)$, and in which the domain corresponds to the unit cell for a periodic heterogeneous material. The differential of the Lagrangian is evaluated using the functional derivative denotes with an overhead bar as

$$L_M := \int_D \left(\frac{\bar{\partial} L_M}{\bar{\partial} A_j} \delta A_j + \frac{\bar{\partial} L_M}{\bar{\partial} \dot{A}_j} \delta \dot{A}_j \right) dx \tag{A2}$$

with the identification of the functional derivatives therein written with the partial derivative notation $\frac{\bar{\partial}(.)}{\bar{\partial}(.)}$ that easily follows as

$$\frac{\bar{\partial} L}{\bar{\partial} A_j} = \frac{\partial l}{\partial A_j} - \partial_i \left(\frac{\partial l}{\partial \left(\partial_i A_j\right)} \right); \quad \frac{\bar{\partial} L}{\bar{\partial} \dot{A}_j} = \frac{\partial l}{\partial \dot{A}_j} \tag{A3}$$

For a continuous system, the variation of the action can be expressed using the functional derivative as

$$\delta S\left[A_j(\mathbf{x},t)\right] := \int_{t_i}^{t_f} dt \int_D dV \frac{\bar{\partial} S}{\bar{\partial} A_j} \delta A_j \tag{A4}$$

The stationary action principle, equation $\frac{\bar{\partial} S}{\bar{\partial} A_j} = 0$, can be made more explicit

$$\delta S\left[A_j(\mathbf{x},t)\right] := \int_{t_i}^{t_f} dt \delta L_M(t) = \int_{t_i}^{t_f} dt \int_D dV \left\{ \frac{\bar{\partial} L_M}{\bar{\partial} A_j} - \frac{d}{dt}\left(\frac{\bar{\partial} L_M}{\bar{\partial} \dot{A}_j} \right) \right\} \delta A_j \Rightarrow \frac{\bar{\partial} S}{\bar{\partial} A_j} = \frac{\bar{\partial} L_M}{\bar{\partial} A_j} - \frac{d}{dt}\left(\frac{\bar{\partial} L_M}{\bar{\partial} \dot{A}_j} \right) = 0 \quad (A5)$$

The use of the functional derivatives leads to field equations that are formally identical to the discrete case. The Hamilton equations of motion for a field shall also take a similar form: let first define the momentum of the field and the Hamiltonian

$$\Pi_j := \frac{\partial L_M}{\partial \dot{A}_j} \Rightarrow H_M := \int_D dV \left(\Pi_j \dot{A}_j - L_M \right) \quad (A6)$$

An easy calculation of the variation of H_M using the functional derivative and the definition of H_M leads to Hamilton equations:

$$\dot{\Pi}_j := \frac{\bar{\partial} H_M}{\bar{\partial} A_j}, \ \dot{A}_j := \frac{\bar{\partial} H_M}{\bar{\partial}_j \Pi_j} \quad (A7)$$

Appendix B: Hill's macrohomogeneity condition for the dynamical strain gradient medium

Let consider a symmetrical stress tensor field $\boldsymbol{\sigma}$ defined in the unit cell, assumed to have a rectangular shape (Fig. B1) compatible allowing space tessellation and verifying the following BVP over the unit cell with anti-periodic traction, and with $\mathbf{f}$ the body force vector:

$$\begin{cases} \nabla_y \cdot \boldsymbol{\sigma} + \mathbf{f} = \rho \ddot{\mathbf{u}} \\ \boldsymbol{\sigma}.\mathbf{n} \quad \text{opposite on opposite edges of } \partial Y \end{cases} \quad (B1)$$

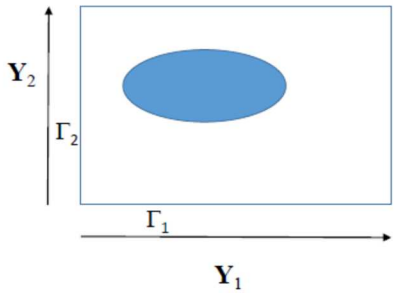

Figure A1: composite unit cell and the associated periodicity vectors $\mathbf{Y}_1, \mathbf{Y}_2$ in a 2D situation

The weak formulation of previous equations is obtained in a conventional way, multiplying Eq. (B1) with an arbitrary differentiable vector field $\boldsymbol{\omega}$ and integrating over the unit cell domain Y an over a given time interval $\left[t_i, t_f\right]$, so that it holds

$$\forall \boldsymbol{\omega}, \quad \int_{t_i}^{t_f} \int_Y \left(\nabla_y \cdot \boldsymbol{\sigma} \right) \cdot \boldsymbol{\omega} dV + \int_{t_i}^{t_f} \int_Y \mathbf{f} \cdot \boldsymbol{\omega} dV = \int_{t_i}^{t_f} \int_Y \rho \ddot{\mathbf{u}} \cdot \boldsymbol{\omega} dV \quad (B2)$$

In the sequel, we will concentrate on the domain (spatial) integral alone, so that time integral in (B2) will be temporarily dropped. Integrating by parts Eq.(B2) and using the divergence theorem delivers the relation

$$-\int_{\mathrm{Y}} \boldsymbol{\sigma} : (\boldsymbol{\omega} \otimes \nabla_{\mathrm{y}}) \mathrm{dV} + \int_{\partial \mathrm{Y}} (\boldsymbol{\sigma} \cdot \mathbf{n}) . \boldsymbol{\omega} \, \mathrm{ds} + \int_{\mathrm{Y}} \mathbf{f} \cdot \boldsymbol{\omega} \mathrm{dV} = \int_{\mathrm{Y}} \rho \ddot{\mathbf{u}} \cdot \boldsymbol{\omega} \mathrm{dV} \tag{B3}$$

Taking into account the boundary condition of Eq. (B1) provides the weak formulation of Eq. (B1) as

$$\forall \boldsymbol{\omega}, \quad -\int_{Y} \boldsymbol{\sigma} : (\boldsymbol{\omega} \otimes \nabla_{y}) dV + \sum_{i=1,2} \int_{\partial Y} (\boldsymbol{\sigma} \cdot \mathbf{n}) \cdot [\![\boldsymbol{\omega}]\!]^{i} ds + \int_{Y} \mathbf{f} \cdot \boldsymbol{\omega} dV = \int_{Y} \rho \ddot{\mathbf{u}} \cdot \boldsymbol{\omega} dV \tag{B4}$$

with the difference of the vector field $\boldsymbol{\omega}$ taken over opposite edges of the unit cell:

$$[\![\boldsymbol{\omega}]\!]^{i} := \boldsymbol{\omega}\left(\mathbf{y} + \mathbf{Y}^{i}\right) - \boldsymbol{\omega}\left(\mathbf{Y}^{i}\right), \ \ \mathrm{i}=1,2 \tag{B5}$$

The traction over the unit cell boundary is identified in (B4) as the vector $\mathbf{t} = \boldsymbol{\sigma} \cdot \mathbf{n}$. By imposing $[\![\boldsymbol{\omega}]\!]^{i} = \mathrm{Constant}$ on the unit cell boundary $\Gamma^{i}, \ i = 1,2$ it holds further

$$-\int_{Y} \boldsymbol{\sigma} : (\boldsymbol{\omega} \otimes \nabla_{y}) dV + \sum_{i=1,2} [\![\boldsymbol{\omega}]\!]^{i} \cdot \int_{\partial Y} (\boldsymbol{\sigma} . \mathbf{n}) ds + \int_{Y} \mathbf{f} \cdot \boldsymbol{\omega} dV = \int_{Y} \rho \ddot{\mathbf{u}} \cdot \boldsymbol{\omega} dV \tag{B6}$$

Assuming $\boldsymbol{\omega}$ of the form

$$\boldsymbol{\omega}(\mathbf{x}, \boldsymbol{\xi}) = \mathbf{V}(\mathbf{x}) + \delta \mathbf{E}(\mathbf{x}) \cdot \boldsymbol{\xi} + \frac{1}{2} \delta \mathbf{K} \cdot (\boldsymbol{\xi} \otimes \boldsymbol{\xi}) \tag{B7}$$

with $\boldsymbol{\xi} := \mathbf{y} - \mathbf{x}$ therein the relative position of the micropoints within Y, $\delta \mathbf{E}(\mathbf{x}), \ \delta \mathbf{K}(\mathbf{x})$ are virtual variations of the macrostrain and macrostrain gradient, and $\mathbf{V}(\mathbf{x}), \delta \mathbf{E}(\mathbf{x}), \delta \mathbf{K}(\mathbf{x})$ are virtual variations of the controlled unit cell kinematic loading, it holds due to Eqs.(B5, B6):

$$\begin{aligned} \boldsymbol{\omega} \otimes \nabla_{y} &= \delta \mathbf{E}(\mathbf{x}) + \delta \mathbf{K}(\mathbf{x}) \cdot \boldsymbol{\xi} \\ [\![\boldsymbol{\omega}]\!]^{i} &= \delta \mathbf{E}(x) \cdot \mathbf{Y}^{i} + \frac{1}{2} \delta \mathbf{K}(\mathbf{x}) \cdot \mathbf{Y}^{i} \cdot \mathbf{Y}^{i} \end{aligned} \tag{B8}$$

Substituting Eqs. (B7), (B8) into Eq. (B6) results after straight forward calculations in

$$-\int_{Y} \boldsymbol{\sigma} : (\boldsymbol{\omega} \otimes \nabla_{y}) dV + \sum_{i=1,2} [\![\boldsymbol{\omega}]\!]^{i} \cdot \int_{\partial Y} (\boldsymbol{\sigma} . \mathbf{n}) ds + \int_{Y} \mathbf{f} \cdot \boldsymbol{\omega} dV = \int_{Y} \rho \ddot{\mathbf{u}} \cdot \boldsymbol{\omega} dV$$

It follows as a consequence the following balance equations:

$$\forall\, \delta\mathbf{V}(\mathbf{x}),\delta\mathbf{E}(\mathbf{x}),\, \delta\mathbf{L}_K(\mathbf{x}),$$

$$\left(\int_Y \mathbf{f}dV\right).\delta\mathbf{V}(\mathbf{x})=\left(\int_Y \rho\ddot{\mathbf{u}}dV\right).\delta\mathbf{V}(\mathbf{x})\Rightarrow\mathbf{F}:=\int_Y \mathbf{f}dV=\int_Y \rho\ddot{\mathbf{u}}dV$$

$$\left\{\int_Y \mathbf{f}\otimes\xi dV-\int_Y \boldsymbol{\sigma}dV+\sum_{i=1,2}\left(\int_{\partial Y}(\boldsymbol{\sigma}\cdot\mathbf{n})ds\right)\otimes\mathbf{Y}^i\right\}:\delta\mathbf{E}(x)=\left(\int_Y \rho\ddot{\mathbf{u}}\otimes\xi dV\right).\delta\mathbf{E}(\mathbf{x})\Rightarrow \tag{B9}$$

$$\langle\mathbf{f}\otimes\xi\rangle_Y=\langle\rho\ddot{\mathbf{u}}\otimes\xi\rangle_Y$$

$$\left\{\frac{1}{2}\int_Y \mathbf{f}\otimes\xi\otimes\xi dV-\int_Y(\xi\otimes\boldsymbol{\sigma})dV+\sum_{i=1,2}\left(\frac{1}{2}\left(\int_{\partial Y}(\boldsymbol{\sigma}\cdot\mathbf{n})ds\right)\otimes\mathbf{Y}^i\otimes\mathbf{Y}^i\right)\right\}.\therefore\delta\mathbf{K}(\mathbf{x})=\frac{1}{2}\left(\int_Y \rho\ddot{\mathbf{u}}\otimes\xi\otimes\xi dV\right).\therefore\delta\mathbf{K}(\mathbf{x})$$

$$\Rightarrow\langle\mathbf{f}\otimes\xi\otimes\xi\rangle_Y=\langle\rho\ddot{\mathbf{u}}\otimes\xi\otimes\xi\rangle_Y$$

Eq.(B9) results in the elaboration of the dynamic stress and hyperstress measures $\boldsymbol{\Sigma}^{dyn},\mathbf{S}^{dyn}$ of the strain gradient (dynamical) effective continuum as the following sums over the unit cell external boundary:

$$\langle\boldsymbol{\sigma}\rangle_Y=\frac{1}{|Y|}\sum_{i=1,2}\left(\int_{\partial Y}(\boldsymbol{\sigma}\cdot\mathbf{n})ds\right)\otimes\mathbf{Y}^i+\frac{1}{|Y|}\int_Y \mathbf{f}\otimes\xi dV-\frac{1}{|Y|}\int_Y \rho\ddot{\mathbf{u}}\otimes\xi dV \tag{B10}$$

$$\Rightarrow\boldsymbol{\Sigma}^{dyn}:=\langle\boldsymbol{\sigma}\rangle_Y+\langle\rho\ddot{\mathbf{u}}\otimes\xi\rangle_Y$$

$$\langle\xi\otimes\boldsymbol{\sigma}\rangle_Y=\frac{1}{2|Y|}\sum_{i=1,2}\left(\int_{\partial Y}(\boldsymbol{\sigma}\cdot\mathbf{n})ds\right)\otimes\mathbf{Y}^i\otimes\mathbf{Y}^i+\frac{1}{2|Y|}\int_Y \mathbf{f}\otimes\xi\otimes\xi dV-\frac{1}{2|Y|}\left(\int_Y \rho\ddot{\mathbf{u}}\otimes(\xi\otimes\xi)dV\right) \tag{B11}$$

$$\Rightarrow\mathbf{S}^{dyn}:=\langle\xi\otimes\boldsymbol{\sigma}\rangle_Y+\langle\rho\ddot{\mathbf{u}}\otimes(\xi\otimes\xi)\rangle_Y$$

with $\boldsymbol{\gamma}(\mathbf{x})$ therein the acceleration of the center of gravity of the unit cell. Using relation (B10) and (B6) leads after straightforward computations to

$$\forall\,\boldsymbol{\omega}^i=\text{Cst on }\Gamma^i,\quad \int_Y \boldsymbol{\sigma}:(\boldsymbol{\omega}\otimes\nabla_y)\mathrm{dV}=\sum_{i=1,2}\boldsymbol{\omega}^i\otimes\mathbf{N}^i.\langle\boldsymbol{\sigma}\rangle_Y \tag{B12}$$

Taking a constant and arbitrary stress in previous formulation, it then holds

$$\forall\,\boldsymbol{\omega}^i=\text{Cst on }\Gamma^i,$$

$$\int_Y(\boldsymbol{\omega}\otimes\nabla_y)\mathrm{dV}=\sum_{i=1,2}\boldsymbol{\omega}^i\otimes\mathbf{N}^i\equiv\int_{\partial V(x)}\boldsymbol{\omega}\otimes\mathbf{N}\mathrm{dS}(\mathbf{x})=\int_{V(x)}\boldsymbol{\omega}\otimes\nabla_y\mathrm{dS}(\mathbf{x}) \tag{B13}$$

Previous relation entails the following definition of the macrostrain (after symmeterization of previous relation) for the real microscopic displacement $\mathbf{u}(\mathbf{y})$:

$$\mathbf{E}(\mathbf{x}):=\left\langle\mathbf{u}(\mathbf{y})\otimes^S\nabla_x\right\rangle_Y \tag{B14}$$

Using then the relation (Caillerie, 2012)

$$\sum_{i=1,2}\mathbf{N}^i\otimes\mathbf{Y}^j=|Y|\mathbf{I}_2 \tag{B15}$$

with $\mathbf{I}_2$ the second order identity tensor, Eq.(B6) can be rewritten selecting a constant difference $[\![\boldsymbol{\omega}]\!]^i$ as

$$\forall \boldsymbol{\omega},\quad [\![\boldsymbol{\omega}]\!]^i = cst \rightarrow \int_Y \boldsymbol{\sigma} : (\boldsymbol{\omega} \otimes \nabla_y) dV = \sum_{i,j=1,2} \delta_{ij} [\![\boldsymbol{\omega}]\!]^i \cdot \int_{\partial Y} (\boldsymbol{\sigma} \cdot \mathbf{n}) ds \tag{B16}$$

Using the relation $\sum_{i=1,2} \mathbf{N}^i . \mathbf{Y}^j = |Y| \delta_{ij}$ arising as a consequence of (B15), see (Caillerie, 2012), Eq.(B16) rewrites:

$$\int_Y \boldsymbol{\sigma} : (\boldsymbol{\omega} \otimes \nabla_y) dV = \frac{1}{|Y|} \sum_{i,j=1,2} N^i \cdot \mathbf{Y}^j [\![\boldsymbol{\omega}]\!]^i \cdot \int_{\partial Y} (\boldsymbol{\sigma} \cdot \mathbf{n}) ds \tag{B17}$$

Eq. (B17)(B17) can be rewritten into the form

$$\int_Y \boldsymbol{\sigma} : (\boldsymbol{\omega} \otimes \nabla_y) dV = \frac{1}{|Y|} \sum_{i=1,2} \left([\![\boldsymbol{\omega}]\!]^i \otimes \mathbf{N}^i \right) : \sum_{j=1,2} \left(\int_{\partial Y} (\boldsymbol{\sigma} \cdot \mathbf{n}) ds \otimes \mathbf{Y}^j \right) \tag{B18}$$

Inserting the two relations in Eq.(B8) into relation (B17) delivers the equality

$$\begin{aligned} &\int_Y \boldsymbol{\sigma} : (\boldsymbol{\omega} \otimes \nabla_y) dV = \frac{1}{|Y|} \sum_{i=1,2} \left(\left(\delta \mathbf{E} \cdot \mathbf{Y}^i \right) \otimes \mathbf{N}^i \right) : \sum_{j=1,2} \left(\int_{\partial Y} (\boldsymbol{\sigma} \cdot \mathbf{n}) ds \otimes \mathbf{Y}^j \right) + \\ &+ \frac{1}{|Y|} \sum_{i=1,2} \left(\left(\frac{1}{2} \delta \mathbf{K} \cdot \mathbf{Y}^i \cdot \mathbf{Y}^i \right) \otimes \mathbf{N}^i \right) : \sum_{j=1,2} \left(\int_{\partial Y} (\boldsymbol{\sigma} \cdot \mathbf{n}) ds \otimes \mathbf{Y}^j \right) \end{aligned} \tag{B19}$$

droping here the macroscopic position for the sake of simplicity of the writing. Using again the relation $\mathbf{N}^i \cdot \mathbf{Y}^j = |Y| \delta_{ij}$, Eq.(B19) can be rewritten after straightforward calculations as

$$\begin{aligned} &\int_Y \boldsymbol{\sigma} : (\boldsymbol{\omega} \otimes \nabla_y) dV = \frac{1}{|Y|} \sum_{i=1,2} \left(\left(\delta \mathbf{E} \cdot \mathbf{Y}^i \right) \otimes \mathbf{N}^i \right) : \sum_{j=1,2} \left(\int_{\partial Y} (\boldsymbol{\sigma} \cdot \mathbf{n}) ds \otimes \mathbf{Y}^j \right) + \\ &+ \sum_{i=1,2} \left(\left(\delta \mathbf{K} \cdot \mathbf{Y}^i \right) \otimes \mathbf{N}^i \right) \therefore \sum_{j=1,2} \left(\frac{1}{2|Y|} \int_{\partial Y} (\boldsymbol{\sigma} \cdot \mathbf{n}) ds \right) \otimes \mathbf{Y}^j \otimes \mathbf{Y}^j = \\ &= \langle \boldsymbol{\sigma} \rangle_Y : \mathbf{E} + \langle \boldsymbol{\xi} \otimes \boldsymbol{\sigma} \rangle_Y \therefore \mathbf{L}_K = \boldsymbol{\Sigma} : \delta \mathbf{E} + \mathbf{S} \therefore \delta \mathbf{K} \end{aligned} \tag{B20}$$

The last relation in Eq.(B20) follows from the use of a symmetrical macrostrain tensor, such that (similar definitions hold for the virtual variations of the same fields)

$$\mathbf{E}(\mathbf{x}) := \left\langle \mathbf{u}(\mathbf{y}) \otimes^{\mathrm{S}} \nabla_{\mathrm{x}} \right\rangle_{\mathrm{Y}} \rightarrow \mathbf{K}(\mathbf{x}) = \mathbf{E}(\mathbf{x}) \otimes \nabla_{\mathrm{x}} \tag{B21}$$

Relation (B20) entails the static version of the virtual power principle:

$$\left\langle \boldsymbol{\sigma} : \boldsymbol{\omega} \otimes^S \nabla_y \right\rangle_Y = \langle \boldsymbol{\sigma} \rangle_Y : \left\langle \boldsymbol{\omega} \otimes^S \nabla_y \right\rangle_Y + \langle \boldsymbol{\sigma} \otimes \boldsymbol{\xi} \rangle_Y \therefore \left\langle \boldsymbol{\omega} \otimes^S \nabla_y \right\rangle_Y \otimes \nabla_x \tag{B22}$$

Its dynamical extension is further formulated. Expanding the virtual velocity as

$$\boldsymbol{\omega} = \mathbf{W} + \boldsymbol{\eta} . \mathbf{y} + \boldsymbol{\tau} : \frac{1}{2} (\mathbf{y} \otimes \mathbf{y}) \tag{B23}$$

with $\mathbf{W}(\mathbf{x}), \boldsymbol{\eta}(\mathbf{x}), \boldsymbol{\tau}(\mathbf{x})$ the virtual velocity, strain rate and rate of strain gradient leads to the expression of the virtual power of inertia forces, with $\rho\ddot{\mathbf{u}} = \rho\boldsymbol{\gamma}(\mathbf{x})$ denoting the acceleration quantities:

$$\begin{aligned}&\int_Y \rho\ddot{\mathbf{u}}\cdot\boldsymbol{\omega} dV = \int_Y dV\left(\rho\boldsymbol{\gamma}(\mathbf{x})\right)\cdot\left(\mathbf{W}+\boldsymbol{\eta}.\mathbf{y}+\boldsymbol{\tau}:\frac{1}{2}(\mathbf{y}\otimes\mathbf{y})\right)dV = \\ &\left(\int_Y dV\,\rho\boldsymbol{\gamma}(\mathbf{x})\right).\mathbf{W}+\int_Y dV\left(\rho\boldsymbol{\gamma}(\mathbf{x})\otimes\mathbf{y}\right)\cdot\boldsymbol{\eta}+\frac{1}{2}\left(\int_Y dV\left(\rho\boldsymbol{\gamma}(\mathbf{x})\otimes\mathbf{y}\otimes\mathbf{y}\right)\right)\therefore\boldsymbol{\tau}\end{aligned} \tag{B24}$$

Equality (B24) relates the average of the power of acceleration quantities $\rho\ddot{\mathbf{u}}$ to its macroscopic average on the right-hand side. Summing up the virtual power of inertia forces with relation (B22) leads using (B23) to

$$\begin{aligned}&\mathbf{W}=\langle\boldsymbol{\omega}\rangle_Y,\ \boldsymbol{\eta}=\langle\boldsymbol{\omega}\otimes\nabla_y\rangle_Y,\ \boldsymbol{\tau}=\langle\boldsymbol{\omega}\otimes\nabla_y\otimes^S\nabla_y\rangle_Y\Rightarrow\\ &\langle\rho\ddot{\mathbf{u}}.\boldsymbol{\omega}+\boldsymbol{\sigma}:\boldsymbol{\omega}\otimes\nabla_y\rangle_Y=\langle\rho\ddot{\mathbf{u}}\rangle_Y.\mathbf{W}+\langle\rho\ddot{\mathbf{u}}\otimes\mathbf{y}\rangle_Y\cdot\boldsymbol{\eta}+\frac{1}{2}\langle\rho\ddot{\mathbf{u}}\otimes\mathbf{y}\otimes\mathbf{y}\rangle_Y\therefore\boldsymbol{\tau}\\ &+\langle\boldsymbol{\sigma}\rangle_Y:\langle\boldsymbol{\omega}\otimes\nabla_y\rangle_Y+\langle\boldsymbol{\sigma}\otimes\boldsymbol{\xi}\rangle_Y\therefore\langle\boldsymbol{\omega}\otimes^S\nabla_y\rangle_Y\otimes\nabla_x\end{aligned} \tag{B25}$$

Whitaker's theorem for situations of continuous internal interfaces between constituents has been used, in the form $\langle\boldsymbol{\omega}\otimes\nabla_y\otimes\nabla_y\rangle_Y\equiv\langle\boldsymbol{\omega}\otimes\nabla_y\rangle_Y\otimes\nabla_x$. Eq.(B25) constitutes the dynamical Hill macrohomogeneity condition for the strain gradient effective continuum, stating that the average of the microscopic Hamiltonian density is identical to the macroscopic Hamiltonian density evaluated over the homogeneous substitution medium. Note that Hill dynamical macrohomogeneity condition for the Cauchy continuum is simply recovered as a specific case of identity (B25) by setting $\boldsymbol{\tau}\equiv\mathbf{0}$ in the expansion of the virtual velocity, Eq.(B23), thus leading to

$$\mathbf{W}=\langle\boldsymbol{\omega}\rangle_Y,\ \boldsymbol{\eta}=\langle\boldsymbol{\omega}\otimes\nabla_y\rangle_Y\Rightarrow\langle\rho\ddot{\mathbf{u}}.\boldsymbol{\omega}+\boldsymbol{\sigma}:\boldsymbol{\omega}\otimes\nabla_y\rangle_Y=\langle\rho\ddot{\mathbf{u}}\rangle_Y.\mathbf{W}+\langle\rho\ddot{\mathbf{u}}\otimes\mathbf{y}\rangle_Y\cdot\boldsymbol{\eta}+\langle\boldsymbol{\sigma}\rangle_Y:\langle\boldsymbol{\omega}\rangle_Y\otimes\nabla_x \tag{B26}$$

wherein Whitaker theorem has been employed to express the last term in alternative form

$$\langle\boldsymbol{\sigma}\rangle_Y:\langle\boldsymbol{\omega}\otimes\nabla_y\rangle_Y=\langle\boldsymbol{\sigma}\rangle_Y:\langle\boldsymbol{\omega}\rangle_Y\otimes\nabla_x \tag{B27}$$

The following identity is easily obtained from Eqs.(B22, A24):

$$\begin{aligned}&\langle\rho\ddot{\mathbf{u}}.\delta\mathbf{u}+\boldsymbol{\sigma}:\delta\mathbf{u}\otimes\nabla_y\rangle_Y=\left(\langle\rho\ddot{\mathbf{u}}\rangle_Y.\delta\mathbf{U}+\langle\rho\ddot{\mathbf{u}}\otimes\mathbf{y}\rangle_Y\cdot\langle\delta\mathbf{U}\otimes\nabla_y\rangle_Y\right)+\frac{1}{2}\langle\rho\ddot{\mathbf{u}}\otimes\mathbf{y}\otimes\mathbf{y}\rangle_Y\therefore\langle\delta\mathbf{U}\otimes^S\nabla_y\rangle_Y\otimes\nabla_x\\ &+\langle\boldsymbol{\sigma}\rangle_Y:\langle\delta\mathbf{U}\otimes\nabla_y\rangle_Y+\langle\boldsymbol{\sigma}\otimes\boldsymbol{\xi}\rangle_Y\therefore\langle\delta\mathbf{U}\otimes^S\nabla_y\rangle_Y\otimes\nabla_x\end{aligned} \tag{B28}$$

Previous variational formulation is further transformed using Maxwell-Betti reciprocity relations at both microscopic and macroscopic levels and performing integration by part in time of acceleration quantities in (B28) after time integration of (B28), adopting nil initial values for the test function $\delta\mathbf{u}$ and its time derivative:

$$
\begin{aligned}
&\left\langle l_\mu(\boldsymbol{\varepsilon},\mathbf{p})\right\rangle_Y := \frac{1}{2}\left\langle \rho\dot{\mathbf{u}}.\dot{\mathbf{u}} - \boldsymbol{\sigma}:\mathbf{u}\otimes\nabla_y\right\rangle_Y = \frac{1}{2}\mathbf{P}.\mathbf{V} - \frac{1}{2}\boldsymbol{\Sigma}^{stat}:\mathbf{E} - \frac{1}{2}\mathbf{S}^{stat}\therefore\mathbf{K} - \frac{1}{2}\boldsymbol{\Sigma}^{dyn}:\dot{\mathbf{E}} - \frac{1}{2}\mathbf{S}^{dyn}\therefore\dot{\mathbf{K}}\\
&=: L_M\left(\mathbf{V},\mathbf{V}\otimes\nabla_x,\mathbf{E},\mathbf{K}\right)\\
&\mathbf{P} := \left\langle\mathbf{p}\right\rangle_Y,\ \mathbf{Q} := \left\langle\mathbf{p}\otimes\mathbf{y}\right\rangle_Y,\\
&\mathbf{E} := \left\langle\mathbf{U}\otimes\nabla_y\right\rangle_Y,\ \ \mathbf{K} := \left\langle\mathbf{U}\otimes^S\nabla_y\right\rangle_Y\otimes\nabla_x\\
&\boldsymbol{\Sigma}^{stat} := \left\langle\boldsymbol{\sigma}\right\rangle_Y, \boldsymbol{\Sigma}^{dyn} := -\left\langle\mathbf{p}\otimes\mathbf{y}\right\rangle_Y,\ \ \mathbf{S}^{stat} := \left\langle\boldsymbol{\sigma}\otimes\boldsymbol{\xi}\right\rangle_Y,\ \mathbf{S}^{dyn} := -\frac{1}{2}\left\langle\mathbf{p}\otimes\mathbf{y}\otimes\mathbf{y}\right\rangle_Y
\end{aligned}
\tag{B29}
$$

Eq.(B28) states that the Y-average of the microscopic Lagrangian is identical to the macroscopic Lagrangian $L_M\left(\mathbf{V},\mathbf{V}\otimes\nabla_x,\mathbf{E},\mathbf{K}\right)$, wherein we have introduced the effective momentum $\mathbf{P}$ and hypermomentum $\mathbf{Q}$, as well as the dynamical stress $\boldsymbol{\Sigma}^{dyn}$ and hyperstress $\mathbf{S}^{dyn}$. An alternative writing of previous Hill type dynamical macrohomogeneity condition can be written involving the macrostrain and macro strain gradients only (without their temporal derivatives as in (B29)):

$$
\begin{aligned}
&\left\langle l_\mu(\boldsymbol{\varepsilon},\mathbf{p})\right\rangle_Y := \frac{1}{2}\left\langle \rho\dot{\mathbf{u}}.\dot{\mathbf{u}} - \boldsymbol{\sigma}:\mathbf{u}\otimes\nabla_y\right\rangle_Y = \frac{1}{2}\mathbf{P}.\mathbf{V} - \frac{1}{2}\boldsymbol{\Sigma}^{dyn}:\mathbf{E} - \frac{1}{2}\mathbf{S}^{dyn}\therefore\mathbf{K} =: L_M\left(\mathbf{E},\mathbf{K},\mathbf{V},\mathbf{V}\otimes\nabla_x\right)\\
&\mathbf{P} := \left\langle\rho\dot{\mathbf{u}}\right\rangle_Y,\ \mathbf{Q} := \left\langle\rho\dot{\mathbf{u}}\otimes\mathbf{y}\right\rangle_Y,\\
&\mathbf{E} := \left\langle\mathbf{U}\otimes\nabla_y\right\rangle_Y,\ \ \mathbf{K} := \left\langle\mathbf{U}\otimes^S\nabla_y\right\rangle_Y\otimes\nabla_x\\
&\boldsymbol{\Sigma}^{dyn} := \left\langle\boldsymbol{\sigma}\right\rangle_Y + \left\langle\rho\ddot{\mathbf{u}}\otimes\mathbf{y}\right\rangle_Y,\ \ \mathbf{S}^{dyn} := \left\langle\boldsymbol{\sigma}\otimes\boldsymbol{\xi}\right\rangle_Y + \frac{1}{2}\left\langle\rho\ddot{\mathbf{u}}\otimes\mathbf{y}\otimes\mathbf{y}\right\rangle_Y
\end{aligned}
\tag{B30}
$$

A similar dynamical macrohomogeneity condition holds for the Hamiltonian $H_M\left(\mathbf{E},\mathbf{P}(\mathbf{V}),\mathbf{Q}(\mathbf{V}\otimes\nabla_x)\right)$, as can be easily proven:

$$
\begin{aligned}
&\left\langle h_\mu(\boldsymbol{\varepsilon},\mathbf{p})\right\rangle_Y := \frac{1}{2}\left\langle \rho\dot{\mathbf{u}}.\dot{\mathbf{u}} + \boldsymbol{\sigma}:\mathbf{u}\otimes\nabla_y\right\rangle_Y = \frac{1}{2}\mathbf{P}.\mathbf{V} + \frac{1}{2}\boldsymbol{\Sigma}^{stat}:\mathbf{E} + \frac{1}{2}\mathbf{S}^{stat}\therefore\mathbf{K} + \frac{1}{2}\boldsymbol{\Sigma}^{dyn}:\dot{\mathbf{E}} + \frac{1}{2}\mathbf{S}^{dyn}\therefore\dot{\mathbf{K}}\\
&=: H_M\left(\mathbf{E},\mathbf{K},\mathbf{P},\mathbf{Q}\right)\\
&\Leftrightarrow \left\langle h_\mu(\boldsymbol{\varepsilon},\mathbf{p})\right\rangle_Y := \frac{1}{2}\left\langle \rho\dot{\mathbf{u}}.\dot{\mathbf{u}} + \boldsymbol{\sigma}:\mathbf{u}\otimes\nabla_y\right\rangle_Y = \frac{1}{2}\mathbf{P}.\mathbf{V} + \frac{1}{2}\boldsymbol{\Sigma}^{dyn}:\mathbf{E} + \frac{1}{2}\mathbf{S}^{dyn}\therefore\mathbf{K} =: H_M\left(\mathbf{E},\mathbf{K},\mathbf{P},\mathbf{Q}\right)\\
&\mathbf{P} := \left\langle\rho\dot{\mathbf{u}}\right\rangle_Y,\ \mathbf{Q} := \left\langle\rho\dot{\mathbf{u}}\otimes\mathbf{y}\right\rangle_Y,\\
&\mathbf{E} := \left\langle\mathbf{U}\otimes^S\nabla_y\right\rangle_Y,\ \ \mathbf{K} := \left\langle\mathbf{U}\otimes^S\nabla_y\right\rangle_Y\otimes\nabla_x\\
&\boldsymbol{\Sigma}^{dyn} := \left\langle\boldsymbol{\sigma} + \rho\ddot{\mathbf{u}}\otimes\mathbf{y}\right\rangle_Y,\ \ \mathbf{S}^{dyn} := \left\langle\boldsymbol{\sigma}\otimes\boldsymbol{\xi} + \frac{1}{2}\rho\dot{\mathbf{u}}\otimes\mathbf{y}\otimes\mathbf{y}\right\rangle_Y
\end{aligned}
\tag{B31}
$$

Two alternative forms in Eq.(B31) involving either static and dynamical stress tensors respectively conjugated to the kinematic variables and to their rates, or dynamical stress tensors only (dual to the strain tensors) and without appearance of strain rates, have been used.

Appendix C: derivation of the homogeneous part of the displacement and velocity fields for the dynamical strain gradient effective medium

The homogeneous contribution of the displacement field is obtained using Hill macrohomogeneity condition relating the microscopic to the macroscopic Lagrangian, both expressed in the space-frequency domain from Eq.(B30):

$$\left\langle l_\mu(\boldsymbol{\varepsilon},\mathbf{v})\right\rangle_Y := \frac{1}{2}\left\langle \mathbf{p}.\mathbf{v}-\boldsymbol{\sigma}:\mathbf{u}\otimes\nabla_y\right\rangle_Y = \frac{1}{2}\mathbf{P}.\mathbf{V}-\frac{1}{2}\boldsymbol{\Sigma}^{dyn}:\mathbf{E}-\frac{1}{2}\mathbf{S}^{dyn}\therefore\mathbf{K} =: L_M(\mathbf{E},\mathbf{K},\mathbf{V},\mathbf{V}\otimes\nabla_x)$$
$$\mathbf{P} := \left\langle \mathbf{p}\right\rangle_Y,\ \mathbf{Q} := \left\langle \mathbf{p}\otimes\mathbf{y}\right\rangle_Y,\ \mathbf{E} := \left\langle \mathbf{U}\otimes\nabla_y\right\rangle_Y,\ \mathbf{K} := \left\langle \mathbf{U}\otimes^S\nabla_y\right\rangle_Y\otimes\nabla_x \tag{C1}$$
$$\boldsymbol{\Sigma}^{dyn} := \left\langle\boldsymbol{\sigma}\right\rangle_Y + \left\langle i\omega\mathbf{p}\otimes\mathbf{y}\right\rangle_Y,\ \mathbf{S}^{dyn} := \left\langle\boldsymbol{\sigma}\otimes\boldsymbol{\xi}\right\rangle_Y + \frac{1}{2}\left\langle\mathbf{p}\otimes\mathbf{y}\otimes\mathbf{y}\right\rangle_Y$$

In the microscopic Lagrangian density, all fields $(\boldsymbol{\sigma},\boldsymbol{\varepsilon},\mathbf{v})$ are expressed in terms of the micro-position and frequency. The macroscopic Cauchy stress and hyperstress tensors together with the macroscopic momentum are obtained exploiting Eq.(B1) and the definition of the Lagrangian obtained in the **Appendix B** as a potential for the macroscopic stress tensor and momentum, as formulated by the macroscopic constitutive equations (3.15) through (3.19):

$$L_M(\mathbf{E},\mathbf{K},\mathbf{V}) = \left\langle l_\mu(\boldsymbol{\varepsilon},\mathbf{v})\right\rangle_Y = \frac{1}{2}\mathbf{P}.\mathbf{V}-\frac{1}{2}\boldsymbol{\Sigma}^{dyn}:\mathbf{E}-\frac{1}{2}\mathbf{S}^{dyn}\therefore\mathbf{K}\Rightarrow$$
$$\forall(\sigma_{pq},p_p):$$
$$\Sigma_{ij}^{dyn} := -\frac{\partial L_M}{\partial E_{ij}(\omega)} = -\frac{\partial}{\partial E_{ij}}\left\langle l_\mu(\boldsymbol{\varepsilon},p)\right\rangle_Y = -\left\langle\frac{\partial l_\mu}{\partial E_{ij}}\right\rangle_Y = -\left\langle\frac{\partial l_\mu}{\partial\varepsilon_{pq}}\frac{\partial\varepsilon_{pq}}{\partial E_{ij}}+\frac{\partial l_\mu}{\partial v_p}\frac{\partial v_p}{\partial E_{ij}}\right\rangle_Y = -\left\langle\sigma_{pq}\tfrac{\partial\varepsilon_{pq}}{\partial E_{ij}}+p_p\frac{\partial v_p}{\partial E_{ij}}\right\rangle_Y, \tag{C2}$$
$$\text{with } \Sigma_{ij}^{dyn} := \left\langle\sigma_{ij}+i\omega p_i y_j\right\rangle_Y$$
$$P_i := \frac{\delta L_M}{\delta V_i(\omega)} = \frac{\delta}{\delta V_i}\left\langle l_\mu(\boldsymbol{\varepsilon},\mathbf{v})\right\rangle_Y = \left\langle\frac{\partial l_\mu}{\partial V_i}\right\rangle_Y = \left\langle\frac{\partial l_\mu}{\partial\varepsilon_{pq}}\frac{\partial\varepsilon_{pq}}{\partial V_i}+\frac{\partial l_\mu}{\partial v_p}\frac{\partial v_p}{\partial V_i}\right\rangle_Y = \left\langle\sigma_{pq}\tfrac{\partial\varepsilon_{pq}}{\partial V_i}+p_p\frac{\partial v_p}{\partial V_i}\right\rangle_Y,$$
$$\text{with } P_i := \left\langle p_i\right\rangle_Y$$

In Eq.(C2), we have used the definitions of the macroscopic dynamical Cauchy stress and hyperstress tensors in Eq.(B31), formulated in the frequency domain. Similarly, the average macroscopic hyperstress and hypermomentum write using Hill lemma and the macroscopic formulation of the Hamiltonian, the first equality in Eq.(C2) as

$$\forall(\sigma_{pq},p_p),$$
$$S_{ijk}^{stat} := -\frac{\partial L_M}{\partial K_{ijk}} = \frac{\partial}{\partial K_{ijk}}\left\langle l_\mu(\boldsymbol{\varepsilon})\right\rangle_Y = \left\langle\frac{\partial l_\mu(\boldsymbol{\varepsilon})}{\partial K_{ijk}}\right\rangle_Y = \left\langle\frac{\partial l_\mu(\boldsymbol{\varepsilon})}{\partial\varepsilon_{pq}}\frac{\partial\varepsilon_{pq}}{\partial K_{ijk}}+\frac{\partial l_\mu}{\partial v_p}\frac{\partial v_p}{\partial K_{ijk}}\right\rangle_Y = \left\langle\sigma_{pq}\tfrac{\partial\varepsilon_{pq}}{\partial K_{ijk}}+p_p\frac{\partial v_p}{\partial K_{ijk}}\right\rangle_Y,$$
$$\text{with } S_{ijk}^{dyn} := \left\langle\sigma_{ij}\xi_k+\frac{1}{2}i\omega p_i y_j y_k\right\rangle_Y, \tag{C3}$$
$$Q_i := \frac{\delta L_M}{\delta V_{i,j}(\omega)} = \frac{\delta}{\delta V_{i,j}}\left\langle l_\mu(\boldsymbol{\varepsilon},\mathbf{v})\right\rangle_Y = \left\langle\frac{\partial l_\mu}{\partial V_{i,j}}\right\rangle_Y = \left\langle\frac{\partial l_\mu}{\partial\varepsilon_{pq}}\frac{\partial\varepsilon_{pq}}{\partial V_{i,j}}+\frac{\partial l_\mu}{\partial v_p}\frac{\partial v_p}{\partial V_{i,j}}\right\rangle_Y = \left\langle\sigma_{pq}\tfrac{\partial\varepsilon_{pq}}{\partial V_{i,j}}+p_p\frac{\partial v_p}{\partial V_{i,j}}\right\rangle_Y,$$
$$\text{with } Q_{ij} = \left\langle p_i y_j\right\rangle_Y$$

These two sets of equalities deliver a set of integral relations for the homogeneous displacement and velocity fields, leading to the determination of the microscopic velocity and deformation field versus the macroscopic variables $(\mathbf{V},\mathbf{E},\mathbf{K})$. Eq.(C2) entails the following system of five integral equations (three for the micro strain and two for the micro velocity versus the macro strain and velocity) in the present planar situation:

$$\forall\left(\sigma_{pq},p_p\right),$$
$$\left\langle\sigma_{ij}+i\omega p_i y_j\right\rangle_Y=\left\langle\sigma_{pq}\frac{\partial\varepsilon_{pq}}{\partial E_{ij}}+p_p\frac{\partial v_p}{\partial E_{ij}}\right\rangle_Y\Rightarrow v_i=i\omega E_{ij}y_j,\ \varepsilon_{ij}=E_{ij} \tag{C4}$$
$$\left\langle p_i\right\rangle_Y=\left\langle\sigma_{pq}\frac{\partial\varepsilon_{pq}}{\partial V_i}+p_p\frac{\partial v_p}{\partial V_i}\right\rangle_Y\Rightarrow v_i=V_i,\ \frac{\partial\varepsilon_{pq}}{\partial V_i}=0$$

Similarly, and for the higher gradient response, Eq.(C3) leads to the following system of integral relations leading to three relations for the micro strain tensor and two for the micro velocity versus the macro strain gradient tensor and macro velocity gradient tensor:

$$\forall\left(\sigma_{pq},p_p\right),$$
$$\left\langle\sigma_{ij}y_k+\frac{1}{2}i\omega p_i y_j y_k\right\rangle_Y=\left\langle\sigma_{pq}\frac{\partial\varepsilon_{pq}}{\partial K_{ijk}}+p_p\frac{\partial v_p}{\partial K_{ijk}}\right\rangle_Y\Rightarrow v_i=i\omega K_{ijk}y_j y_k,\ \varepsilon_{ij}=K_{ijk}y_k, \tag{C5}$$
$$\left\langle p_i y_j\right\rangle_Y=\left\langle\sigma_{pq}\frac{\partial\varepsilon_{pq}}{\partial V_{i,j}}+p_p\frac{\partial v_p}{\partial V_{i,j}}\right\rangle_Y\Rightarrow v_i=V_{i,j}y_j,\ \frac{\partial\varepsilon_{pq}}{\partial V_{i,j}}=0$$

Summarizing the dependencies obtained in Eq.(C4-C5), the simultaneous satisfaction of the system of resulting equalities leads to the following form of the microscopic velocity and strain fields in space-frequency domain versus the macroscopic kinematic control variables applied over the unit cell, namely the (macroscopic) velocity vector and the strain and strain gradient tensors:

$$\begin{aligned}&v_i=V_i+V_{i,j}y_j+i\omega E_{ij}y_j+i\omega K_{ijk}y_j y_k,\\&\varepsilon_{ij}=E_{ij}+K_{ijk}y_k\end{aligned} \tag{C6}$$

Appendix D: Hamilton principle for strain gradient dynamical homogenization

The macroscopic Lagrangian in the framework of strain gradient dynamical homogenization writes as follows:

$$\begin{aligned}&L_M\left(\mathbf{E},\mathbf{K},\mathbf{V},\mathbf{V}\otimes^S\nabla_x,\left(\mathbf{V}\otimes^S\nabla_x\otimes\nabla_x\right),\mathbf{\Lambda}\right)\\&=\underset{\tilde{\mathbf{u}},\tilde{\mathbf{v}}\in K}{\mathrm{Min}}\frac{1}{2}\left\{\begin{array}{l}\int_Y dV_y\rho\left(\mathbf{A}^V.\mathbf{V}+\mathbf{H}^{VE}:i\omega\mathbf{E}+\mathbf{H}^{VK}:i\omega\mathbf{K}\right).\left(\mathbf{A}^V.\mathbf{V}+\mathbf{H}^{VE}:i\omega\mathbf{E}+\mathbf{H}^{VK}:i\omega\mathbf{K}\right)-\\\left(\mathbf{E}+\mathbf{K}.\mathbf{x}+\left(\mathbf{H}^{EE}\otimes\nabla_y:\mathbf{E}+\mathbf{H}^{EK}\otimes\nabla_y:\mathbf{K}+\left(\mathbf{H}^{EV}\otimes\nabla_y\right).\mathbf{V}\right)\right):\\\mathbf{C}:\left(\mathbf{E}+\mathbf{K}.\mathbf{x}+\left(\mathbf{H}^{EE}\otimes\nabla_y:\mathbf{E}+\mathbf{H}^{EK}\otimes\nabla_y:\mathbf{K}+\left(\mathbf{H}^{EV}\otimes\nabla_y\right).\mathbf{V}\right)\right)+\\\frac{\mathbf{\Lambda}}{|Y|}.\left(\mathbf{V}-\left(\mathbf{V}\otimes^S\nabla_x\right)\cdot\mathbf{x}-\left(\mathbf{V}\otimes^S\nabla_x\otimes\nabla_x\right):\mathbf{G}_2\right)\end{array}\right\}=\\&\underset{\tilde{\mathbf{u}},\tilde{\mathbf{v}}\in K}{\mathrm{Min}}\frac{1}{2}\left\{\begin{array}{l}\int_Y dV_y\rho\left(\mathbf{A}^V.\mathbf{V}+\mathbf{H}^{VE}:i\omega\mathbf{E}+\mathbf{H}^{VK}:i\omega\mathbf{K}\right).\left(\mathbf{A}^V.\mathbf{V}+\mathbf{H}^{VE}:i\omega\mathbf{E}+\mathbf{H}^{VK}:i\omega\mathbf{K}\right)-\\\left(\mathbf{A}^E:\mathbf{E}+\mathbf{A}\therefore\mathbf{K}+\left(\mathbf{H}^{EV}\otimes\nabla_y\right).\mathbf{V}\right):\mathbf{C}:\left(\mathbf{A}^E:\mathbf{E}+\mathbf{A}\therefore\mathbf{K}+\left(\mathbf{H}^{EV}\otimes\nabla_y\right).\mathbf{V}\right)+\\\frac{\mathbf{\Lambda}}{|Y|}.\left(\mathbf{V}-\left(\mathbf{V}\otimes^S\nabla_x\right)\cdot\mathbf{x}-\left(\mathbf{V}\otimes^S\nabla_x\otimes\nabla_x\right):\mathbf{G}_2\right)\end{array}\right\}\end{aligned} \tag{D1}$$

We have introduced in the last equality the strain and velocity localization operators

$$\begin{aligned}
&\mathbf{A}^{\mathrm{E}}(\mathbf{y},\omega) := \mathbf{I}_4 + \mathbf{H}^{\mathrm{E}}(\mathbf{y},\omega)\otimes\nabla_{\mathrm{y}},\\
&\mathbf{A}^{\mathrm{K}}(\mathbf{y},\omega) := \left(\mathbf{I}_4\otimes\mathbf{x} + \mathbf{H}^{\mathrm{K}}(\mathbf{y},\omega)\otimes\nabla_{\mathrm{y}}\right),\\
&\mathbf{A}^{\mathrm{V}}(\mathbf{y},\omega) := \mathbf{H}^{\mathrm{VV}}(\mathbf{y},\omega)
\end{aligned} \tag{D2}$$

The dynamical strain gradient constitutive law follows from Hill macrohomogeneity condition written in Eq.(3.5), wherein minimization and partial derivatives with respect to the macroscopic kinematic variables has been done (using similar argumentation as for the first gradient situation previously exposed):

$$\begin{aligned}
&\boldsymbol{\Sigma}^{\mathrm{dyn}} := -\underset{\tilde{\mathbf{u}},\tilde{\mathbf{v}}\in\mathrm{V_K}}{\mathrm{Min}}\frac{\delta \mathrm{L_M}\left(\mathbf{E},\mathbf{K},\mathbf{V},\mathbf{V}\otimes^{\mathrm{S}}\nabla_{\mathrm{x}},\left(\mathbf{V}\otimes^{\mathrm{S}}\nabla_{\mathrm{x}}\otimes\nabla_{\mathrm{x}}\right),\boldsymbol{\Lambda}\right)}{\delta\mathbf{E}}\\
&=\int_{\mathrm{Y}}\left\{-\frac{\mathrm{d}}{\mathrm{dt}}\left[\rho\left(\mathbf{A}^{\mathrm{V}}.\mathbf{V}+\mathbf{H}^{\mathrm{VE}}:\mathbf{E}+\mathbf{H}^{\mathrm{VK}}\therefore\mathbf{K}\right)\right].\mathbf{H}^{\mathrm{VE}}+\left(\mathbf{A}^{\mathrm{E}}+\mathbf{A}\therefore\mathbf{K}+\left(\mathbf{H}^{\mathrm{EV}}\otimes\nabla_{\mathrm{y}}\right).\mathbf{V}\right):\mathbf{C}:\mathbf{A}^{\mathrm{E}}\right\}\mathrm{dV_y}
\end{aligned} \tag{D3}$$

$$\begin{aligned}
&\mathbf{S}^{\mathrm{dyn}} := -\underset{\tilde{\mathbf{u}},\tilde{\mathbf{v}}\in\mathrm{V_K}}{\mathrm{Min}}\frac{\partial \mathrm{L_M}\left(\mathbf{E},\mathbf{K},\mathbf{V},\mathbf{V}\otimes^{\mathrm{S}}\nabla_{\mathrm{x}},\left(\mathbf{V}\otimes^{\mathrm{S}}\nabla_{\mathrm{x}}\otimes\nabla_{\mathrm{x}}\right),\boldsymbol{\Lambda}\right)}{\partial\mathbf{K}}\\
&=-\int_{\mathrm{Y}}\mathrm{dV_y}\left\{-\frac{\mathrm{d}}{\mathrm{dt}}\left(\rho\left(\mathbf{A}^{\mathrm{V}}.\mathbf{V}+\mathbf{H}^{\mathrm{VE}}:\mathbf{E}+\mathbf{H}^{\mathrm{VK}}:\mathbf{K}\right)\right).\mathbf{H}^{\mathrm{VK}}+\left(\mathbf{A}^{\mathrm{E}}:\mathbf{E}+\mathbf{A}^{\mathrm{K}}\therefore\mathbf{K}+\left(\mathbf{H}^{\mathrm{EV}}\otimes\nabla_{\mathrm{y}}\right).\mathbf{V}\right):\mathbf{C}:\mathbf{A}^{\mathrm{K}}\right\}
\end{aligned} \tag{D4}$$

$$\begin{aligned}
&\mathbf{P} := \underset{\tilde{\mathbf{u}},\tilde{\mathbf{v}}\in\mathrm{V_K}}{\mathrm{Min}}\frac{\partial \mathrm{L_M}\left(\mathbf{E},\mathbf{K},\mathbf{V},\mathbf{V}\otimes^{\mathrm{S}}\nabla_{\mathrm{x}},\left(\mathbf{V}\otimes^{\mathrm{S}}\nabla_{\mathrm{x}}\otimes\nabla_{\mathrm{x}}\right),\boldsymbol{\Lambda}\right)}{\partial\mathbf{V}} =\\
&\int_{\mathrm{Y}}\mathrm{dV_y}\rho\left(\mathbf{A}^{\mathrm{V}}.\mathbf{V}+\mathbf{H}^{\mathrm{VE}}:\mathbf{E}+\mathbf{H}^{\mathrm{VK}}:\mathbf{K}\right).\mathbf{A}^{\mathrm{V}}-\left(\mathbf{A}^{\mathrm{E}}:\mathbf{E}+\mathbf{A}^{\mathrm{K}}\therefore\mathbf{K}+\left(\mathbf{H}^{\mathrm{EV}}\otimes\nabla_{\mathrm{y}}\right).\mathbf{V}\right):\mathbf{C}:\left(\mathbf{H}^{\mathrm{EV}}\otimes\nabla_{\mathrm{y}}\right)+\\
&\boldsymbol{\Lambda}\left(\mathbf{E},\mathbf{K},\mathbf{V},\mathbf{Q}\right)+\frac{\partial\boldsymbol{\Lambda}}{\partial\mathbf{V}}.\left(\mathbf{V}-\left(\mathbf{V}\otimes^{\mathrm{S}}\nabla_{\mathrm{x}}\right)\cdot\mathbf{x}-\left(\mathbf{V}\otimes^{\mathrm{S}}\nabla_{\mathrm{x}}\otimes\nabla_{\mathrm{x}}\right):\mathbf{G}_2\right) =\\
&\left\{\int_{\mathrm{Y}}\mathrm{dV_y}\rho\mathbf{H}^{\mathrm{VE}}.\left(\mathbf{A}^{\mathrm{V}}\right)^{\mathrm{T}}-\left(\mathbf{A}^{\mathrm{E}}:\mathbf{E}\right):\mathbf{C}:\left(\mathbf{H}^{\mathrm{EV}}\otimes\nabla_{\mathrm{y}}\right)^{\mathrm{T}}\right\}:\mathbf{E}+\\
&\left\{\int_{\mathrm{Y}}\mathrm{dV_y}\rho\left(\mathbf{H}^{\mathrm{VK}}:\mathbf{K}\right).\mathbf{A}^{\mathrm{V}}-\left(\mathbf{A}^{\mathrm{K}}\therefore\mathbf{K}\right):\mathbf{C}:\left(\mathbf{H}^{\mathrm{EV}}\otimes\nabla_{\mathrm{y}}\right)^{\mathrm{T}}\right\}\therefore\mathbf{K}+\\
&\left\{\int_{\mathrm{Y}}\mathrm{dV_y}\rho\mathbf{A}^{\mathrm{V}}.\left(\mathbf{A}^{\mathrm{V}}\right)^{\mathrm{T}}-\left(\mathbf{H}^{\mathrm{EV}}\otimes\nabla_{\mathrm{y}}\right):\mathbf{C}:\left(\mathbf{H}^{\mathrm{EV}}\otimes\nabla_{\mathrm{y}}\right)^{\mathrm{T}}\right\}.\mathbf{V}+\boldsymbol{\Lambda}
\end{aligned} \tag{D5}$$

$$\mathbf{Q} := \underset{\tilde{\mathbf{u}},\tilde{\mathbf{v}}\in\mathrm{K}}{\mathrm{Min}}\frac{\partial \mathrm{L_M}\left(\mathbf{E},\mathbf{K},\mathbf{V},\mathbf{V}\otimes^{\mathrm{S}}\nabla_{\mathrm{x}},\left(\mathbf{V}\otimes^{\mathrm{S}}\nabla_{\mathrm{x}}\otimes\nabla_{\mathrm{x}}\right),\boldsymbol{\Lambda}\right)}{\partial\left(\mathbf{V}\otimes\nabla_{\mathrm{x}}\right)} =: -\boldsymbol{\Lambda}^{\mathrm{S}}\left(\mathbf{E},\mathbf{K},\mathbf{V},\mathbf{V}\otimes\nabla_{\mathrm{x}}\right) \tag{D6}$$

Thereby, Eq.(D6) shows that the Lagrange multiplier takes the sense of (minus) the hypermomentum; note that only the symmetrical part of the Lagrange multiplier can be determined, since the introduced macroscopic kinematics involves the symmetrical part of the velocity gradient. Note that all factors in previous constitutive law involving derivatives of the Lagrange multipliers vanish wen the kinematic constraint Eq.(3.9) is satisfied.

After expressing the macroscopic force type arguments of the macroscopic Lagrangian versus their dual kinematic variables, it incorporates the second gradient of the average velocity, which pairs to the second displacement gradient, thus one obtains in addition the second

hypermomentum given from Eqs.(3.10) by the relation (dropping here the frequency-dependency of the variables):

$$\mathbf{R} \coloneqq \underset{\tilde{\mathbf{u}},\tilde{\mathbf{v}}\in K}{\mathrm{Min}} \frac{\partial L_M\left(\mathbf{E},\mathbf{K},\mathbf{V},\mathbf{V}\otimes^S\nabla_x,\left(\mathbf{V}\otimes^S\nabla_x\otimes\nabla_x\right),\boldsymbol{\Lambda}\right)}{\partial\left(\mathbf{V}\otimes\nabla_x\otimes\nabla_x\right)} = -\boldsymbol{\Lambda}.\mathbf{G}_2 = \mathbf{Q}.\mathbf{G}_2 \qquad \text{(D7)}$$

The second order momentum writes accordingly as the integral of the hypermomentum weighted by the second order moment of inertia, introducing anisotropy in the higher order dynamical response.